


UNIVERSITY OF CALABRIA

Department of Biology, Ecology and Heart Sciences

PhD Program in Operation Research

'La presente tesi è cofinanziata con il sostegno della Commissione Europea, Fondo Sociale Europeo e della Regione Calabria. L'autore è il solo responsabile di questa tesi e la Commissione Europea e la Regione Calabria declinano ogni responsabilità sull'uso che potrà essere fatto delle informazioni in essa contenute.'

CYCLE XXVI

Inositol pyrophosphates in *Dictyostelium discoideum*: Developing the model

(Disciplinary field MAT/09)

Co-ordinator: *Prof. Lucio Grandinetti*

Supervisors: *Prof. Giuseppina Rose*

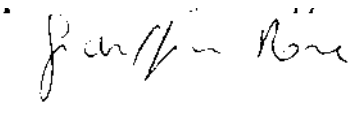

Dr. Adolfo Saiardi

Candidate: *Francesca Pisani*

2013

INDEX

SOMMARIO

Il lavoro di tesi qui presentato è stato realizzato in collaborazione con il Dr. Adolfo Saiardi che attualmente lavora al *Medical Research Council Laboratory for Molecular Cell Biology* (LMCB), all'interno del campus della *University College London* (UCL), a Londra. Da diversi anni il Dr. Saiardi si occupa dello studio degli inositoli polifosfati, importanti molecole di segnale che svolgono un ruolo sostanziale in diverse patologie umane come il cancro, il diabete e l'obesità. Il più descritto tra queste molecole è il fattore di rilascio del calcio I(1,4,5)P_3 o (IP_3) che rappresenta un classico esempio di secondo messaggero utilizzato nella trasduzione del segnale cellulare. Negli ultimi anni il ruolo fisiologico degli inositoli polifosfati ha suscitato un forte interesse da parte della comunità scientifica in quanto sarebbe interessante capire quali funzioni svolgono gli inositoli che contengono nel loro interno legami pirofosforici ovvero legami ad alta energia. I più caratterizzati e descritti tra gli inositoli pirofosfati sono l'IP_7 o PP-IP_5 e l'IP_8 o $[PP]_2$-IP_4. I legami ad alta energia presenti in queste molecole costituiscono un importante potenziale energetico per diverse reazioni molecolari e la loro particolare struttura suggerisce come queste molecole possano rappresentare una nuova classe di secondi messaggeri con funzioni importanti ma ancora non completamente note. Inoltre, la recente scoperta che il gruppo fosfato, presente nella frazione pirofosforica della molecola, possa essere donato direttamente alle proteine prefosforilate ha permesso di ipotizzare l'esistenza di un nuovo tipo di modificazione post-traduzionale e potrebbe aprire un altro campo in quello che è il già così vasto settore di ricerca della trasduzione del segnale.

Considerato che l'inositolo è stato utilizzato nel corso dell'evoluzione per produrre diverse molecole di segnale metabolicamente interconnesse, l'obiettivo principale della ricerca è stato quello di comprendere come molecole antichissime quali gli inositoli polifosfati, con funzioni limitate, si possano essere evolute fino a generare il sofisticato sistema di molecole di segnale presente nelle nostre cellule. Utilizzando un'ameba unicellulare, *Dictyostelium discoideum*, che condivide molti percorsi metabolici con gli organismi superiori e possiede caratteristiche peculiari che lo rendono un buon organismo modello, abbiamo cercato di sviluppare un sistema in cui analizzare il metabolismo degli inositoli pirofosfati e le vie di segnalazione in cui queste molecole sono implicate. Nel complesso, i risultati ottenuti ci permettono di affermare che *Dictyostelium* non solo possiede IP_6 ma anche gli inositoli pirofosfati che da esso derivano; la sintesi di IP_7 e IP_8 non è però indotta dall'cAMP come precedentemente riportato.

Per di più, i livelli di IP_8 riscontrati nella fase vegetativa del ciclo vitale di *Dictyostelium* sono molto più alti rispetto a quanto pubblicato in precedenza. Siamo anche riusciti ad identificare altre due importanti molecole di segnale: IP_5 (*Dictyostelium* ne possiede tre diverse isoforme) e IP_9. Questi risultati sono riportati in un articolo scientifico 'Analysis of *Dictyostelium discoideum* inositol pyrophosphate metabolism by gel electrophoresis' (PlosOne – In corso di stampa).

Nella prima parte del mio programma di Dottorato ho inoltre collaborato ad uno studio rivolto a valutare il ruolo svolto dalla variabilità dei geni che codificano per le ossido nitrico sintasi (NOS) nell'invecchiamento umano. I risultati di tale studio hanno portato ad una pubblicazione scientifica, 'Common polymorphisms in nitric oxide synthase (NOS) genes influence quality of aging and longevity in humans' (Biogerentology), riportata in appendice.

SUMMARY

This thesis has been realized in collaboration with Dr. Adolfo Saiardi who currently works at the *Medical Research Council Laboratory for Molecular Cell Biology* (LMCB), *University College London* (UCL), in London. For many years, Dr. Saiardi has studied the inositol polyphosphates, important signaling molecules playing a substantial role in several human diseases such as cancer, diabetes and obesity. Among the inositol polyphosphates the best characterized is the calcium releasing factor I(1,4,5)P_3 (IP_3), which represents a classical example of a secondary messenger molecule used in cellular signal transduction. In recent years, the physiological role played by inositol polyphosphates has fascinated the scientific community because it would be interesting to understand which functions are carried out by inositols that contain high-energy pyrophosphate bonds. The best characterized inositol pyrophosphates are diphosphoinositol pentakisphosphate (IP_7 or PP-IP_5) and bis-diphosphoinositol tetrakisphosphate (IP_8 or $[PP]_2$-IP_4). The high-energy bonds present in these molecules have the potential energy for many molecular reactions and their distinctive structure suggests that inositol pyrophosphates could represent a new class of second messengers with basic and not yet completely characterized functions. Moreover, the discovery that the high-energy phosphate of the pyrophosphate moiety can be directly donated to pre-phosphorylated proteins provided a novel type of post-translational modification (protein pyro-phosphorylation) and could possibly open a new field in signal transduction.

Considering that evolution used the inositol module to create different signaling entities that are metabolically interconnected, the current research was focused on understanding how ancient inositol polyphosphates with restricted functions have evolved into the sophisticated system of signaling molecules present in our cells. Using an unicellular amoeba, *Dictyostelium discoideum*, which shares many metabolic pathways with higher organisms and possesses characteristics that make it a good model organism, we attempted to develop a system in which to analyse inositol pyrophosphate metabolism and the signaling pathways involving these molecules. On the whole, these results allowed us to assert that *Dictyostelium* possesses IP_6 and its derivative inositol pyrophosphates IP_7 and IP_8. We also demonstrated that cAMP does not induce inositol pyrophosphates synthesis as previously reported. Furthermore, our study revealed much higher levels of IP_8 in the vegetative state of *D. discoideum* than previously detected. In addition, we also identified two other important signaling molecules namely IP_5 (three different isoforms are present in *Dictyostelium*) and

IP_9. In detail the work is reported in a scientific paper entitled 'Analysis of *Dictyostelium discoideum* inositol pyrophosphate metabolism by gel electrophoresis' (PlosOne – In Press).

In the first part of my PhD program, I participated in a study conducted to evaluate the role of the genetic variability of nitric oxide synthase (NOS) genes in the human aging. The results of this study are summarized in the published paper ‘Common polymorphisms in nitric oxide synthase (NOS) genes influence quality of aging and longevity in humans’ (Biogerontology) that is presented in the appendix.

CHAPTER I

Introduction

1. Inositol Poly- and Pyro-phosphates

The inositol polyphosphates are molecules that have a well-known place in the field of cell signaling and in many other important areas of cell biology. Recently, the di-phosphoinositol phosphates or inositol pyrophosphates have been added to the inositide family.

The name inositol derives from the Greek '*ino*' that means '*sinew*', indicating its role as a vitamin. Using *myo*-inositol as a starting point, the creation of an enormous range of molecules with different cellular functions is enabled.

Myo-inositol (1,2,3,4,5,6-cyclohexanol), the most copious inositol in nature, was discovered by a German medical scientist, Johann Joseph Scherer. It represents just one of the nine possible inositol isomeric isoforms; the other isoforms are: *cis*-, *epi*-, *allo*-, *muco*-, *neo*-, *D-chiro*(+)-, *L-chiro*(-)-, and *scyllo*-inositol (Scherer, 1850). All isomers are mesomeric forms aside from the enantiomeric *chiro*-inositol.

The special chair conformation of *myo*-inositol contains one single axial (assigned to position 2) and five equatorial hydroxyl moieties. The inner mirror symmetry of the molecule is due to the presence of this isomerism. The mirror plane contains the 2- and the 5-hydroxyl C-O bonds and normally stands perpendicular to the ring with a chair conformation (**Figure 1**). A large set of mesomeric and enantiomeric derivates is produced when carrying substituents of the ring hydroxyls in this particular structure.

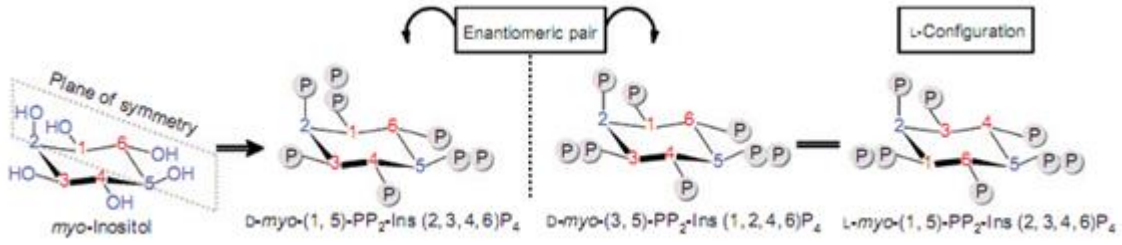

Figure 1. *Nomenclature of inositol phosphates (Wundenberg and Mayr, 2012).*

The success of this vast family is founded on the stereochemistry of *myo*-inositol itself. The orientation of the hydroxyls around the *myo*-inositol permits the phosphorylation of the

cyclohexane ring in a series of combinations which can give up to 63 stereo-chemically distinctive forms (**Table 1**). A great part of them has been shown to be of biological significance.

	Number of phosphates at *myo*-inositol or number of pyrophosphates at *myo*-$InsP_6$						
	1	2	3	4	5	6	Total
Total isomers	6	15	20	15	6	1	63
Mesomeric	2	3	4	3	2	1	15
Enantiomeric	2×2	2×6	2×8	2×6	2×2	0	48
HPLC separable	4	9	12	9	4	1	39

Table 1. *Number of all mathematically possible myo-inositol phosphate isomers (Wundenberg and Mayr, 2012).*

Agranoff was the first to suggest the use, for the relaxed rule for numbering of substituted inositols, of a 'turtle with head up' concept to symbolize the inositol ring, where the right forelimb is assigned to 1-, the head to 2-position, and, by moving counterclock-wise around the turtle's limbs, the tail is at the 5-position (Agranoff, 1978) (**Figure 2**).

Until that time, the standard IUPAC system for carbohydrates was used with the D/L-notation for pairs of enantiomers following the 'lowest number rule' (NC-IUB, 1989).

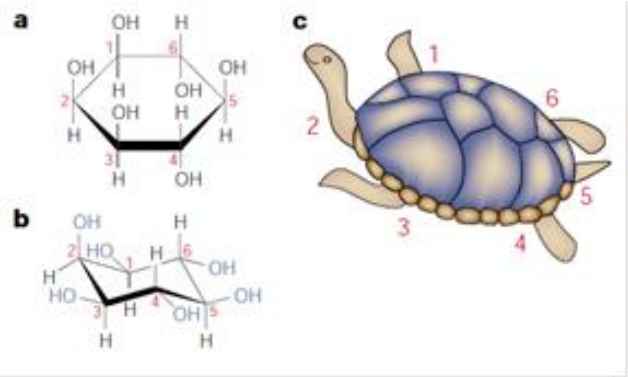

Figure 2. *Agranoff's turtle. (a) Shows myo-inositol as a Haworth projection and (b) shows a more accurate representation of the 'chair' structure that Agranoff noted is similar to a turtle (c) (Irvine and Schell, 2001).*

The history of inositol phosphates starts at the beginning of the 20th century, however, this research area almost disappeared in the successive decades. A noticeable breakthrough came in the 1980s. Inositol-1,4,5-trisphosphate, Ins(1,4,5)P_3 or IP_3, was established as a phosphoinositide-derived second messenger that regulates the release of Ca^{2+} from intracellular stores (Streb et al., 1983).

This discovery was the first to demonstrate the importance of inositol phosphates. Subsequently, other inositol phosphate isomers were identified whose functions have been partially characterized. The variety of soluble inositols varies from unphosphorylated *myo*-inositol to the fully phosphorylated inositol hexakisphosphate (also named IP_6 or phytic acid) and beyond (Irvine and Schell, 2001).

The signaling roles for inositol polyphosphates are very complex in all eukaryotic organisms; in fact IP_3 represents the predecessor of a large range of inositol polyphosphates (Irvine and Schell, 2001) (Resnick and Saiardi, 2008). A characteristic of these molecules is their duality of function, acting as transient metabolites in the synthetic pathways of further or less phosphorylated inositol species and in addition as signaling molecules themselves (Resnick and Saiardi, 2008) (Saiardi and Cockcroft, 2008).

Although the inositol polyphosphates are implicated in different aspects of cell biology, from plasma membrane ion channel regulation to nuclear mRNA export, it has been hard to identify detailed signaling pathways for these molecules (Bennett et al., 2006).

Just 10 years after the discovery of the function of IP_3, the field was ignited again by the discovery that more than six phosphates can be bound to the six-carbon inositol ring, demonstrating the existence of pyrophosphate groups. This finding has been attributed to two papers, from two different research groups, both published in the Journal of Biological Chemistry in early 1993 (Menniti et al., 1993) (Stephens et al., 1993). In the years since their discovery, these molecules have been found in every eukaryote, from yeast to mammalian neurons (Bennett et al., 2006).

IP_6 is the precursor of the best characterized inositol pyrophosphates IP_7 (or PP-IP_5; 5-diphosphoinositol pentakisphosphate) and IP_8 (or $(PP)_2$-IP_4; bisdiphosphoinositol tetrakisphosphate). Respectively, these molecules have seven or eight phosphate groups attached to the six-carbon inositol ring and as a result have one and two pyrophosphate moieties (**Figure 3**).

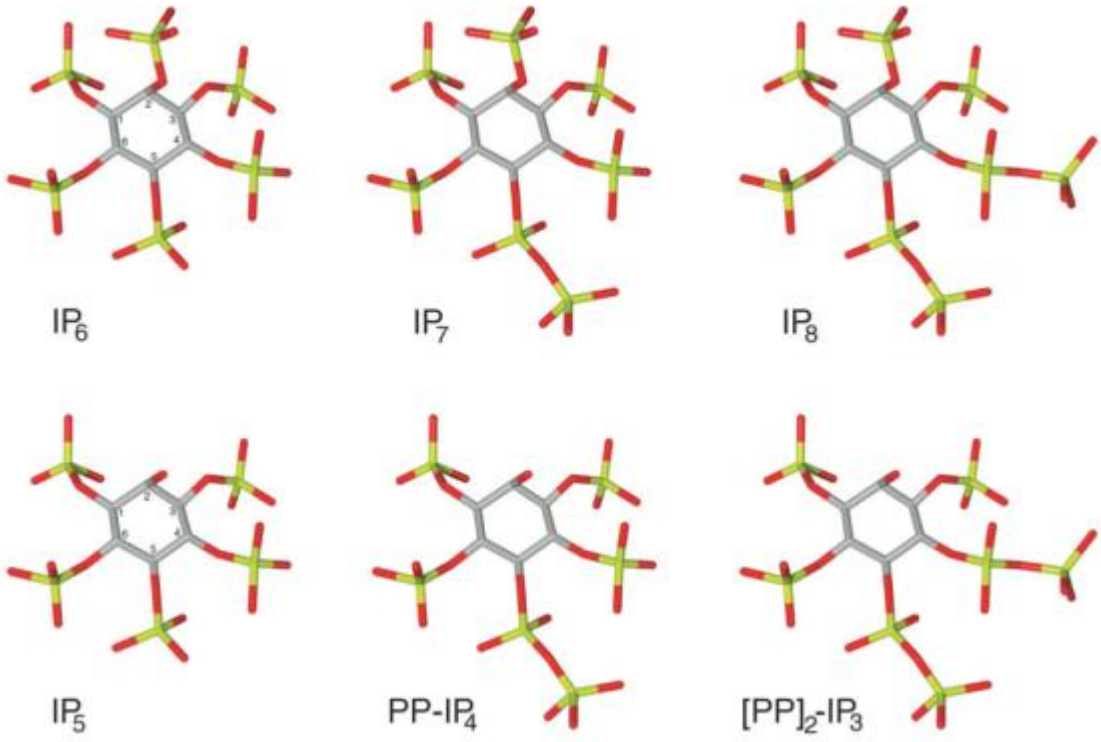

Figure 3. *The figure shows the chemical structure of IP_6 with its pyrophosphate derivates IP_7 and IP_8, as well as IP_5, with its derived pyrophosphates PP-IP_4 and $[PP]_2$-IP_3 (Bennett et al., 2006).*

At the moment, even if the *pyro*-nomenclature is generally used, it is important to note that the correct IUPAC definition for this moiety is *diphospho*-, so the correct chemical name of IP_7 is diphosphoinositol pentakiphosphate (PP-IP_5). The different nomenclatures that indicate the scientific name and the common name of these molecules are shown below (**Table 2**).

Common name	IUPAC Nomenclature	Alternative name	Isomeric forms
IP_6	Inositol hexakisphosphate $InsP_6$	phytic acid	
IP_7 $PP\text{-}IP_5$	Diphosphoinositol pentakisphosphate $PP\text{-}InsP_5$	$InsP_7$	$1PP\text{-}IP_5$ $5PP\text{-}IP_5$
IP_8 $(PP)_2\text{-}IP_4$	Bis-diphosphoinositol tetrakisphosphate $(PP)_2\text{-}InsP_4$	$InsP_8$	$1,5PP\text{-}IP_4$ Mammal $5,6PP\text{-}IP_4$ *D. discoideum*
IP_5	Inositol pentakisphosphate $Ins(1,3,4,5,6)P_5$	$InsP_5$	
$PP\text{-}IP_4$	Diphosphoinositol tetrakisphosphate	$PP\text{-}InsP_4$	$(1/3)PP\text{-}IP_4$ $5PP\text{-}IP_4$
$(PP)_2\text{-}IP_3$	Bis-diphosphoinositol trisphosphate	$(PP)_2\text{-}InsP_3$	

Table 2. *This table summarizes the nomenclature of the inositol pyrophosphates, with the correct IUPAC nomenclature, the alternative names infrequently present in the literature, and the identified biological isomers (Wilson et al., 2013).*

In eukaryotic cells, IP_6 is the most abundant inositol polyphosphate with a concentration in mammalian cells in the range of 10-60µM (Pittet et al., 1989) (Szwergold et al., 1987) and up to 0.7mM in slime moulds such as *Dictyostelium discoideum* (*D. discoideum*) (Martin et al., 1987) (Laussmann et al., 2000). In general, IP_6 has housekeeping functions as a phosphate storage molecule and as an antioxidant (Raboy, 2003) (Shears, 2001), and in addition is a signaling molecule that is involved in the regulation of vesicular trafficking (Shears, 2001) as well as quite in a lot of nuclear events (York et al., 1999) (Shears, 2001).

IP_7 and IP_8 are present in all eukaryotic cells. In mammalian cells, these molecules are present in sub-micromolar amounts, representing less than 5% of their precursor IP_6 (Bennett et al., 2006). Though the inositol pyrophosphate species levels are low and constant, this concentration hides an extraordinary turnover that has been calculated (using fluoride inhibition of phosphatases in mammalian cells) to convert up to 50% of the IP_6 pool every hour to its pyrophosphorylated derivatives (Menniti et al., 1993). This most probably reveals an important signaling function in the cell.

In contrast to mammalian cells, *D. discoideum* has IP_7 and IP_8 levels in the 100–200mM range (Laussmann et al., 2000), and the structures of these molecules has been elucidated by $^{1}H\text{-}^{31}P$ 2D NMR spectroscopy (Laussmann et al., 1996) and isomeric analysis using stereo-specific inositol phosphatases (Laussmann et al., 1997).

The results revealed a single IP_8 isomer present as 5,6-$[PP]_2$-IP_4, and two IP_7 isomers, 5-PP-IP_5 and 6-PP-IP_5 (Albert et al., 1997), with a relatively higher abundance *in vivo* of the 6-pyrophosphorylated species. The IP_8 species from another amoeba, *Polysphondylium pallidum*, has been identified as 1,5-$[PP]_2$-IP_4 (Laussmann et al., 1998), while an IP_7 species from *Entamoeba histolyticaas* was found to be 5-PP-IP_5 (Martin et al., 2000).

Consequently, the results from structural analyses have shown that the inositol pyrophosphates are structurally different and may also suggest that organisms possess various inositol pyrophosphate species with diverse functions.

2. Synthesis: kinases and phosphatases

In *Saccharomyces cerevisiae* (*S. cerevisiae*), the yeast experimental model, the synthesis of inositol phosphates begins with the well-known second messenger IP_3 (**Figure 4**) that is the product of cleavage of the lipid $PI(4,5)P_2$ by phospholipase C (Mikoshiba et al., 1993). Subsequent to liberation from its diacyl glycerol (DAG) tail, this molecule can be dephosphorylated to *myo*-inositol, or it can be additionally phosphorylated to the completely phosphorylated IP_6 ring and further, to form the inositol pyrophosphates IP_7 and IP_8 (**Figure 4**) (Laussmann et al., 1998).

While *S. cerevisiae* synthesizes inositol phosphates by this lipid path (Stephens and Irvine, 1990), *D. discoideum* synthesizes IP_6 by the cytosolic path. In this amoeba phospholipase C activity is not necessary to synthesize the higher phosphorylated inositols, because the synthesis happens directly from *myo*-inositol to IP_6 (**Figure 4**) (Stephens and Irvine, 1990).

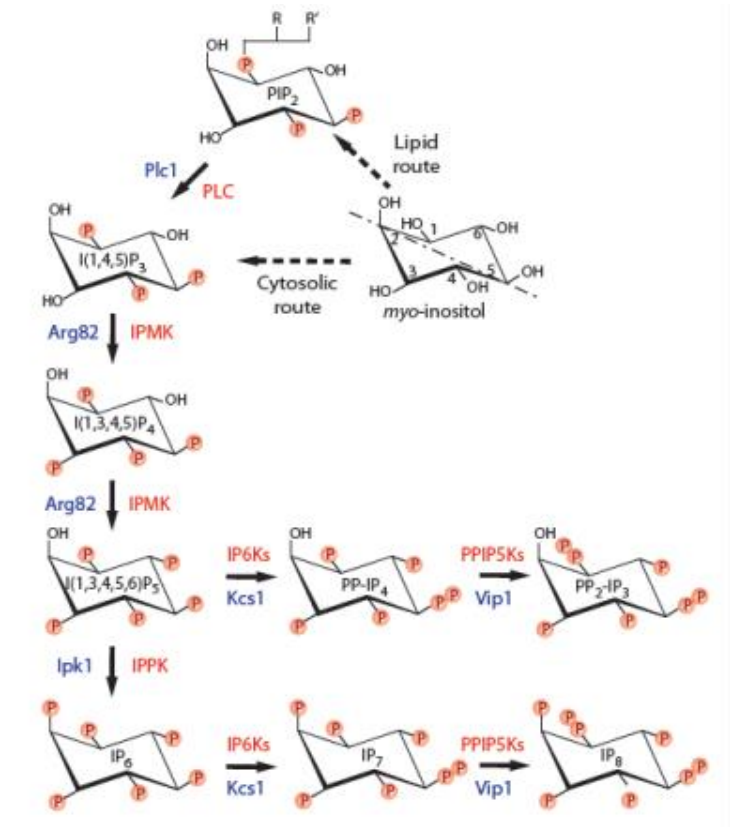

Figure 4. *This linear pathway shows the production of inositol pyrophosphates starting from myo-inositol. In S. cerevisiae this occurs via the lipid route, whereas in D. discoideum they are produced by the cytosolic route (Wilson et al., 2013).*

Two different classes of enzymes are able to synthesize inositol pyrophosphates: the IP_6 kinases (IP6K) and the PP-IP_5 kinases (PPIP5K), *Kcs1* and *Vip1* respectively in *S. cerevisiae*. The difference between these enzymes consist of a difference in catalytic activity against different positions on the ring, IP6Ks place a phosphate group at the β position of carbon 5 on the fully phosphorylated IP_6 ring (Draskovic et al., 2008), whereas the PPIP5Ks phosphorylate position 1 (Lin et al., 2009) (**Figure 4**).

In mammalian cells, the isomeric form of IP_8 that is present has been identified as 1,5-PP-IP_4 (Chakraborty et al., 2011) whereas in *D. discoideum* the 5,6-PP-IP_4 isomer of IP_8 is present (Chakraborty et al., 2011), probably because the two metabolisms are different (**Figure 4**).

In vitro, PPIP5Ks do not act on the main inositol pentakisphosphate isomer, I(1,3,4,5,6)P_5, while the IP6K enzymes are capable of phosphorylating this isomer, mostly but not completely at the enantiomeric positions (1,3), producing (1/3)PP-IP_4. Further phosphorylation by IP6K or PPIP5K can generate $(PP)_2$-IP_3 (Wang et al., 2011).

However, *in vivo*, it has been shown that yeast *Kcs1* generates inositol pyrophosphate even using IP_3 and IP_4 (Seeds et al., 2005). Meanwhile, *in vitro* the IP6Ks are also able to generate a tri-phosphate PPP-IP_5 form of 'IP_8' (Draskovic et al., 2008).

The high conservation of IP6Ks has facilitated not only the identification of these enzymes from different organisms, but also helped to identify another family of inositol polyphosphate kinases, known as inositol polyphosphate multi-kinases (IPMKs). These enzymes are able to phosphorylate IP_3 and IP_4 isoforms as well as phosphorylating the phosphoinositide lipid PtdIns(4,5)P_2 to PtdIns(3,4,5)P_3.

Consequently, the IP6Ks, IMPKs and IP_3-3Ks belong to an inositol polyphosphate kinase family, the IPKs that generated from a common ancestor. The most important characteristic of this family is the presence of the conserved PxxxDxKxG motif in the inositol-binding region (Bennett et al., 2006). Phylogenetic analysis of their sequences indicates that in fact IP6Ks are the most ancient members of this family (**Figure 5**).

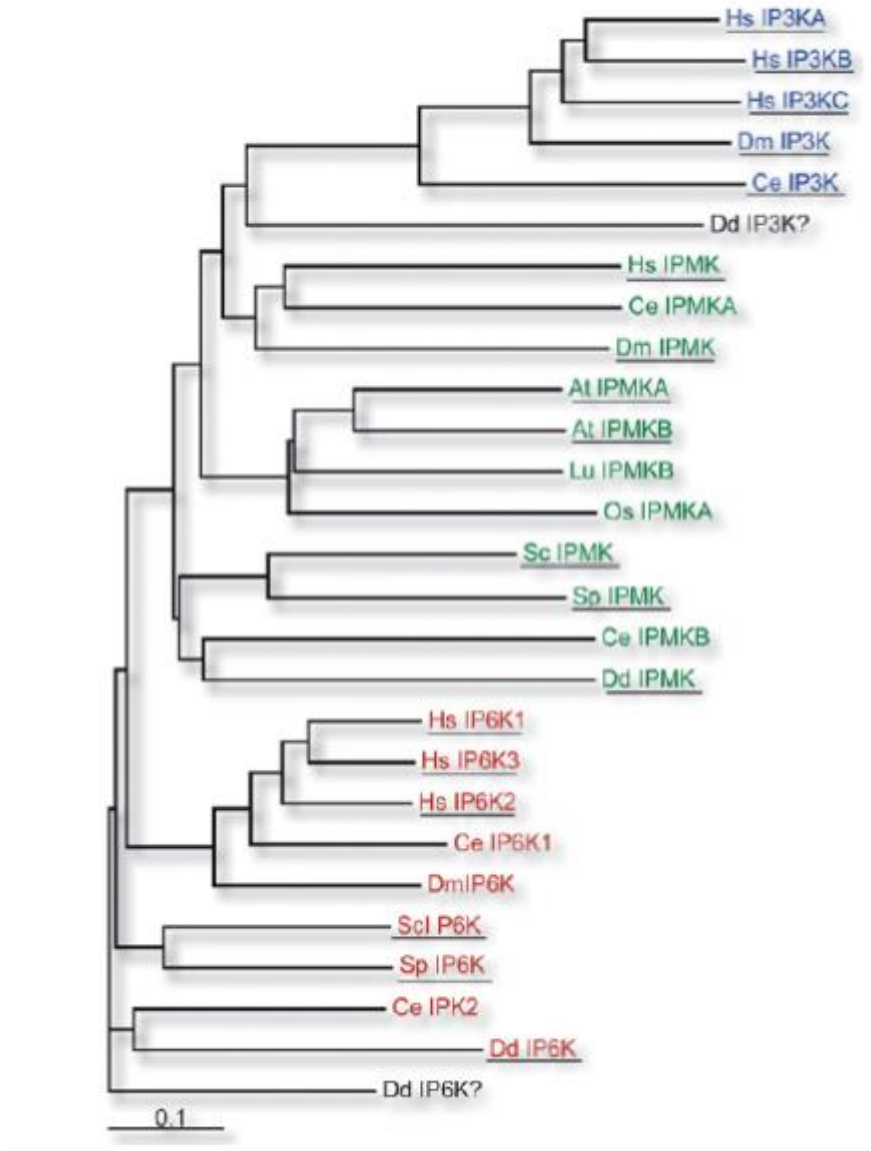

Figure 5. *Phylogenetic tree of IPK proteins family members (Bennett et al., 2006).*

In addition to the consensus PxxxDxKxG motif, all three family members share a common carboxy-terminal catalytic domain containing the conserved SSLL and IDF motifs (El Bakkoury et al., 2000) (Irvine and Schell, 2001). There is an extra 30 amino acid residue insertion in the inositol binding domain of IP_3-3Ks over IPMK and IP6Ks, while IPMK has a more open binding domain which corresponds to its greater substrate versatility (Holmes and Jogl, 2006). There is also a large 129 amino acid insert in the N-terminal region of the IP_6 kinases that may be involved in the specific regulation of this enzyme (**Figure 6**).

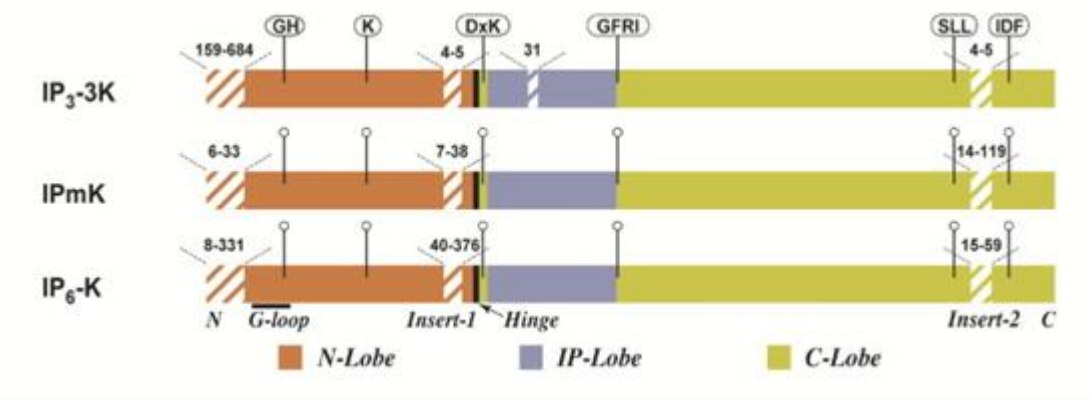

Figure 6. *Schematic diagram of common IPK catalytic domain structural elements. The three major subdomains of the IPKs are indicated with different colors. Hatched lines signify non-conserved insert regions, and the numbers over these regions indicate the range in the number of residues observed among all identifiable IPKs. Flagged regions show conserved motifs present in most IPK members (Gonzáles et al., 2004).*

The IP6Ks were first purified in Solomon Snyder's laboratory (Voglmaier et al., 1996). Three mammalian genes IP6K1, 2 and 3 were identified, one of which, IP6K2, had previously been identified as PiUS (inorganic phosphate uptake stimulator) (Voglmaier et al., 1996) (Saiardi et al., 2001). *In vitro*, all three mammalian IP6Ks as well as the yeast *Kcs1* are capable of phosphorylating IP_6 to IP_7, as well as IP_5 to PP-IP_4 (Saiardi et al., 1999).

IP6K1 possesses high amino acid similarity in a number of different species, for example 99% between mouse and rat and 95% between rat-human and mouse-human. The human gene is found on chromosome 3 (3p21.3) and codes for a 50-kDa protein. Studies have shown strong levels of expression in different mouse tissues such as brain and testis in addition to pancreatic β-cells (Illies et al., 2007), with a weak expression in heart, kidney, liver, lung and spleen (Saiardi et al., 1999).

IP6K2 has also been mapped to chromosome 3 (3p21.31) and this gene encodes for a protein of ~49-kDa. By alternative splicing two different variants have been identified that lack most of the C-terminal part of the whole protein. Northern blot analysis has shown a tissue distribution which is highest in brain and lung and lower in liver, kidney, and testis (Saiardi et al., 1999).

IP6K3 is located on chromosome 6 (6p21.31), has a smaller mass (46-kDa) and is most enriched in the brain where its levels resemble that of IP6K1 and IP6K2 (Saiardi et al., 2001).

IP6K3 shows 50 and 45% sequence identity to IP6K1 and IP6K2, respectively and possess a less acidic character than the other two enzymes. It has been shown by over-expression studies that IP6K2 is exclusively nuclear, IP6K3 is predominant in the cytoplasm, and IP6K1 displays comparable nuclear and cytosolic densities (Saiardi et al., 2001).

All these proteins possess a similar structure nevertheless showing some differences (**Figure 6**). In fact, it is not clear how protein-protein interactions occur and/or the regions where these connections happen. These proteins possess diverse binding partners such as GRAB (Luo et al., 2001), heat-shock protein 90 (HSP90) (Chakraborty et al., 2008) and tumor necrosis factor receptor-associated factor 2 (TRAF2) (**Figure 7**).

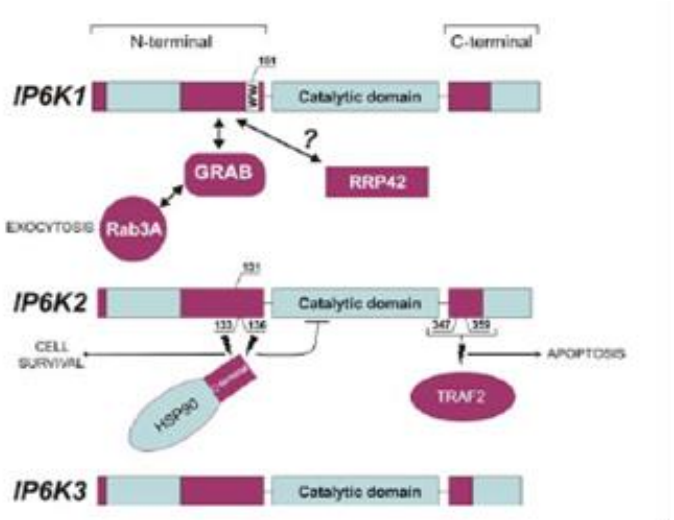

Figure 7. *IP6Ks showing basic structure of proteins. In blue the similarities between the proteins are shown, while purple shows the differences (Barker et al., 2009).*

In 2007 the York laboratory identified the second class of kinases: the yeast enzyme *Vip1* (Fridy et al., 2007). It is able to phosphorylate at the 1/3 enantiomeric positions generating 1/3PP-InsP_5 or 1/3,5(PP_2)-InsP_4 from IP_6 and 5PP-InsP_5 respectively (Lin et al., 2009). Two mammalian homologues, PPIP5K1 and PPIP5K2, were also identified (Shears et al., 2013). These proteins do not belong to the inositol phosphate kinase family; they possess two different domains: kinase domain and histidine acid phosphatase-like domain in the C terminal portion of the protein.

It has been supposed that the phosphatase domain is responsible for the allosteric regulation of PPIP5K by IP_6 (Shears et al., 2013) but it is catalytically inactive. However, truncated PPIP5K constructs lacking the phosphatase domain show increased activity when over-expressed, indicating that this domain is active. It may antagonize the kinase domain, specifically dephosphorylating 1PP-IP_5, the IP_7 isomer produced by the kinase domain.

Although *in vitro*, PPIP5K can phosphorylate IP_6 to 1PP-IP_5 (Shears et al., 2013), while *in vivo*, this activity is masked by phosphatase activity and cannot be easily detected, suggesting that the major physiological target of the PPIP5Ks is IP_7. This is further supported by the increase in levels of IP_7 in *vip1Δ* mutants, whilst levels of IP_6 remain unchanged (Shears et al., 2013).

Phosphatases are enzymes that show the reverse capability of kinases; in fact they are able to hydrolyze pyrophosphate groups. Two different proteins have been discovered: MIPP (multiple inositol polyphosphate phosphatase) and DIPP (diphosphoinositol phosphate phosphohydrolase). DIPPs were first cloned (Safrany et al., 1998) before the IP6Ks but there is at the moment no more than modest information on their physiological role.

MIPP is located in the endoplasmic reticulum (Ali et al., 1993) and is able to hydrolyze the 5β-phosphates *in vitro*, however it does not play a role in inositol pyrophosphate degradation *in vivo* (Shears et al., 1995).

In human and mouse, there are five different DIPP isoforms (1, 2α, 2β, 3α, 3β) while there is only one DIPP in *S. cerevisae* (Ddp1p/Yor163w) (Safrany et al., 1999) and one in *S. pombe* (Aps1) (Ingram et al., 2003).

DIPP1 is the product of the NUDT3 gene. DIPP2α and DIPP2β, only differing by one amino acid (glutamine Q86), are the products of the NUDT4 gene (Caffrey et al., 2001). DIPP3α and DIPP3β are the products of the NUDT10 and NUDT11 genes, respectively (Leslie et al., 2002) (Hidaka et al., 2002).

DIPP3α is also called hAsp2 whilst DIPP3β is called hAsp1. These two proteins are identical in mouse while in humans differ through one amino acid (Hua et al., 2003).

DIPP1 and DIPP2 are expressed in a large range of tissues (Chu et al., 2004) (Hua et al., 2001) whereas DIPP3 shown a more restricted expression in fact has been found in testis, liver, kidney and brain (Hua et al., 2003).

DIPPs have a common catalytic site used to hydrolyze inositol pyrophosphates and diadenosine polyphosphates, as well as PRPP (5-phosphoribosyl 1-pyrophosphate pyrophosphatase) (Fisher et al., 2002) that is not a substrate for these enzyme in vivo (Hidaka et al., 2002) (**Figure 8**).

Between these enzymes, DIPP1 is the most catalytically active (Hua et al., 2003), DIPP2α is more active than DIPP2β, probably because they differ by one amino acid that has a strong influence on catalytic function (Caffrey et al., 2000), whereas DIPP3α and DIPP3β are the least active against inositol pyrophosphates (Leslie et al., 2002).

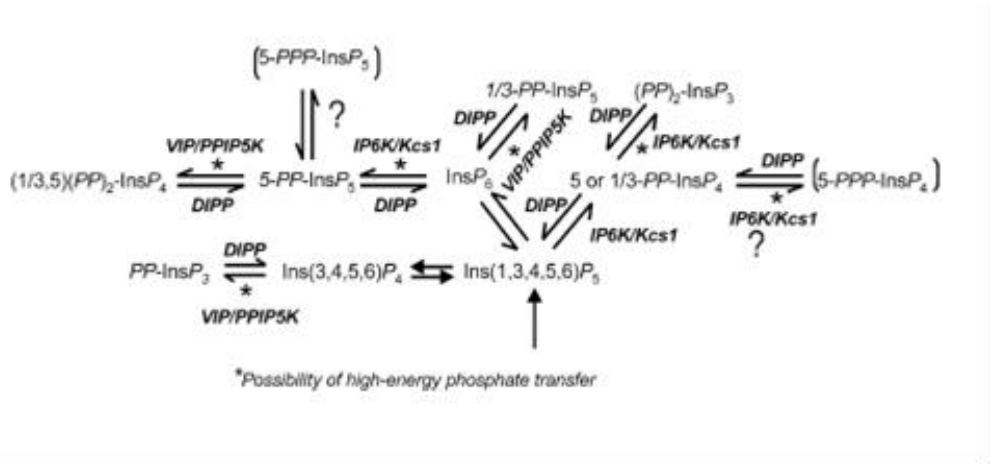

Figure 8. *Metabolic interrelationships between inositol pyrophosphates and enzymes responsible for their synthesis and degradation (Barker et al., 2009).*

The DIPPs hydrolyze their substrate in a site-specific order, indeed in 1,5PP_2-IP_4 they hydrolyze first position 1 and then position 5 (Caffrey et al., 2000). For complete activity, DIPPs require a free Mg^{2+} of 1.5-2mM (Safrany et al., 1999), on the contrary fluoride inhibits their activity with a K_i around 10μM (Leslie et al., 2002).

3. Functions of inositol pyrophosphates

Inositol pyrophosphates are recognized to control a variety of cellular activities such as apoptosis (Morrison et al., 2005), telomere maintenance (Saiardi et al., 2005) (York et al., 2005) and vesicular trafficking (Saiardi et al., 2002). This variety of activities underlines the biological significance of these molecules though until recently it was not clear how these molecules controlled all these cellular functions.

It was published that inositol pyrophosphates play a role as metabolic messengers (Shears, 2009), regulators of cell homoeostasis (Wunderberg and Mayr, 2012) and regulators of cellular energetic metabolism (Szijgyarto et al., 2011). These functions are summarized in the following figure (**Figure 9**) in which is shown the link between inositol pyrophosphates and the metabolism at molecular, cellular and organismal levels.

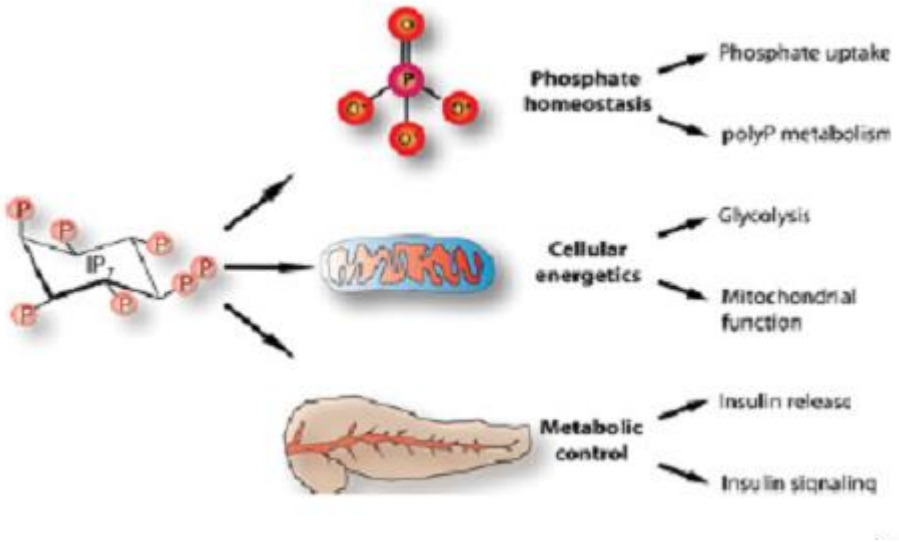

Figure 9. *Diverse controls that inositol pyrophosphates (IP_7) perform on the metabolism at different levels (Wilson et al., 2013).*

The synthesis of inositol pyrophosphates is linked to ATP levels for the reason that the IP6K enzymes show high affinity for ATP. Startlingly, it has been demonstrated that in cells that do not possess or cells that have low levels of inositol pyrophosphates that they have an increased cellular ATP concentration while ADP and AMP levels are reduced, producing an increase in the adenylate pool and to an increase in adenylate energy charge (AEC) (Szijgyarto et al., 2011).

On the contrary, in the wild-type yeast cells that shown increased levels of IP_7 since there is an over-expression of mammalian IP6K1, the concentration of ATP is decreased. In the yeast system it was revealed that protein pyrophosphorylation was influencing the interactions of the crucial yeast glycolytic transcription factors Gcr1, Gcr2 and Rap1 (Barbara et al., 2007). Pyrophosphorylation of Gcr1 decreases its capability to bind Gcr2, thus inhibiting the transcription of genes encoding glycolytic enzymes. Thus, the *kcs1Δ* yeast consumed glucose more rapidly than wild-type yeast (Szijgyarto et al., 2011).

Unexpectedly, in the *kcs1Δ* yeast given the increase in cellular ATP concentration, the mitochondria were malfunctioning. Generally, yeast produce energy and intermediates by fermentation, however it is possible to achieve mitochondrial metabolism/oxidative phosphorylation by providing just a non-fermentable carbon source. The *kcs1Δ* yeast are unable to grow in these conditions.

Instead, the high ATP level and the reduced oxygen consumption of $IP6K1^{-/-}$ MEFs compared with wild-type MEFs evidence that the regulation of cellular metabolism by inositol pyrophosphate is evolutionarily conserved. ATP availability is underpins virtually all other cellular activity.

In *D. discoideum* it has been shown that inositol pyrophosphates furthermore control chemotaxis (Luo et al., 2003). In wild-type cells, starvation and successive cAMP signaling and chemotaxis induces formation of a multicellular fruiting body. The *ip6k* knockout was more responsive to cAMP and aggregated more rapidly than wild-type cells responding to starvation (Luo et al., 2003).

These results suggest that in wild-type cells there is an antagonism between IP_7 and PIP_3 in binding the PH domain of Crac, a protein related to cAMP-dependent chemotaxis. During *D. discoideum* aggregation PIP_3 is not able to be the principal regulatory molecule, as deletion of every PI3K capable of producing PIP_3 did not inhibit chemotaxis to cAMP (Hoeller and Kay, 2007). Furthermore, as IP_7 influences energetic metabolism in addition to the adenine nucleotide level, the high level of ATP could lead to an increased cAMP concentration and then the more rapidly chemotaxic response observed in *D. discoideum ip6k* knockout.

In addition, it has been shown that inositol pyrophosphates are molecules involved also in the regulation of organismal metabolism. In pancreatic β-cells, the overexpression of IP6K1 or the addition of IP_7 generate induction of exocytosis (Illies et al., 2007). This result is confirmed by $IP6K1^{-/-}$ mouse characterization: it possesses weak levels of plasma insulin,

hypersensitivity to insulin and decrease in fatty tissue levels (defective mitochondria cannot synthesize the intermediates for fatty acid synthesis) (Hiltunen et al., 2010).

However, it has been shown that the interaction between the inositol pyrophosphates levels and AEC generates a link that regulates the connections between insulin and plasma glucose concentration.

Additionally, the IP6K2$^{-/-}$ mouse characterization has shown that IP6K2 could be the most important isoform in cell death regulation by inositol pyrophosphates. Particularly, seems that IP6K2 interacts with two different proteins, HSP90 and p53, by a via unknown and independent of inositol pyrophosphates synthesis (Koldobskiy et al., 2010).

Another important link is established between metabolism and aging (Passarino et al., 2010). It has been shown that high levels of IP_6 and IP_7 are present in hepatocytes from old wild-type mice but not in younger mice. Also, one probable link between metabolism and aging has been found in the telomere length; indeed shorter telomeres are associated with aging in mammals (Mather et al., 2011).

The *kcs1Δ* yeast has longer telomeres than wild-type whilst *ipk1Δ* yeast has shorter telomeres; (Saiardi et al., 2005) perhaps these results are due to Tel1 which is a telomere regulator inhibited by inositol pyrophosphates. Furthermore it has been supposed that inositol pyrophosphates can also influence other important proteins involved in DNA damage signaling/DNA repair (Lovejoy and Cortez, 2009) such as Ku protein (Ma and Lieber, 2002).

In recent years, it has been shown that inositol pyrophosphates are also able to regulate the process of DNA repair. In yeast, ROS signaling is generally studied using the exposure to exogenous agents for example H_2O_2, which causes DNA base modification, single- and double-strand breaks, and the formation of apurinic/apyrimidinic lesions (Letavayova et al., 2006). To generate DNA-damage, it is usually appropriate to use sub-lethal concentrations of H_2O_2 (Leroy et al., 2001).

Yeast mutants which are deficient in inositol pyrophosphates have a higher threshold of resistance to the lethal effects of H_2O_2, but not to other DNA-damaging agents. This specific resistance to H_2O_2 connects with a constant activation of Rad53 and as a result promotion of DNA repair mechanisms. Further it has been reported that H_2O_2 regulates higher inositide metabolism, producing a decrease in cellular levels of inositol pyrophosphates (Onnebo and Saiardi, 2009).

Inositol pyrophosphates also possess the ability to regulate phosphate metabolism (Saiardi, 2012). Inositol pyrophosphates regulate the access of phosphate into the cells (Norbis et al., 1997), suggesting that they could affect phosphate uptake either directly, for example stimulating a transporter, or indirectly by helping 'fixing' free phosphates in organic molecules.

Additionally, many hypotheses have been formulated to elucidate the biological link between phosphate, inositol pyrophosphates and *polyP* that is a linear polymer of phosphodiester bound. Indeed, the synthesis of *polyP* may be related to phosphate ingress into the cell. Inositol pyrophosphate control of energy metabolism (Szijgyarto et al., 2011) influences not only ATP levels but it can also change the total cellular balance of adenine nucleotides. The phosphate transfer reactions generally use ATP as a means of transport for the phosphate groups, so inositol pyrophosphate could influence phosphate metabolism by regulating the adenylate cellular pool. Moreover, the existence of a feedback mechanism that coordinates the metabolic balance between ATP, phosphate and inositol pyrophosphates has been suggested.

Inositol pyrophosphates could either contribute to the regulation of *polyP* synthesis, play a role in *polyP* degradation, or both. The analysis of yeast mutant that are not able to synthesize inositol pyrophosphates has shown a striking correlation between the lack of inositol pyrophosphates and the absence of *polyP* (Auesukaree et al., 2005) (Lonetti et al., 2011).

It has even been reported that increasing cellular IP_7 levels augments cell sensitivity to cell death. The phosphorylation of mammalian target of rapamycin (mTOR) was also depressed in cells that over-express IP6Ks, suggesting that the mTOR pathway regulates autophagosomes generated by IP6Ks. These results suppose that IP6Ks support autophagy and provoke caspase-independent cell death (Nagata et al., 2011).

Different experiments have been conducted to demonstrate the existence of a link between inositol pyrophosphates and autophagy in yeast. These results indicate that inositol phosphates are implicated in the regulation of autophagy, however the precise role of each inositol phosphate species in this process is not clear (Taylor et al., 2012).

4. Mechanism of action

To transduce signals, the inositol pyrophosphates may use two different mechanisms of action: binding (Lemmon, 2008) and pyro-phosphorylation (Bhandari et al., 2007). In cells, these two mechanisms are not exclusive but coexist. Usually, the first mechanism happens through the binding of small molecules to specific protein targets, such as cAMP to protein kinase A otherwise lipid hormone to specific receptors.

Inositol polyphosphates bind to several proteins containing specific domains such as PH (pleckstrin homology), PX (phagocyte oxidase homology) or FYVE (for Fab1, YOTB, Vac1 and EEA1) domains (Alcázar-Román and Wente, 2008). The best characterized mechanism of action in this area is the binding of IP_3 to its receptor (IP_3-receptor) that leads to an alteration of the tridimensional structure of the channel, which in turn allows Ca^{2+} efflux (Mikoshiba et al., 1993) (Irvine, 2003).

The similar mechanism of action has been theorized for inositol pyrophosphates that may also signal through allosteric interactions with proteins indeed, *in vitro*, IP_7 is able to bind several proteins such as AP3/AP180 (Saiardi et al., 2002), the Golgi coatomer (Ali et al., 1995) and the clathrin-assembly adaptors AP2 (Voglmaier et al., 1992). Further, IP_7 competes for binding to the *D. discoideum* chemotaxis protein Crac (cytosolic regulator of adenylate cyclase) and mammalian Akt (Luo et al., 2003).

The proteins that bind to IP_7 also bind to IP_6, though to a more modest extent, and IP_6 has been proposed to be the more essential ligand *in vivo* (Cremona and De Camilli, 2001). As the concentration of inositol pyrophosphates is low, a severe specificity of binding for IP_7 over IP_6 is required. To solve this problem it is possible to induce the IP_6 kinase activity inducing increase in the IP_7/IP_6 ratio.

However, the importance of binding as a mechanism of action has been confirmed by IP_7-mediated competition for the binding of $PI(3,4,5)P_3$ to the PH domain-containing CRAC that is consequently inhibitory to chemotaxis (Luo et al., 2003).

It was also revealed that IP_6 is only 1–2% as potent as IP_7, and then IP_7 is more likely to be the physiological binding partner during aggregation (Laussmann et al., 2000). IP_7 was found to bind to a variety of other PH-domain containing proteins, including, *in vitro*, mammalian Akt (Luo et al., 2003).

In addition, a further recent study demonstrated the inability of the PH-domain of phosphoinositide-dependent protein kinase 1 (PDK1) to bind IP_7 (Komander et al., 2004).

Allosteric interaction has been also suggested like a mechanism for controlling the Pho85/Pho80/Pho81 cyclin dependent kinase/cyclin/cyclin-dependent kinase inhibitor complex of the yeast *S. cerevisiae* (Lee et al., 2008). The binding of 1/3PP-IP_5, the IP_7 isomer generated by *Vip1*, to the Pho85/Pho80/Pho81 complex inhibits its action: the transcription factor Pho4 is now not hyper-phosphorylated by Pho85 so is able to go into the nucleus to activate the PHO pathway (Lee et al., 2007).

The second mechanism of action is the pyro-phosphorylation that occur by donation of the β-phosphate from the pyrophosphate group to proteins (Saiardi et al., 2004). The process of pyro-phosphorylation is due to the presence of a functional group: the pyro-phosphate group. Furthermore the mechanism of action is shown in the following figure (**Figure 10**) (Saiardi et al., 2004).

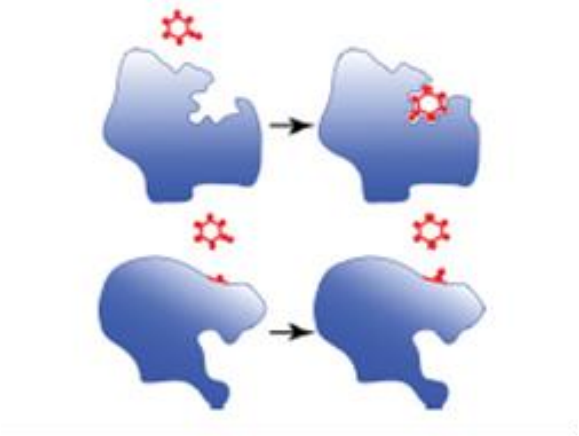

Figure 10. *The proposed mechanisms of action for inositol pyrophosphates: the direct binding mechanism when a protein target has a particular pocket able to distinguish IP_7 (upper panel) and the pyro-phosphorylation modification of a protein carried out by IP_7 (lower panel) (Wilson et al., 2013).*

In recent years, the pyrophosphate constituent of IP_7 has been shown to act as a phosphate donor to proteins, in a non-enzymatic and temperature-dependent reaction (Saiardi et al., 2004).

In yeast, have been identified three different potential IP_7 substrates: NSR1 (a nuclear protein implicated in ribosome assembly and export), YGR130c (protein with unknown function),

SRP40 (protein that acts as a ribosomal chaperone). All these proteins have regions of similar sequence, as everyone contains regions of serine residues surrounded by acidic residues.

Generally, proteins that are phosphorylated by IP_7 in eukaryotic cells are no longer phosphorylated if expressed in bacteria, indicating that substrate priming, across a post-translation modification, is an necessary requisite for IP_7-driven phosphorylation (York and Hunter, 2004).

Pyro-phosphorylation mediated by IP_7 may cause functional alterations in protein conformation and then may give rise to variations in the protein's interactions, activity or localization (Azevedo et al., 2009) (Szijgyarto et al., 2011). Further investigation into the mechanism of action of IP_7 will confidently provide insight into its regulation in the cell and coordination with further signaling pathways.

5. Physiological role

To study the physiological role of inositol pyrophosphates yeast cells that don't have IP6K enzymes (*kcsI*Δ) and consequently don't possess inositol pyrophosphates are generally used (Saiardi et al., 2002). Morphologically, these mutants are abnormal, suggestive of important functions for inositol pyrophosphates. The *kcsI*Δ mutants are bigger and grow slower than wild-type cells, and appear to be hypersensitive to salt stress however appear unaffected by osmotic challenge with sorbitol (Dubois et al., 2002).

Problems in cell wall integrity have also been observed as well as a disjointed vacuolar morphology (Saiardi et al., 2002). These findings suggest that inositol pyrophosphates play important functions in central cellular processes such as growth, endocytosis and response to stress.

In mammalian cells, where three different isoforms of IP6K and two different isoforms of PP-IP5K are present, it is more complicated to establish the effects of a lack of inositol pyrophosphates.

Therefore to elucidate which phenotypic abnormalities are related to the deficiency of inositol pyrophosphates further studies are needed to comprehend if these molecules are truly involved also in complex signaling functions in mammalian cells.

6. *D. discoideum* as a model to study inositol pyrophosphates

D. discoideum is a small soil-living amoeba that possesses a haploid genome having six completely sequenced chromosomes (Eichinger et al., 2005). Commonly referred to as slime mold, is a eukaryote that shifts from a collection of unicellular amoebae into a multicellular slug and then into a fruiting body within its lifetime. This organism also contains many proteins and molecular processes that were previously thought to be present only in metazoa. For example, the *D. discoideum* genome possesses 24 classes of protein kinase that are not present in the yeast *S. cerevisiae* (Annesley and Fisher, 2009), so the presence of these proteins in this amoeba proposes that they are derived from ancestral pathways abandoned in the yeast heredity. *D. discoideum* has an exclusively asexual lifecycle including four different stages: vegetative, aggregation, migration, and culmination (**Figure 11**).

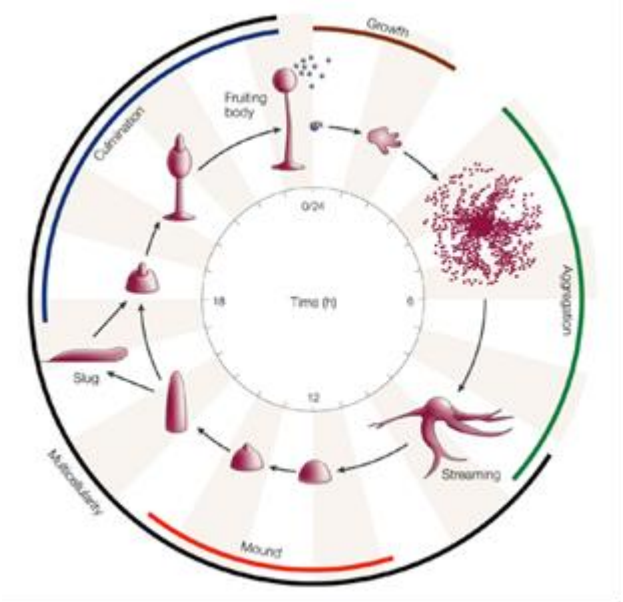

Figure 11. *The life cycle of D. discoideum begins as a vegetative amoeba and ends with the formation of the mature fruiting body (Fey et al., 2007).*

Developmental morphogenesis starts from single and vegetative amoebae and ends with the formation of the mature fruiting body, which contains diverse spores on top of a stalk. Myxamoebae hatch from the spores under warm and moist conditions. Throughout the vegetative stage, the myxamoebae divide by mitosis as they feed on bacteria. The bacteria secrete folic acid, attracting the myxamoebae. When the supply of bacteria is depleted, the myxamoebae go into the aggregation stage.

During aggregation, starvation starts the formation of a biochemical process involving glycoproteins and adenylyl cyclase (Gilbert, 2006). The glycoproteins permit cell-cell adhesion, and adenylyl cyclase produces cAMP that is secreted by the amoebas to attract adjacent cells to an inner location. Moving towards the signal, they impact into each other and stick together by the use of glycoprotein adhesion molecules.

The migration phase starts once the amoebas have produced a tight aggregate; the amoebas work together as a motile pseudo-plasmodium also known as a slug. The slug is about 2–4 mm long, composed of up to 100,000 cells (Cooper and Geoffrey, 2000), and is capable of movement by producing a cellulose scabbard in its anterior cells through which the slug shifts (Tyler, 2000).

The formation of different cell types is helped by cAMP and DIF (differentiation-inducing factor) (Tyler, 2000). The slug gets differentiated into pre-stalk and pre-spore cells that go to the anterior and posterior ends, respectively. Once established in an appropriate environment, the anterior end of the slug will create the stalk of the fruiting body and the posterior end will produce the spores of the fruiting body (Tyler, 2000). The culmination stage begins when the slug settles into one spot, the posterior end spreads out with the anterior end raised in the air, forming a structure looking like a 'hat'.

The anterior end of the 'hat' forms a cellulose tube, which allows the cells to move (Tyler, 2000). To obtain the mature fruiting body takes 8–10 hours (Tyler, 2000). The fruiting body is then capable of starting the entire cycle over again by releasing the mature spores that can be converted into myxamoebae.

Usually *D. discoideum* are capable of reproducing asexually but are still able to reproduce sexually if there are certain conditions. During aggregation, if two amoebae of different mating types are present in a dark and wet environment, they can combine to create an enormous cell that will phagocytizes the other cells in the aggregate furthermore collect the entire aggregate in a cellulose wall to defend it. This is also known as a macro-cyst where inside the enormous cell divides first through meiosis, then through mitosis to produce many haploid amoebae.

D. discoideum is commonly used as a model organism not just because has a simple life cycle but also because it possesses a restricted number of cell types and the growth is typically very rapid (Tyler, 2000).

It is used to study different cellular processes such as cell differentiation, chemotaxis and programmed cell death or other aspects of development including phagocytosis and signal transduction. These processes and aspects of development are not present or too complex to view easily in other model organisms, so these features make *D. discoideum* a good candidate model organism (Nag and Tikhonenko, 2008).

Furthermore, *D. discoideum* is often used as a model to study inositol polyphosphate signaling for the reason that it has high levels of IP_7 and IP_8, important in the initial identification of their structures and functions (Stephens et al., 1993). The inositol pyrophosphate levels are not high during the vegetative state but they increase dramatically in the aggregation state and chemotaxis, which depend on cAMP signaling (Luo et al., 2003), reaching the equivalent levels of IP_6 (Laussmann et al., 2000).

In *D. discoideum* 7 genes belonging to the IPK family are present. One of these genes, namely I6KA was identified as an IP6K (Luo et al., 2003). The activity of this enzyme has not been tested in vitro, however destroying I6KA by homologous recombination produced a dramatically decrease in the inositol pyrophosphate levels. Regarding the phenotype, mutant cells possess similar shape and size; in addition they show equal growth rate comparate to wild-type cells. However during starvation, aggregation occurs that is faster in the mutants than in wild-type cells. Mutants exhibit high sensitivity to chemotactants, responding rapidly to low concentrations of cAMP. These results suggest that in the mutants there is an alteration of chemotactic pathways (Luo et al., 2003).

The translocation of CRAC to the membrane, mediated by the PH domain, is an indispensable step for directional sensing, since either decreasing the amount of $PI(3,4,5)P_3$, by disrupting PI3K genes, or abnormally increasing $PI(3,4,5)P_3$ levels by disruption of PTEN decreases the ability of cells to orientate and to move in response to chemotactic gradients (Iijima and Devreotes, 2002). The lack of IP_7 in the null mutant would free the CRAC-PH domain to bind to $PI(3,4,5)P_3$, and its translocation to the membrane would consequently increase.

In addition to being an excellent experimental model, during *D. discoideum* development the most dramatic modulation of the levels of inositol pyrophosphates has been seen (Stephens et al., 1993).

In mammalian cells, it has been possible to use fluoride to dramatically modulate the levels of inositol pyrophosphates, and in addition to discover that 50% of IP_6 is converted, every hour, to IP_7. Because IP_7 levels only represent 2-8% of IP_6 concentration, IP_7 itself is turning over

many times each hour (Glennon and Shears, 1993) (Menniti et al., 1993). These results suggest that inositol pyrophosphates are signaling molecules with 'molecular switch activity' though their physiological significance remains unknown. Fluoride inhibits the DIPP phosphohydrolases and is a common phosphatase inhibitor with many effects on cell signaling (Bollen and Stalmans, 1988); the specific effect on inositol metabolism is unclear. Overall these results suggest that in mammalian cells inositol pyrophosphates are dynamic molecules that turnover very rapidly, and that cells spend a lot of energy to keep their levels constant.

However, the best example of modulation of inositol pyrophosphate levels has been observed in *D. discoideum*, where during starvation-induced aggregation it is possible to observe a considerable increase in the levels of IP_7 and IP_8 (Laussmann et al., 2000). During starvation cAMP is secreted that induces elevation in the IP_7 and IP_8 levels (Luo et al., 2003).

In fact, a decrease in extracellular inorganic phosphate concentration led to a dramatic rise in the intracellular levels of inositol pyrophosphates, in particular IP_7 (Mulugu et al., 2007).

More studies are needed to elucidate this result that is controversial as usually reduction of phosphate causes a reduction of ATP, which is fundamental for the synthesis of inositol pyrophosphates (Boer et al., 2010).

7. Plan of the thesis

Chapter II reports one manuscript (PlosOne – In Press) aimed at investigating the inositol pyrophosphate metabolism in *D. discoideum*. In particular, in the manuscript 'Analysis of *Dictyostelium discoideum* inositol pyrophosphate metabolism by gel electrophoresis' we report results obtained using polyacrylamide gel electrophoresis (PAGE) to resolve and detect inositol pyrophosphate species in this amoeba. We have achieved three major findings:

- *D. discoideum* possesses three bands correspond to IP_6 and its derivative inositol pyrophosphates, IP_7 and IP_8;
- there is another band that correspond to IP_9;
- this amoeba possesses three different IP_5 isomers;
- during development there is a three times increase of inositol pyrophosphates and not the 25 times previous reported;
- cAMP does not induce inositol pyrophosphates synthesis.

In the thesis is also included an appendix which reports the integral version of the published paper (Montesanto et al., 2013), 'Common polymorphisms in nitric oxide synthase (NOS) genes influence quality of aging and longevity in humans' Biogerontology 14(2):177-86.

REFERENCES

1. Agranoff, B. W., (1978) Cyclitol confusion. Trends Biochem Sci 3, N283-N285.
2. Alcázar-Román, A. R., Wente, S. R., (2008) Inositol polyphosphates: a new frontier for regulating gene expression. Chromosoma 117, 1-13.
3. Albert, C., Safrany, S. T., Bembenek, M. E., Reddy, K. M., Reddy, K., Falck, J., Bröcker, M., Shears, S. B., Mayr, G. W., (1997) Biological variability in the structures of diphosphoinositol polyphosphates in *Dictyostelium discoideum* and mammalian cells. Biochem J 327, 553-560.
4. Ali, N., Craxton, A., Shears, S. B., (1993) Hepatic Ins(1,3,4,5)P_4 3-phosphatase is compartmentalized inside endoplasmic reticulum. J Biol Chem 268, 6161-6167.
5. Ali, N., Duden, R., Bembenek, M. E., Shears, S. B., (1995) The interaction of coatomer with inositol polyphosphates is conserved in *Saccharomyces cerevisiae*. Biochem J 310, 279-284.
6. Annesley, S. J., Fisher, P. R., (2009) *Dictyostelium discoideum* – a model for many reasons. Mol Cell Biochem 329, 73-91.
7. Auesukaree, C., Tochio, H., Shirakawa, M., Kaneko, Y., Harashima, S., (2005) Plc1p, Arg82p, and Kcs1p, enzymes involved in inositol pyrophosphate synthesis, are essential for phosphate regulation and polyphosphate accumulation in *Saccharomyces cerevisiae*. J Biol Chem 280, 25127-25133.
8. Azevedo, C., Burton, A., Ruiz-Mateos, E., Marsh, M., Saiardi, A., (2009) Inositol pyrophosphate mediated pyrophosphorylation of AP3B1 regulates HIV-1 Gag release. Proc Natl Acad Sci U S A 106, 21161-21166.
9. Barbara, K. E., Haley, T. M., Willis, K. A., Santangelo, G. M., (2007) The transcription factor Gcr1 stimulates cell growth by participating in nutrient-responsive gene expression on a global level. Mol Genet Genomics 277, 171-188.
10. Barker, C. J., Illies, C., Gaboardi, G. C., Berggren, P. O., (2009) Inositol pyrophosphates: structure, enzymology and function. Cell Mol Life Sci 66, 3851-3871.
11. Bhandari, R., Saiardi, A., Ahmadibeni, Y., Snowman, A. M., Resnick, A. C., Kristiansen, T. Z., Molina, H., Pandey, A., Werner, J. K. Jr, Juluri, K. R., Xu, Y., Prestwich, G. D., Parang, K., Snyder, S. H., (2007) Protein pyrophosphorylation by inositol pyrophosphates is a posttranslational event. Proc Natl Acad Sci U S A 104, 15305-15310.
12. Bennett, M., Onnebo, S. M., Azevedo, C., Saiardi, A., (2006) Inositol pyrophosphates: metabolism and signaling. Cell Mol Life Sci 63, 552-564.
13. Boer, V. M., Crutchfield, C.A., Bradley, P. H., Botstein, D., Rabinowitz, J. D., (2010) Growth-limiting intracellular metabolites in yeast growing under diverse nutrient limitations. Mol Biol Cell 21, 198-211.
14. Bollen, M., Stalmans, W., (1988) Fluorine compounds inhibit the conversion of active type-1 protein phosphatases into the ATP Mg-dependent form. Biochem J 255, 327-333.
15. Caffrey, J. J., Darden, T., Wenk, M. R., Shears, S.B., (2001) Expanding coincident signaling by PTEN through its inositol 1,3,4,5,6-pentakisphosphate 3-phosphatase activity. FEBS Lett 499, 6-10.

16. Caffrey, J. J., Safrany, S. T., Yang, X., Shears, S. B., (2000) Discovery of molecular and catalytic diversity among human diphosphoinositol-polyphosphate phosphohydrolases. An expanding Nudt family. J Biol Chem 275, 12730-12736.
17. Chakraborty, A., Kim, S., Snyder, S. H., (2011) Inositol Pyrophosphates as Mammalian Cell Signals. Sci Signal 4, 188.
18. Chakraborty, A., Koldobskiy, M. A., Sixt, K. M., Juluri, K. R., Mustafa, A. K., Snowman, A. M., van Rossum, D. B., Patterson, R. L., Snyder, S. H., (2008) HSP90 regulates cell survival via inositol hexakisphosphate kinase-2. Proc Natl Acad Sci U S A 105, 1134-1139.
19. Chu, C., Alapat, D., Wen, X., Timo, K., Burstein, D., Lisanti, M., Shears, S., Kohtz, D. S., (2004) Ectopic expression of murine diphosphoinositol polyphosphate phosphohydrolase 1 attenuates signaling through the erk 1/2 pathway. Cell Signal 16, 1045-1059.
20. Cooper, G. J., Geoffrey, M., (2000) Chapter 1. An Overview of Cells and Cell Research. The Cell (Work in NCBI Bookshelf) Part I.
21. Cremona, O., De Camilli, P., (2001) Phosphoinositides in membrane traffic at the synapse. J Cell Sci 114, 1041-52.
22. Draskovic, P., Saiardi, A., Bhandari, R., Burton, A., Ilc, G., Kovacevic, M., Snyder, S. H., Podobnik, M., (2008) Inositol hexakisphosphate kinase products contain diphosphate and triphosphate groups. Chem Biol 15, 274-286.
23. Dubois, E., Scherens, B., Vierendeels, F., Ho, M. M., Messenguy, F., Shears, S. B., (2002) In *Saccharomyces cerevisiae*, the inositol polyphosphate kinase activity of Kcs1p is required for resistance to salt stress, cell wall integrity, and vacuolar morphogenesis. J Biol Chem 277, 23755-23763.
24. Eichinger, L., Pachebat, J. A., Glöckner, G., Rajandream, M. A., Sucgang, R., Berriman, M., Song, J., Olsen, R., Szafranski, K., Xu, Q., Tunggal, B., Kummerfeld, S., Madera, M., Konfortov, B. A., Rivero, F., Bankier, A. T., Lehmann, R., Hamlin, N., Davies, R., Gaudet, P., Fey, P., Pilcher, K., Chen, G., Saunders, D., Sodergren, E., Davis, P., Kerhornou, A., Nie, X., Hall, N., Anjard, C., Hemphill, L., Bason, N., Farbrother, P., Desany, B., Just, E., Morio, T., Rost, R., Churcher, C., Cooper, J., Haydock, S., van Driessche, N., Cronin, A., Goodhead, I., Muzny, D., Mourier, T., Pain, A., Lu, M., Harper, D., Lindsay, R., Hauser, H., James, K., Quiles, M., Madan Babu, M., Saito, T., Buchrieser, C., Wardroper, A., Felder, M., Thangavelu, M., Johnson, D., Knights, A., Loulseged, H., Mungall, K., Oliver, K., Price, C., Quail, M. A., Urushihara, H., Hernandez, J., Rabbinowitsch, E., Steffen, D., Sanders, M., Ma, J., Kohara, Y., Sharp, S., Simmonds, M., Spiegler, S., Tivey, A., Sugano, S., White, B., Walker, D., Woodward, J., Winckler, T., Tanaka, Y., Shaulsky, G., Schleicher, M., Weinstock, G., Rosenthal, A., Cox, E. C., Chisholm, R. L., Gibbs, R., Loomis, W. F., Platzer, M., Kay, R. R., Williams, J., Dear, P. H., Noegel, A. A., Barrell, B., Kuspa, A., (2005) The genome of the social amoeba *Dictyostelium discoideum*. Nature 435, 43-57.
25. El Bakkoury, M., Dubois, E., Messenguy, F., (2000) Recruitment of the yeast MADS-box proteins, ArgRI and Mcm1 by the pleiotropic factor ArgRIII is required for their stability. Mol Microbiol 35, 15-31.
26. Fey, P., Kowal, A. S., Gaudet, P., Pilcher, K. E., Chisholm, R. L., (2007) Protocols for growth and development of *Dictyostelium discoideum*. Nat Protoc 2, 1307-1316.

27. Fisher, D. I., Safrany, S. T., Strike, P., McLennan, A. G., Cartwright, J. L., (2002) Nudix hydrolases that degrade dinucleoside and diphosphoinositol polyphosphates also have 5-phosphoribosyl 1-pyrophosphate (PRPP) pyrophosphatase activity that generates the glycolytic activator ribose 1,5-bisphosphate. J Biol Chem 277, 47313-47317.
28. Fridy, P. C., Otto, J. C., Dollins, D. E., York, J. D., (2007) Cloning and characterization of two human VIP1-like inositol hexakisphosphate and diphosphoinositol pentakisphosphate kinases. J Biol Chem 282, 30754-30762.
29. Gilbert, S. F., (2006) Developmental Biology. 8th ed. Sunderland (MA) Sinauer p. 36-39.
30. Glennon, M. C., Shears, S. B., (1993) Turnover of inositol pentakisphosphates, inositol hexakisphosphate and diphosphoinositol polyphosphates in primary cultured hepatocytes. Biochem J 293 (Pt 2), 583-590.
31. Gonzalez, B., Schell, M.J., Letcher, A.J., Veprintsev, D.B., Irvine, R.F., and Williams, R.L., (2004) Structure of a human inositol 1,4,5-trisphosphate 3-kinase: substrate binding reveals why it is not a phosphoinositide 3-kinase. Mol Cell 15, 689–701.
32. Hidaka, K., Caffrey, J. J., Hua, L., Zhang, T., Falck, J. R., Nickel, G. C., Carrel, L., Barnes, L. D., Shears, S. B., (2002) An adjacent pair of human NUDT genes on chromosome X are preferentially expressed in testis and encode two new isoforms of diphosphoinositol polyphosphate phosphohydrolase. J Biol Chem 277, 32730-32738.
33. Hiltunen, J. K., Autio, K. J., Schonauer, M.S., Kursu, V.A., Dieckmann, C. L., Kastaniotis, A. J., (2010) Mitochondrial fatty acid synthesis and respiration. Biochim Biophys Acta 1797, 1195-1202.
34. Hoeller, O., Kay, R. R., (2007) Chemotaxis in the absence of PIP_3 gradients. Curr Biol 17, 813-817.
35. Holmes, W., Jogl, G., (2006) Crystal structure of inositol phosphate multikinase 2 and implications for substrate specificity. J Biol Chem 281, 38109-16.
36. Hua, L.V., Green, M., Warsh, J.J., Li, P.P., (2001) Molecular cloning of a novel isoform of diphosphoinositol polyphosphate phosphohydrolase: a potential target of lithium therapy. Neuropsychopharmacology 24, 640-651.
37. Hua, L. V., Hidaka, K., Pesesse, X., Barnes, L. D., Shears, S. B., (2003) Paralogous murine Nudt10 and Nudt11 genes have differential expression patterns but encode identical proteins that are physiologically competent diphosphoinositol polyphosphate phosphohydrolases. Biochem J 373, 81-89.
38. Iijima, M., Devreotes, P., (2002) Tumor suppressor PTEN mediates sensing of chemoattractant gradients. Cell 109, 599-610.
39. Illies, C., Gromada, J., Fiume, R., Leibiger, B., Yu, J., Juhl, K., Yang, S. N., Barma, D. K., Falck, J. R., Saiardi, A., Barker, C. J., Berggren, P. O., (2007) Requirement of inositol pyrophosphates for full exocytotic capacity in pancreatic beta cells. Science 318, 1299-1302.
40. Ingram, S. W., Safrany, S.T., Barnes, L. D., (2003) Disruption and overexpression of the *Schizosaccharomyces pombe* aps1 gene, and effects on growth rate, morphology and intracellular diadenosine 5',5'''-P1,P5-pentaphosphate and diphosphoinositol polyphosphate concentrations. Biochem J 369, 519-528.
41. Irvine, R. F., (2003) 20 years of $Ins(1,4,5)P_3$, and 40 years before. Nat Rev Mol Cell Biol 4, 586-590.

42. Irvine, R. F., Schell, M. J., (2001) Back in the water: the return of the inositol phosphates. Nat Rev Mol Cell Biol 2, 327-338.
43. Koldobskiy, M. A., Chakraborty, A., Werner, J. K. Jr, Snowman, A. M., Juluri, K. R., Vandiver, M.S., Kim, S., Heletz, S., Snyder, S. H., (2010) p53-mediated apoptosis requires inositol hexakisphosphate kinase-2. Proc Natl Acad Sci U S A 107, 20947-51.
44. Komander, D., Fairservice, A., Deak, M., Kular, G. S., Prescott, A. R, Peter Downes, C., Safrany, S. T., Alessi, D. R., van Aalten, D. M., (2004) Structural insights into the regulation of PDK1 by phosphoinositides and inositol phosphates. Embo J 23, 3918-3928.
45. Laussmann, T., Eujen, R., Weisshuhn, C. M., Thiel, U., Vogel, G., (1996) Structures of diphospho-myo-inositol pentakisphosphate and bisdiphospho-myo-inositol tetrakisphosphate from *Dictyostelium* resolved by NMR analysis. Biochem J 315, 715-720.
46. Laussmann, T., Hansen, A., Reddy, K. M., Reddy, K. K., Falck, J. R., Vogel, G., (1998) Diphospho-myo-inositol phosphates in *Dictyostelium* and *Polysphondylium*: identification of a new bisdiphospho-myo-inositol tetrakisphosphate. FEBS Lett 426, 145-150.
47. Laussmann, T., Pikzack, C., Thiel, U., Mayr, G. W., Vogel, G., (2000) Diphospho-*myo*-inositol phosphates during the life cycle of *Dictyostelium* and *Polysphondylium*. Eur J Biochem 267, 2447-2451.
48. Laussmann, T., Reddy, K. M., Reddy, K. K., Falck, J. R., Vogel, G., (1997) Diphospho-*myo*-inositol phosphates from *Dictyostelium* identified as D-6-diphospho-*myo*-inositol pentakisphosphate and D-5,6-bisdiphospho-myo-inositol tetrakisphosphate. Biochem J 322, 31-33.
49. Lee, Y. S., Huang, K., Quiocho, F. A., O'Shea, E. K., (2008) Molecular basis of cyclin-CDK-CKI regulation by reversible binding of an inositol pyrophosphate. Nat Chem Biol 4, 25-32.
50. Lee, Y. S., Mulugu, S., York, J. D., O'Shea, E. K., (2007) Regulation of a cyclin-CDK-CDK inhibitor complex by inositol pyrophosphates. Science 316, 109-112.
51. Lemmon, M. A., (2008) Membrane recognition by phospholipid-binding domains. Nat Rev Mol Cell Biol 9, 99-111.
52. Leroy, C., Mann, C., Marsolier, M. C., (2001) Silent repair accounts for cell cycle specificity in the signaling of oxidative DNA lesions. Embo J 20, 2896-2906.
53. Leslie, N. R., McLennan, A. G., Safrany, S. T., (2002) Cloning and characterisation of hAps1 and hAps2, human diadenosine polyphosphate-metabolising Nudix hydrolases. BMC Biochem 3: 20.
54. Letavayová, L., Marková, E., Hermanská, K., Vlcková, V., Vlasáková, D., Chovanec, M., Brozmanová, J., (2006) Relative contribution of homologous recombination and non-homologous end-joining to DNA double-strand break repair after oxidative stress in *Saccharomyces cerevisiae*. DNA Repair (Amst) 5, 602-610.
55. Lin, H., Fridy, P. C., Ribeiro, A. A., Choi, J. H., Barma, D. K., Vogel, G., Falck, J. R., Shears, S. B., York, J. D., Mayr, G. W., (2009) Structural analysis and detection of biological inositol pyrophosphates reveal that the family of VIP/diphosphoinositol pentakiphosphatase kinases are 1/3-kinases. J Biol Chem 284, 1863-1872.

56. Lonetti, A., Szijgyarto, Z., Bosch, D., Loss, O., Azevedo, C., Saiardi, A., (2011) Identification of an evolutionarily conserved family of inorganic polyphosphate endopolyphosphatases. J Biol Chem 286, 31966-31974.
57. Lovejoy, C. A., Cortez, D., (2009) Common mechanisms of PIKK regulation. DNA Repair (Amst) 8, 1004-1008.
58. Luo, H. R., Huang, Y. E., Chen, J. C., Saiardi, A., Iijima, M., Ye, K., Huang, Y., Nagata, E., Devreotes, P., Snyder, S. H., (2003) Inositol pyrophosphates mediate chemotaxis in *Dictyostelium* via pleckstr in homology domain-PtdIns(3,4,5)P_3 interactions. Cell 114, 559-572.
59. Luo, H. R., Saiardi, A., Nagata, E., Ye, K., Yu, H., Jung, T. S., Luo, X., Jain, S., Sawa, A., Snyder, S. H., (2001) GRAB: a physiologic guanine nucleotide exchange factor for Rab3A, which interacts with inositol hexakisphosphate kinase. Neuron 31, 439-451.
60. Ma, Y., Lieber, M., R., (2002) Binding of inositol hexakiphosphatase (IP_6) to Ku but not to DNA-PKcs. J Biol Chem 277, 10756-10759.
61. Martin, J. B., Foray, M. F., Klein, G., Satre, M., (1987) Identification of inositol hexaphosphate in ^{31}P-NMR spectra of *Dictyostelium discoideum* amoebae. Relevance to intracellular pH determination. Biochim Biophys Acta 931, 16-25.
62. Martin, J. B., Laussmann, T., Bakker-Grunwald, T., Vogel, G., Klein, G., (2000) Neo-inositol polyphosphates in the amoeba *Entamoeba histolytica*. J Biol Chem 275, 10134-10140.
63. Mather, K. A., Jorm, A. F., Parslow, R. A., Christensen, H., (2011) Is telomere length a biomarker of aging? A review. J Gerontol A Biol Sci Med Sci 66, 202-213.
64. Menniti, F. S., Miller, R. N., Putney, J. W. Jr, Shears, S. B., (1993) Turnover of inositol polyphosphate pyrophosphates in pancreatoma cells. J Biol Chem 268 3850-3856.
65. Mikoshiba, K., Furuichi, T., Miyawaki, A., Yoshikawa, S., Nakade, S., Michikawa, T., Nakagawa, T., Okano, H., Kume, S., Muto, A., et al. (1993) Structure and function of inositol 1,4,5-trisphosphate receptor. Ann N Y Acad Sci 707: 178-197.
66. Morrison, B. H., Tang, Z., Jacobs, B. S., Bauer, J. A., Lindner, D. J., (2005) Apo2L/TRAIL induction and nuclear translocation of inositol hexakisphosphate kinase 2 during IFN-beta-induced apoptosis in ovarian carcinoma. Biochem J 385, 595-603.
67. Mulugu, S., Bai, W., Fridy, P. C., Bastidas, R. J., Otto, J. C., Dollins, D. E., Haystead, T. A., Ribeiro, A. A., York, J. D., (2007) A conserved family of enzymes that phosphorylate inositol hexakisphosphate. Science 316, 106-109.
68. Nag, D. K., Tikhonenko, I., Soga, I., Koonce, M. P., (2008) Disruption of four kinesin genes in *Dictyostelium*. BMC Cell Biol 1186/1471-2121-9-21.
69. Nagata, E., Saiardi, A., Tsukamoto, H., Okada, Y., Itoh, Y., Satoh, T., Itoh, J., Margolis, R. L., Takizawa, S., Sawa, A., Takagi, S., (2011) Inositol hexakisphosphate kinases induce cell death in Huntington disease. J Biol Chem 286, 26680-26686.
70. No authors listed, (1989) Nomenclature of initiation, elongation and termination factors for translation in eukaryotes. Recommendations 1988. Nomenclature Committee of the International Union of Biochemistry (NC-IUB). Eur J Biochem 186, 1-3.

71. Norbis, F., Boll, M., Stange, G., Markovich, D., Verrey, F., Biber, J., Murer, H., (1997) Identification of a cDNA/protein leading to an increased Pi-uptake in *Xenopus laevis* oocytes. J Membr Biol 156, 19-24.
72. Onnebo, S. M., Saiardi, A., (2009) Inositol pyrophosphates modulate hydrogen peroxide signalling. Biochem J 423, 109-118.
73. Passarino, G., Rose, G., Bellizzi, D., (2010) Mitochondrial function, mitochondrial DNA and ageing: a reappraisal. Biogerontology 11, 575-588.
74. Pittet, D., Schlegel, W., Lew, D. P., Monod, A., Mayr, G. W., (1989) Mass changes in inositol tetrakis- and pentakisphosphate isomers induced by chemotactic peptide stimulation in HL-60 cells. J Biol Chem 264, 18489-18493.
75. Raboy, V., (2003) *Myo*-inositol-1,2,3,4,5,6-hexakisphosphate. Phytochemistry 64, 1033-1043.
76. Resnick, A. C., Saiardi, A., (2008) Inositol polyphosphate multikinase: metabolic architect of nuclear inositides. Front Biosci 13: 856-866.
77. Safrany, S. T., Caffrey, J. J., Yang, X., Bembenek, M. E., Moyer, M. B., Burkhart, W. A., Shears, S. B., (1998) A novel context for the 'MutT' module, a guardian of cell integrity, in a diphosphoinositol polyphosphate phosphohydrolase. Embo J 17, 6599-6607.
78. Safrany, S. T., Ingram, S. W., Cartwright, J. L., Falck, J. R., McLennan, A. G., Barnes, L. D., Shears, S. B., (1999) The diadenosine hexaphosphate hydrolases from *Schizosaccharomyces pombe* and *Saccharomyces cerevisiae* are homologues of the human diphosphoinositol polyphosphate phosphohydrolase. Overlapping substrate specificities in a MutT-type protein. J Biol Chem 274, 21735-21740.
79. Saiardi, A., (2012) How inositol pyrophosphates control cellular phosphate homeostasis? Adv Biol Regul 52, 351-359.
80. Saiardi, A., Bhandari, R., Resnick, A. C., Snowman, A. M., Snyder, S. H., (2004) Phosphorylation of proteins by inositol pyrophosphates. Science 306, 2101-2105.
81. Saiardi, A., Cockcroft, S., (2008) Human ITPK1: a reversible inositol phosphate kinase/phosphatase that links receptor-dependent phospholipase C to Ca^{2+}-activated chloride channels. Sci Signal 1, pe5.
82. Saiardi, A., Erdjument-Bromage, H., Snowman, A. M., Tempst, P., Snyder, S. H., (1999) Synthesis of diphosphoinositol pentakisphosphate by a newly identified family of higher inositol polyphosphate kinases. Curr Biol 9, 1323-1326.
83. Saiardi, A., Nagata, E., Luo, H. R., Snowman, A. M., Snyder, S. H., (2001) Identification and characterization of a novel inositol hexakisphosphate kinase. J Biol Chem 276, 39179-39185.
84. Saiardi, A., Resnick, A. C., Snowman, A. M., Wendland, B., Snyder, S. H., (2005) Inositol pyrophosphates regulate cell death and telomere length through phosphoinositide 3-kinase-related protein kinases. Proc Natl Acad Sci U S A 102, 1911-1914.
85. Saiardi, A., Sciambi, C., McCaffery, J. M., Wendland, B., Snyder, S. H., (2002) Inositol pyrophosphates regulate endocytic trafficking. Proc Natl Acad Sci U S A 99, 14206-14211.
86. Seeds, A. M., Bastidas, R. J., York, J. D., (2005) Molecular definition of a novel inositol polyphosphate metabolic pathway initiated by inositol 1,4,5-trisphosphate 3-kinase activity in Saccharomyces cerevisiae. J Biol Chem 280, 27654-27661.
87. Shears, S. B., (2001) Assessing the omnipotence of inositol hexakisphosphate. Cell Signal 13, 151-158.

88. Shears, S. B., (2009) Diphosphoinositol polyphosphates: metabolic messengers? Mol Pharmacol 76, 236-252.

89. Shears, S. B., Ali, N., Craxton, A., Bembenek, M. E., (1995) Synthesis and metabolism of bis-diphosphoinositol tetrakisphosphate *in vitro* and *in vivo*. J Biol Chem 270, 10489-10497.

90. Shears, S. B., Weaver, J. D., Wang, H., (2013) Structural insight into inositol pyrophosphate turnover. Adv Biol Regul 53, 19-27.

91. Scherer, J., (1850) Ü ber eine neue, aus dem Muskelfl eische gewonnene Zuckerart. Justus Liebigs Ann Chem 73, 322–328.

92. Stephens, L. R., Irvine, R. F., (1990) Stepwise phosphorylation of *myo*-inositol leading to *myo*-inositol hexakisphosphate in *Dictyostelium*. Nature 346, 580-583.

93. Stephens, L., Radenberg, T., Thiel, U., Vogel, G., Khoo, K. H., Dell, A., Jackson, T. R., Hawkins, P. T., Mayr, G. W., (1993) The detection, purification, structural characterization, and metabolism of diphosphoinositol pentakisphosphate(s) and bisdiphosphoinositol tetrakisphosphate(s). J Biol Chem 268, 4009-4015.

94. Streb, H., Irvine, R. F., Berridge, M. J., Schulz, I., (1983) Release of Ca^{2+} from a non-mitochondrial intracellular store in pancreatic acinar cells by inositol-1,4,5-trisphosphate. Nature 306, 67-69.

95. Szijgyarto, Z., Garedew, A., Azevedo, C., Saiardi, A., (2011) Influence of inositol pyrophosphates on cellular energy dynamics. Science 334, 802-805.

96. Szwergold, B. S., Graham, R. A., Brown, T. R., (1987) Observation of inositol pentakis- and hexakis-phosphates in mammalian tissues by ^{31}P NMR. Biochem Biophys Res Commun 149, 874-881.

97. Taylor, R. Jr, Chen, P. H., Chou, C. C., Patel, J., Jin, S. V., (2012) KCS1 deletion in *Saccharomyces cerevisiae* leads to a defect in translocation of autophagic proteins and reduces autophagosome formation. Autophagy 8, 1300-1311.

98. Tyler, M., S., (2000) Developmental Biology A Guide for Experimental Study. 2nd ed Sunderland (MA): Sinauer pp. 31–34.

99. Voglmaier, S. M., Bembenek, M. E., Kaplin, A. I., Dormán, G., Olszewski, J. D., Prestwich, G. D., Snyder, S. H., (1996) Purified inositol hexakisphosphate kinase is an ATP synthase: diphosphoinositol pentakisphosphate as a high-energy phosphate donor. Proc Natl Acad Sci U S A 93, 4305-4310.

100. Voglmaier, S. M., Keen, J. H., Murphy, J. E., Ferris, C. D., Prestwich, G. D., Snyder, S. H., Theibert, A. B., (1992) Inositol hexakisphosphate receptor identified as the clathrin assembly protein AP-2. Biochem Biophys Res Commun 187, 158-163.

101. Wang, H., Falck, J. R., Traci, M., Tanaka, H., Shears, S. B., (2011) Structural basis for an inositol pyrophosphate kinase surmounting phosphate crowding. Nat Chem Biol 8, 111-116.

102. Wilson, M. S., Livermore, T. M., Saiardi, A., (2013) Inositol pyrophosphates: between signalling and metabolism. Biochem J 452, 369-79.

103. Wundenberg, T., Mayr, G. W., (2012) Synthesis and biological actions of diphosphoinositol phosphates (inositol pyrophosphates), regulators of cell homeostasis. Biol Chem 393, 979-998.

104. York, J. D., Hunter, T., (2004) Signal transduction. Unexpected mediators of protein phosphorylation. Science 306, 2053-2055.

105. York, J. D., Odom, A. R., Murphy, R., Ives, E. B., Wente, S. R., (1999) A phospholipase C-dependent inositol polyphosphate kinase pathway required for efficient messenger RNA export. Science 285, 96-100.

106. York, S. J., Armbruster, B. N., Greenwell, P., Petes, T. D., York, J. D., (2005) Inositol diphosphate signaling regulates telomere length. J Biol Chem 280, 4264-4269.

CHAPTER II

Analysis of *Dictyostelium discoideum* inositol pyrophosphate metabolism by gel electrophoresis

Pisani Francesca[1,2], Livermore Thomas[1], Rose Giuseppina[2], Chubb Jonathan R.[1], Gaspari Marco[3] and Saiardi Adolfo[1]

Authors' copy of Pisani et al., Analysis of *Dictyostelium discoideum* inositol pyrophosphate metabolism by gel electrophoresis - *PlosOne (In Press)*

[1]*Medical Research Council Laboratory for Molecular Cell Biology, University College London, London, UK.*
[2]*Department of Biology, Ecology and Earth Science, University of Calabria, Rende, Italy.*
[3]*Laboratory of Proteomics and Mass Spectrometry, Department of Experimental and Clinical Medicine, "Magna Græcia" University of Catanzaro, Catanzaro, Italy.*

Abstract

The social amoeba *Dictyostelium discoideum* was instrumental in the discovery and early characterization of inositol pyrophosphates, a class of molecules possessing highly-energetic pyrophosphate bonds. Inositol pyrophosphates regulate diverse biological processes and are attracting attention due to their ability to control energy metabolism and insulin signaling. However, inositol pyrophosphate research has been hampered by the lack of simple experimental procedures to study them. The recent development of polyacrylamide gel electrophoresis (PAGE) and simple staining to resolve and detect inositol pyrophosphate species has opened new investigative possibilities. This technology is now commonly applied to study in vitro enzymatic reactions. Here we employ PAGE technology to characterize the *D. discoideum* inositol pyrophosphate metabolism. Surprisingly, only three major bands are detectable after resolving acidic extract on PAGE. We have demonstrated that these three bands correspond to inositol hexakisphosphate (IP_6 or Phytic acid) and its derivative inositol pyrophosphates, IP_7 and IP_8. Biochemical analyses and genetic evidence were used to establish the genuine inositol phosphate nature of these bands. We also identified IP_9 in *D. discoideum* cells, a molecule so far detected only from in vitro biochemical reactions. Furthermore, we discovered that this amoeba possesses three different inositol pentakisphosphates (IP_5) isomers, which are largely metabolised to inositol pyrophosphates. Comparison of PAGE with traditional Sax-HPLC revealed an underestimation of the cellular abundance of inositol pyrophosphates by traditional methods. In fact our study revealed much higher levels of inositol pyrophosphates in *D. discoideum* in the vegetative state than previously detected. A three-fold increase in IP_8 was observed during development of *D. discoideum* a value lower that previously reported. Analysis of inositol pyrophosphate metabolism using *ip6k* null amoeba revealed the absence of developmentally-induced synthesis of inositol pyrophosphates, suggesting that the alternative class of enzyme responsible for pyrophosphate synthesis, PP-IP_5K, doesn't' play a major role in the IP_8 developmental increase.

Introduction

The model organism *Dictyostelium discoideum*, originally developed to study the transition to multicellularity, has subsequently been utilised in several areas of biology from chemotaxis [1] to transcriptional control [2]. Upon exhaustion of nutrients, the Dictyosteliidae slime moulds are able to aggregate into multicellular forms, a process regulated by cAMP signaling [3]. The aggregated slugs develop into fruiting bodies (or sporocarp) compromised of two main cell types; stalk cells and thousands of spore cells. Much of the early work with this amoeba focused on this fascinating behavior. However, in the late 1980s this model organism began to offer insight into the metabolism of inositol phosphates [4]. In fact, it was in *D. discoideum* that the synthesis of inositol hexakisphosphates (IP_6) through direct phosphorylation of inositol was discovered [5]. *D. discoideum* has also been instrumental in the discovery of inositol pyrophosphates (also known as diphosphoinositol phosphates) (For reviews see [6,7]) molecules containing highly energetic pyrophosphate moiety(ies) recently implicated into the regulation of cellular homeostasis [8,9,10]. Inositol pyrophosphates were identified in 1993 in *D. discoideum* [11] and in mammalian cell [12]. During the 1990s the synthesis of the inositol pyrophosphate IP_7 (diphosphoinositol pentakisphosphate or PP-IP_5) and, in particular, IP_8 (bisdiphosphoinositoltetrakisphosphate or $(PP)_2$-IP_4) was linked to the *D. discoideum* developmental program [13]. Furthermore, thanks to the high concentration of these molecules in this amoeba, NMR could be used to resolve the isomeric nature of IP_7 and IP_8 extracted from *D. discoideum* cells. The structure of these isoforms - the 5PP-IP_5 isomer of IP_7 and the 5,6$(PP)_2$-IP_4 isomer of IP_8 [14] are, to date, the only resolved structures of inositol pyrophosphates extracted from cells.

Despite the influence of this organism, *D. discoideum* has faded from the attentions of inositol phosphate scientists over time. The last study demonstrating the importance of inositol pyrophosphate in regulating *Dictyostelium* chemotaxis was published over 10 years ago [15]. This disengagement is in part due to the emergence of another experimental model, the yeast *Saccharomyces cerevisiae* [16,17] but also to the difficulty in promptly labelling the amoeba with tritium inositol (^{3}H-inositol) [18]. Therefore the use of routine Sax-HPLC (Strong anion exchange chromatography) to resolve the different radiolabeled inositol phosphates becomes cumbersome and expensive to apply to amoeba cells. Thus, chromatographic separation of inositol phosphates in *Dictyostelium* is normally performed using metal dye detector post-colum derivatization (MDD-HPLC) [11,19] requiring a dedicated three pump HPLC apparatus and therefore is not a widespread technology. Two different classes of enzymes are

able to synthesize inositol pyrophosphates: the inositol hexakisphosphate kinases IP6Ks (*Kcs1* in yeast) [20] and the PP-IP_5Kinases (*Vip1* in yeast) [21,22]. These enzyme are mainly characterised from mammalian sources and possess the ability to pyro-phosphorylate position 5 of the inositol ring (IP6K) [23] and position 1 ($PPIP_5K$) [24] *in vitro*. Thus, it is believed that mammalian cells possess a different isomer of IP_8, namely the 1,5$(PP)_2$-IP_4 species [25]. The recent discovery that higher inositol phosphates can be resolved by polyacrylamide gel electrophoresis (PAGE) [26] and visualised by simple staining, bypassing the need to use radio labelled material, has enormously improved in vitro studies of inositol pyrophosphates [27]. In particular, this has facilitated characterisation of the inositol pyrophosphate synthesizing kinases; the inositol hexakisphosphate kinases (IP6Ks in mammals, *Kcs1* in yeast) and the diphosphoinositol pentakisphosphate kinases (PP-IP_5Ks in mammals, *Vip1* in yeast) [26]. In the current work we applied this PAGE technology to samples obtained from live cells, allowing us to analyse the in vivo inositol phosphate metabolism by PAGE for the first time. We demonstrated the existence of different inositol pyrophosphate species by both DAPI and Toluidine Blue staining, and reveal a complex metabolism comprising inositol pyrophosphates derived from both IP_6 and inositol pentakisphosphates (IP_5). Furthermore, the analysis of inositol pyrophosphate metabolism during *D. discoideum* development revealed a far less dramatic increase in levels of IP_8 than has been previously described.

Results

Resolving D. discoideum cell extract by PAGE revealed the presence of IP_6, IP_7 and IP_8.

Inositol polyphosphates are routinely extracted using strong acid solutions, usually Perchloric Acid. If appropriately labelled with ^{3}H-inositol this cell extract can be neutralized and analysed by Strong anion exchange chromatography (Sax-HPLC) [28]. The high levels of inositol pyrophosphates in *D. discoideum* prompted us to analyse a fraction (1/20 by volume) of the neutralised unlabeled cells extract, equivalent to 1-2 10^6 cells, by PAGE [26]. Sample migration during PAGE is normal when just 20-40 microlitres of cell extract is loaded (Fig. 1). To our surprise, extract from vegetative Wild Type AX2 (WT) *D. discoideum* cells reveals the presence of three major bands by Toluidine staining. The fastest migrating band co-migrates with the commercially available IP_6 standard (Fig. 1). Staining with DAPI also reveals the same three major bands (Fig. 1). Interestingly, DAPI is heavily photobleached (resulting in negative staining) by the two slower migrating bands and not by that which co-migrates with IP_6. This method of staining reveals a further weaker band, which migrates still slower and is not always detectable by Toluidine. It was previously demonstrated that the ability to photobleach DAPI is a typical characteristic of the pyrophosphate moiety [26], however the large amount of IP_6 present in *D. discoideum* extract is able to induce some DAPI photo-bleaching, though at a much lower efficiency. Thus, besides IP_6 the other bands are expected to be IP_7, IP_8 and, newly detected, endogenous IP_9, previously identified only in vitro [23]. To confirm the nature of these bands we use several approaches. First genetic; the analysis of acidic extract of Inositol Hexakisphosphate Kinase (IP6K) null amoeba (gene I6KA, DDB_G0278739) [15] reveals only the presence of a band co-migrating with IP_6 and a weaker band, detectable only by DAPI, co-migrating with IP_7 (Fig.1). The virtual absence of IP_7, and the total deficiency of the respective IP_8 and IP_9 bands phenocopies the yeast *ip6k* mutant (*kcs1*Δ*)* that lack any detectable inositol pyrophosphates [16,29]. Using traditional ^{3}H-inositol labelling and Sax-HPLC analysis, the absence of any inositol pyrophosphates in *ip6k* null amoeba has been previously verified [15]. Interestingly, DAPI analysis reveals the presence of a new, retarded band in *ip6k* null amoeba (labelled nd in Fig.1B). This band is of undetermined nature although DAPI photo-bleaching ability suggests the presence of pyrophosphate moieties. The analysis of phospholipase C (PLC) mutant cells reveals a pattern of bands similar to WT cells in striking contrast of the yeast *plc1*Δ strain that lacks the synthesis of any highly phosphorylated forms of inositol phosphates [17]. However, our result is coherent with previous reports that demonstrate normal levels of inositol pyrophosphates in *D. discoideum plc* null cells (gene pipA, DDB_G0292736) [18,30] and with the ability of the

amoeba to synthesize IP_6 directly from inositol independently from lipid cleavage [5]. Secondly, we use enzymology to confirm the nature of these bands as genuine inositol phosphates. The treatment of WT extract with phytase, an enzyme capable of fully dephosphorylating IP_6 (also call Phytic Acid), resulted in the complete disappearance of the three major bands (Fig. 2A). The treatment of WT extract with DDP1 (Fig. 2B), a phosphatases that specifically degrades the pyrophosphate moiety, resulted in an almost complete degradation of IP_7 and IP_8 with the corresponding formation of IP_6. Phosphoanhydride bonds (the pyrophosphate moiety) are rapidly hydrolysed in acid at higher temperatures. Consequently, we also incubated the acidic extract at 90^oC for 10 minutes before neutralization. This treatment (Fig. 2C) revealed the complete degradation of the IP_7 and IP_8 bands and the resultant formation of IP_6 as well as three further fast migrating bands. These three extra bands migrate as expected of IP_5, which is almost undetectable in untreated cell extract (Fig. 1, 2, 3). This suggests the existence of an elaborate inositol pyrophosphate metabolism (see below). Finally we use mass spectrometry to determine the mass of the purified bands (Fig. 3A). The analysis of the putative IP_7 band reveals, in the *m/z* range 500-1000, two major peaks at 738.822 and 760.793 *m/z*. These *m/z* values are well in accordance with the theoretical mass of deprotonated IP_7 and its sodium adduct respectively (Fig.3B). The detection of an intense peak at +22 *m/z* with respect to the deprotonated molecule is an additional confirmation of the presence of phosphate moieties on the analyte. Similarly, the analysis of the putative IP_8 band reveals a major peak at 840.590 *m/z*, and a minor peak at 818.627 *m/z* (Fig. 3C). These values correspond to the theoretical mass of, respectively, the sodium adduct of deprotonated IP_8 and deprotonated IP_8. The increased relative intensity of the sodium adduct is an additional confirmation of the increased number of phosphate moieties attached to the analyte in the putative IP_8 band compared to the putative IP_7 band. Unfortunately, we observed a decrease in mass spectrometry ionization efficiency with increasing number of phosphate groups, as can be appreciated by comparing absolute intensities of IP_7 and IP_8 MALDI-TOF spectra in (Fig. 3B and C). Therefore, we were unable to determine the mass of the IP_9 band. Nevertheless, taken together these genetic and biochemical studies prove that the bands observable in *D. discoideum* extract are bona fide inositol pyrophosphates.

Presence of a complex IP_5 derived inositol pyrophosphates metabolism.

The appearance of bands migrating faster that IP_6 after acidic hydrolysis prompted us to perform further analysis with the aim to determine their exact nature. We split a cell extract (from 5ml culture growth at a density of 2-4×10^6 cells/ ml) into two halves and subjected one half to acidic hydrolysis. After neutralisation this half as well as the untreated half were analysed by PAGE. We employed IP_6 as a standard as well the six IP_5 isomers (Fig. 4A). Loading a larger amount of cell extract allowed us to detect fast migrating three weak bands in the untreated sample lane. These bands co-migrate with distinct IP_5 standards. The acidic treated samples reveals a robust increase of both IP_6, due to the conversion of IP_7 and IP_8 to IP_6, and the three IP_5 isomers. This indicates presence of inositol pyrophosphate generated from IP_5, such as PP-IP_4 and likely also $(PP)_2$-IP_3, which are converted back to IP_5 by acidic treatment. The inositol pyrophosphates PP-IP_4 and $(PP)_2$-IP_3 possessing six and seven phosphates groups migrate very closely (or co-migrate) with the more abundant IP_6 and IP_7 species and thus cannot be directly detected in untreated WT cell extract. Densitometry analysis of treated IP_6 and IP_5s versus untreated counterpart reveals that ~60% of the IP_6 pool is converted to IP_7 and IP_8 while >90% of IP_5 pool is converted to inositol pyrophosphate species (Fig. 4B). This indicates that pyrophosphates derived from IP_5 and IP_6 have differing metabolism and turnover. The extraordinary ability of PAGE to resolve different IP_5 isomer and the densitometry analysis of the three IP_5 bands reveal that the IP_5 pool of *D. discoideum* cell is distributed as follows, ~10% I(1,2,3,4,6)P_5; ~30% I(2,3,4,5,6,)P_5 and/or I(1,2,4,5,6)P_5; ~60% I(1,3,4,5,6)P_5 and/or I(1,2,3,5,6)P_5 and/or I(1,2,3,4,5)P_5. The presence of at least three IP_5 isomers is confirmed by an early report [5,31]. However these earlier studies, which relied on HPLC revealed differing relative distributions of the IP_5 isomeric species[31]. It is important to note that strong acidic conditions (such as those used in HPLC analysis) can induce phosphate groups to move to adjacent hydroxyl positions, altering the isomeric nature of inositol phosphates, a well-known phenomena during phosphoinositide (inositol lipid) purification [32]. High temperature and acidity are also able to induce movement of phosphate groups around the hydroxyl groups of the inositol ring in IP_5 (Figure S1). However, the presence of the three IP_5 species in untreated samples (Fig. 4A) is supportive of the genuine existence of at least three different IP_5 isomers in *D. discoideum*. The fact that all of these IP_5 species are enriched after pyrophosphate hydrolysis indicates that multiple IP_5 isomers are precursors of inositol pyrophosphate species indicating a complex isomeric mixture of pyrophosphates derived from IP_5.

PAGE analysis revealed high levels of inositol pyrophosphates.

Previous studies aiming to analyse the level of inositol pyrophosphate during *D. discoideum* development have estimated the levels of IP_7 and IP_8 in vegetative stage cells to be 3-6% of the levels of IP_6, a ratio comparable to that observable in mammalian cells. This data, obtained using MDD-HPLC [13], was subsequently confirmed by traditional metabolic ^{3}H-inositol labelling and Sax-HPLC technology [15]. Strikingly, however, our extraction and PAGE analysis reveals substantially higher levels of inositol pyrophosphates during vegetative state growth (Fig. 1, 2, 3, 4). DAPI analysis reveals a markedly darker stain of the IP_8 band over IP_6 (Fig. 1B). This can be attributed to the favorable ability of the pyrophosphates moiety to photobleach DAPI [26]. The monoaminic Toluidine, however, stains the single phosphates groups with similar efficiency. Therefore a molecule of IP_8 possessing 8 phosphate groups, compared to just 6 on a molecule of IP_6 groups should stain more intensely than IP_6. Experimentally this value has been calculated to be 1.27+/-0.08 (see material and methods for details and Figure S2). However, even taking into account this correction factor, densitometry measurement of PAGE analysis revealed the ratio of IP_8 to IP_6 in the vegetative state to be in the range 30-40% (Fig. 1, 2, 3, 4). Therefore, traditional HPLC technology substantially underestimates the level of cellular inositol pyrophosphates. It is likely that this effect is due to the fact that pyrophosphate (phosphoanhydride) bonds are acid labile and prone to degradation during acidic HPLC running conditions. To further confirm this observation we ran cultures in parallel; one labelled with ^{3}H-inositol and analysed by HPLC, while the second was run by PAGE and analysed by Toluidine staining. We rapidly extracted the inositol phosphates at 4°C to minimise the duration and effect of the acidic conditions. This parallel analysis, reveals that the IP_8 level as ratio over IP_6 was 27.5%+/-6.9 (n=4) and 36.3%+/-4.7 (n=4) analysed by Sax-HPLC or PAGE respectively. Therefore traditional HPLC analysis results in a substantial 1/4 underestimation of IP_8 cellular levels. Application of PAGE to this in vivo system for the first time allows us to determine the intracellular concentration of highly phosphorylated inositol phosphates by simple densitometry (using IP_6 concentration standards to simply calculate a linear regression curve). Our study reveals that in vegetative state, estimating a cell volume of 0.20pL, the concentration of IP_6, IP_7 and IP_8 are ~520, 60 and 180µM respectively. Interestingly, the IP_6 value is in accordance with previous estimates [5,33].

Inositol pyrophosphates cellular levels increase during development.

Dictyostelium development occurs upon exhaustion of food supply. This starvation response can be induced by shifting vegetative *D. discoideum* cells to agar plates made with a simple phosphate buffer (see material and methods). The regulation of inositol pyrophosphate metabolism during the slime mould's developmental program has been previously investigated [13]. This study revealed the most dramatic cellular concentration change in IP_7 and IP_8 so far reported, with a 25-fold increase of IP_8 level [13]. However, our observations that IP_7 and IP_8 are present at high levels in vegetative cells (Fig. 1 to 4) led us to question the scale of this dramatic increase. Therefore we subjected WT and *ip6k* null cells to starvation, inducing the developmental program. Cells were grown to a density of 2×10^6 cells/ml, washed in phosphate buffer and then plated onto 20mM phosphate buffer agar plates. Cells were collected at 5 time points; time zero, whilst still in the vegetative state; after one hour of starvation; upon first visual signs of aggregation (6-9hrs depending on strain); during the "slug" stage 15-17hrs after induction of starvation and finally after 24hrs as mature fruiting bodies. Analysis of acidic cell extract shows a clear increase of IP_8 (in comparison to IP_6) of 2,6 fold during the developmental time course. Therefore, although we observe a clear and substantial increase in IP_8 levels (Fig. 5A), it is in the region of three fold, well below the 25-fold seen previously by HPLC analysis [13]. We also performed developmental study of *ip6k* null stain (fig. 1) [15]. This analysis revealed the lack of induction of any inositol pyrophosphate forms (Fig. 5B). This data indicates that the *D. discoideum* PP-IP_5K homologous gene (DDB_G0284617) does not play any major role in the developmental increase of inositol pyrophosphates. The *D. discoideum* development program is elicited by cAMP signal and it was reported that cAMP stimulation induced a rapid (within minutes) threefold increase in inositol pyrophosphate levels [15]. We repeated these studies and failed to see any significant change in IP_7 and IP_8 levels in response to cAMP when analysed by PAGE (Fig. 6).

Discussion

The recently developed PAGE technology to resolve and visualise inositol phosphates has been previously employed to characterise *in vitro* enzymatic reaction [26,27]. Here we show the huge potential of this technology to study inositol pyrophosphate metabolism in *D. discoideum*. The high abundance of this class of molecules in *D. discoideum*, coupled with the ease of analysis by PAGE has allowed us to re-evaluate the regulation of inositol pyrophosphate metabolism during the amoeba development. This re-evaluation has revealed a 3-fold increase in IP_8 levels reached in mature fruiting bodies a value far below the 25-fold increase that was previously determined by MDD-HPLC [13]. MDD-HPLC technology requires the extracted samples to be resolved using an elution buffer containing 0.1M Hydrochloric Acid [13]. This condition is likely to result in the hydrolysis of pyrophosphate bonds and thus increased variability between samples. Therefore, the difference of IP_8 induction during *Dictyostelium* development between our PAGE analysis and the previous study [13] is most likely due to the acidic sensitivity of the pyrophosphate moiety and its degradation during the strong acidic conditions associated with MDD-HPLC. In agreement with this, analysis of ^{3}H-inositol labelled inositol pyrophosphates by Sax-HPLC, a technology that requires less acidic conditions (Ammonium Phosphate buffer at pH3.8) reveals that the IP_8 ratio over IP_6 is ~27% higher than previous studies suggested [13]. However, pyrophosphate hydrolysis still occurs in the mildly acidic Sax-HPLC running conditions. In fact, when the IP_8 ratio over IP_6 ratio was measured by PAGE and densitometry (sample resolved in 1XTBE, buffer pH8.0) this value was still higher at ~36%. Therefore both in vitro study [26] and also the current in vivo PAGE analysis suggest that HPLC analysis underestimates the cellular levels of inositol pyrophosphates. Unfortunately, technical problems still preclude the application of PAGE analysis to mammalian cells. As such, HPLC analysis remains, at least for now, the only viable method for this system. We have also demonstrated that PAGE can resolve several of the different IP_5 isomeric species (Fig. 4A). This has allowed us to observe at least three different IP_5 isomers in vegetative *D. discoideum* consistent with early reports [5,31]. This is not a surprise as mammalian cells also possess multiple IP_5 species [34,35]. Unexpectedly, all the IP_5s species are precursors of inositol pyrophosphates. Therefore, the inositol pyrophosphates derived from IP_5 are quite complex in compositions, with multiple isomeric forms of PP-IP_4 and $(PP)_2$-IP_3 existing *in vivo*. The same enzymes that generate IP_7 from IP_6, the IP6Ks, also generate these inositol pyrophosphates species in vitro [16,29]. Thus the relative cellular abundance between IP_7/IP_8 and PP-IP_4/$(PP)_2$-IP_3 might depend on the levels of IP_5 versus IP_6. While in *D. discoideum* IP_6

is far more abundant of IP_5 this is not the case the majority of mammalian cell lines where the cellular concentration of these two inositol polyphosphates are similar and regulated in neuron by neurotrofine signal [36]. Consequently inositol pyrophosphate derived from both IP_5 and IP_6 precursors are likely to have similar cellular abundance and physiological importance. More attention needs to be invested to study the functions of the IP_5 derived inositol pyrophosphates. The fact that PP-IP_4 is often undetected on Sax-HPLC (due to co-migration with IP_6), is neither an indicator of its absence nor of a lack of physiological roles. The simple, inexpensive and reliable PAGE analysis leads to clear qualitative and quantitative information by using simple densitometry. Classical ^{3}H-inositol labelling and Sax-HPLC analysis of highly phosphorylated inositol perhaps retains the advantage of a higher dynamic range to calculate the relative abundance of the inositol polyphosphates. However, the use of radioactive material and HPLC apparatus has limited the implementation of inositol phosphate research to the large majority of cell biology laboratories. Here we have demonstrated the huge potential of PAGE technology to study *D. discoideum* inositol phosphate metabolism. PAGE analysis coupled with the generation of the knockout mutant strains for the several inositol phosphate kinases present in the amoeba genome will create a genetic system that will easily surpass the *S. cerevisiae* model, due to the higher complexity and greater similarity to the mammalian system . The obvious future objective is to apply this PAGE technology to analyse inositol pyrophosphate metabolism in mammalian experimental models. However, because of the low abundance of inositol polyphosphate in mammalian cells, the direct application of PAGE technology to this system is not yet possible (Saiardi lab unpublished result). On the other hand, the effortless nature of PAGE technology should encourage further effort towards this goal, thereby opening new avenues for investigation.

Acknowledgments

We thank Antonella Riccio for suggestions and helpful comments and the members of Saiardi lab for discussion.

Materials and methods

Strains, Media and Reagents.

We used the axenic *D. discoideum* strain AX2, *ip6k* null (axeA2,axeB2,axeC2,I6KA [KOvector], bsR) and *plc* null (axeA1, axeB1, axeC1, plc-[pNeoPLCko], neoR) background have been previously described [15,18] and were obtained from dictyBase (http://dictybase.org). *D. discoideum* was generally grown in HL/5 or SIH acquired from Foremedium in presence of penicillin and streptomycin (Gibco). Polyacrylamides, TEMED, ammonium persulfate, were acquired from National Diagnostic. Inositol phosphates were acquired from Calbiochem (IP_6) and Sichem (IP_5s). All others reagents were purchased from the Sigma-Aldrich. Recombinant His-DDP1 was expressed and purified as previously described [8].

Culture condition and cAMP treatment.

Amoeba cells were inoculated at a density of 1×10^5 cells/ml in HL5 in a glass flask, and incubated with shaking at 22°C, 120 RPM. To keep the cells in the vegetative state, stock cultures were diluted every 2-3 days such that cell density didn't surpass $5\text{-}6\times10^6$ cells/ml. Every 2-3 weeks new *D. discoideum* were started from DMSO stock. Treatment with cAMP was performed on active growing vegetative stage cell. cAMP was added to a final concentration of 50µM to100µl of cells and the treatments were terminate by adding 100µl of Perchloric Acid 2M to initiate inositol phosphate extraction.

Inositol phosphates Extraction.

The inositol polyphosphate extraction procedure is an adaptation of the yeast protocol previously described [28]. *D. discoideum* cells were collected during the exponential growth phase ($1\text{-}3\times10^6$ cells/ml) washed twice with KPO_4H buffer 20mM pH6.0 and centrifuged at 1500 RPM on a Sorval RC-3C centrifuge for 3min. The cell pellets were transferred to eppendorf tubes, resuspended in 1M Perchloric acid, vortexed for 5min at 4°C and centrifuged at 14000 RPM at 4°C for 5min. The supernatants were transferred to a new tube and neutralised using 1M Potassium Carbonate containing 3mM EDTA. The samples were placed on ice for 2-3 hours and subsequently spun for 10min. The supernatants were transferred to new tubes and stored at 4^oC. If required, the supernatants volume was reduced using a speed vacuum.

PAGE analysis and band intensity analysis.

To resolve inositol phosphates we used 24×16×0.1 cm glass plates, using 35% polyacrylamide in 1XTBE. Samples were mixed with 6×Dye (0.01% Orange G or Bromophenol Blue; 30% glycerol; 10mM TrisHCl pH7.4; 1mM EDTA). Gels were pre-run for 30min at 300V and run at 600V 6mA overnight at 4°C until the Orange G had run through 2/3 of the gel. Gels were stained with DAPI or Toluidine Blue as described previously [26]. After scanning, the Tiff format file, band densitometry was performed using ImageJ software (http://rsbweb.nih.gov/ij/). To determine the differential Toluidine Blue staining efficiency pure IP_8 and IP_7 were converted to IP_6 by acid hydrolysis and resolved by PAGE. The different densitometry intensity of IP_7 and IP_8 untreated samples versus the generated IP_6 was then calculated (Supporting Fig. 2). IP8 is 1.27+/-0.08 (average +/- standard deviation, n=5) times more strongly labelled that than corresponded generated IP_6, in good accordance with the theoretical value of 1.33. To determine the amount of inositol phosphates present in *D. discoideum*, cell extracts were run together with IP_6 concentration standards from 1nM to 8nM. By determining the densitometry value of the IP_6 standard a linear regression curve was calculated. The densitometry value of the IP_6 present in the cell extract was calculated from the linear regression curve to determine its molar amount. The values for IP_7 and IP_8 were calculated determining the densitometry of the respective bands normalized for the Toluidine staining efficiency (1.27 for IP_8 and 1.15 for IP_7). The cellular concentration of inositol phosphate was then calculated estimating a cell volume of 0.20pL.

Enzymatic Reactions and Acid Hydrolysis.

Neutralised *D. discoideum* cell extract, or purified inositol phosphate, were incubated in 30µl enzymatic reactions containing 5XBuffer (100mM Hepes pH6.8; 250mM NaCl; 30mM MgSO4; 5mM DTT; 5mM NaF), 2µl of recombinant purified Ddp1 (10-2-ng) or Phytase (Sigma). Reactions were incubated at 37°C for 2hrs or overnight and stopped by the addition of 2µl EDTA (100mM). Acidic pyrophosphate hydrolysis was performed by incubating the cell extract at 90°C for 20min prior to neutralisation. After this treatment the samples were neutralised using Potassium Carbonate as described above.

Mass spectrometry.

Inositol phosphates from *D. discoideum* cell extract were purified as described above and previously [28] and directly subjected to mass spectrometry [37]. Matrix-assisted laser desorption ionization (MALDI) mass spectrometry was performed on a Voyager DE-STR

(Applied Biosystems, Framingham, MA), equipped with a MALDI ion source and a time-of-flight mass analyzer (MALDI-TOF). 9-aminoacridine (9-AA, Sigma-Aldrich) was used as matrix, due to its superior performance in revealing acidic analytes in negative ion mode [37]. A double deposition sample preparation procedure was adopted. Typically, 0.5μL of matrix solution, consisting of 7 mg/mL 9-AA in a 1:1 mixture (v/v) of acetonitrile and water was spotted on the stainless steel MALDI sample stage and air-dried. Then, 0.5μL of the analyte solution, either pure or diluted 1:5 (v/v) in water, was spotted on to the matrix crystals and allowed to dry. Mass spectra were acquired in delayed extraction, reflectron negative ion mode using the following settings: accelerating voltage 20,000V, grid voltage 73%, extraction delay time 300nsec, acquisition mass range 300-1,500 *m/z*. Each spectrum was the average of 400-500 individual laser shots acquired in series of 100 consecutive shots.

Sax-HPLC analysis.

D. discoideum were cultured in inositol free SIH media containing 50μCi/ml [^{3}H]-inositol. Cell culture (6ml) were seeded at 1×10^5 cells/ml and grown at 22°C for 3-4 days to get a cell density of $2\text{-}3\times10^6$/ml. Cells were collected and washed once with KPO_4H buffer 20mM pH6.0. Inositol phosphates were extracted as described above and resolved by HPLC as previously described [28].

D. discoideum development.

D. discoideum were cultured in HL/5 media to a density of 2.0×10^6 cells/ml The cells were washed twice with KPO_4H buffer 20mM pH6.0 and resuspended at 1×10^7 cells/ml in the same buffer. Cells were then transferred in solution to 35mm, 20mM phosphate agar plates such that each plate contained 1×10^7 cells. The cells were allowed to settle before aspirating the phosphate buffer. The cells were then allowed to develop in a humidity chamber at 22^{o}C. 10 plates (equivalent to a 1×10^8 cells at the start of the time course) were harvested from plates at 5 time points; 0hr during vegetative state; after 1hr starvation; upon first signs of aggregation (6-9hrs); during the "slug" stage (15hrs); and finally as mature fruiting bodies (24-25hrs). Cells pellets were frozen at -80°C. Inositol polyphosphates were extracted as described above, normalised by protein concentration and analysed by PAGE.

References

1. Franca-Koh, J., Kamimura, Y., Devreotes, P., (2006) Navigating signaling networks: chemotaxis in *Dictyostelium discoideum*. Curr Opin Genet Dev 16: 333-338.

2. Muramoto, T., Cannon, D., Gierlinski, M., Corrigan, A., Barton, G. J., et al., (2012) Live imaging of nascent RNA dynamics reveals distinct types of transcriptional pulse regulation. Proc Natl Acad Sci U S A 109: 7350-7355.

3. Van Haastert, P. J., (1995) Transduction of the chemotactic cAMP signal across the plasma membrane of *Dictyostelium* cells. Experientia 51: 1144-1154.

4. Newell, P. C., Europe-Finner, G. N., Small, N. V., Liu, G., (1988) Inositol phosphates, G-proteins and ras genes involved in chemotactic signal transduction of *Dictyostelium*. J Cell Sci 89 (Pt 2): 123-127.

5. Stephens, L. R., Irvine, R. F., (1990) Stepwise phosphorylation of *myo*-inositol leading to *myo*-inositol hexakisphosphate in *Dictyostelium*. Nature 346: 580-583.

6. Saiardi, A., (2012) Cell signalling by inositol pyrophosphates. Subcell Biochem 59: 413-443.

7. Wilson, M. S., Livermore, T. M., Saiardi, A., (2013) Inositol pyrophosphates: between signalling and metabolism. Biochem J 452: 369-379.

8. Lonetti, A., Szijgyarto, Z., Bosch, D., Loss, O., Azevedo, C., et al., (2011) Identification of an evolutionarily conserved family of inorganic polyphosphate endopolyphosphatases. J Biol Chem 286: 31966-31974.

9. Saiardi, A., (2012) How inositol pyrophosphates control cellular phosphate homeostasis? Adv Biol Regul 52: 351-359.

10. Szijgyarto, Z., Garedew, A., Azevedo, C., Saiardi, A., (2011) Influence of inositol pyrophosphates on cellular energy dynamics. Science 334: 802-805.

11. Stephens, L., Radenberg, T., Thiel, U., Vogel, G., Khoo, K. H., et al., (1993) The detection, purification, structural characterization, and metabolism of diphosphoinositol pentakisphosphate(s) and bisdiphosphoinositol tetrakisphosphate(s). J Biol Chem 268: 4009-4015.

12. Menniti, F. S., Miller, R. N., Putney, J. W. Jr., Shears, S. B., (1993) Turnover of inositol polyphosphate pyrophosphates in pancreatoma cells. J Biol Chem 268: 3850-3856.

13. Laussmann, T., Pikzack, C., Thiel, U., Mayr, G. W., Vogel, G., (2000) Diphospho-*myo*-inositol phosphates during the life cycle of *Dictyostelium* and *Polysphondylium*. Eur J Biochem 267: 2447-2451.

14. Laussmann, T., Reddy, K. M., Reddy, K. K., Falck, J. R., Vogel, G., (1997) Diphospho-*myo*-inositol phosphates from *Dictyostelium* identified as D-6-diphospho-*myo*-inositol pentakisphosphate and D-5,6-bisdiphospho-*myo*-inositol tetrakisphosphate. Biochem J 322 (Pt 1): 31-33.

15. Luo, H. R., Huang, Y. E., Chen, J. C., Saiardi, A., Iijima, M., et al., (2003) Inositol pyrophosphates mediate chemotaxis in *Dictyostelium* via pleckstrin homology domain-PtdIns(3,4,5)P_3 interactions. Cell 114: 559-572.

16. Saiardi, A., Sciambi, C., McCaffery, J. M., Wendland, B., Snyder, S. H., (2002) Inositol pyrophosphates regulate endocytic trafficking. Proc Natl Acad Sci U S A 99: 14206-14211.

17. York, J. D., Odom, A. R., Murphy, R., Ives, E. B., Wente, S. R., (1999) A phospholipase C-dependent inositol polyphosphate kinase pathway required for efficient messenger RNA export. Science 285: 96-100.

18. Drayer, A. L., Van der Kaay, J., Mayr, G. W., Van Haastert, P. J., (1994) Role of phospholipase C in *Dictyostelium*: formation of inositol 1,4,5-trisphosphate and normal development in cells lacking phospholipase C activity. Embo J 13: 1601-1609.

19. Mayr, G. W., (1988) A novel metal-dye detection system permits picomolar-range h.p.l.c. analysis of inositol polyphosphates from non-radioactively labeled cell or tissue specimens. Biochem J 254: 585-591.

20. Saiardi, A., Erdjument-Bromage, H., Snowman, A. M., Tempst, P., Snyder, S. H., (1999) Synthesis of diphosphoinositol pentakisphosphate by a newly identified family of higher inositol polyphosphate kinases. Curr Biol 9: 1323-1326.

21. Fridy, P. C., Otto, J. C., Dollins, D. E., York, J. D., (2007) Cloning and characterization of two human VIP1-like inositol hexakisphosphate and diphosphoinositol pentakisphosphate kinases. J Biol Chem 282: 30754-30762.

22. Choi, J. H., Williams, J., Cho, J., Falck, J. R., Shears, S. B., (2007) Purification, sequencing, and molecular identification of a mammalian PP-InsP_5 kinase that is activated when cells are exposed to hyperosmotic stress. J Biol Chem 282: 30763-30775.

23. Draskovic, P., Saiardi, A., Bhandari, R., Burton, A., Ilc, G., et al., (2008) Inositol hexakisphosphate kinase products contain diphosphate and triphosphate groups. Chem Biol 15: 274-286.

24. Wang, H., Falck, J. R., Hall, T. M., Shears, S. B., (2011) Structural basis for an inositol pyrophosphate kinase surmounting phosphate crowding. Nat Chem Biol 8: 111-116.

25. Lin, H., Fridy, P. C., Ribeiro, A. A., Choi, J. H., Barma, D. K., et al., (2009) Structural analysis and detection of biological inositol pyrophosphates reveal that the family of VIP/diphosphoinositol pentakisphosphate kinases are 1/3-kinases. J Biol Chem 284: 1863-1872.

26. Losito, O., Szijgyarto, Z., Resnick, A. C., Saiardi, A., (2009) Inositol pyrophosphates and their unique metabolic complexity: analysis by gel electrophoresis. PLoS One 4: e5580.

27. Kilari, R. S., Weaver, J. D., Shears, S. B., Safrany, S. T., (2013) Understanding inositol pyrophosphate metabolism and function: Kinetic characterization of the DIPPs. FEBS Lett 587(21): 3464-70.

28. Azevedo, C., Saiardi, A., (2006) Extraction and analysis of soluble inositol polyphosphates from yeast. Nat Protoc 1: 2416-2422.

29. Saiardi, A., Caffrey, J. J., Snyder, S. H., Shears, S. B., (2000) The inositol hexakisphosphate kinase family. Catalytic flexibility and function in yeast vacuole biogenesis. J Biol Chem 275: 24686-24692.

30. Van Dijken, P., de Haas, J. R., Craxton, A., Erneux, C., Shears, S. B., et al., (1995) A novel, phospholipase C-independent pathway of inositol 1,4,5-trisphosphate formation in *Dictyostelium* and rat liver. J Biol Chem 270: 29724-29731.

31. Stephens, L. R., Hawkins, P. T., Stanley, A. F., Moore, T., Poyner, D. R., et al., (1991) *myo*-inositol pentakisphosphates. Structure, biological occurrence and phosphorylation to *myo*-inositol hexakisphosphate. Biochem J 275 (Pt 2): 485-499.

32. Dove, S. K., Michell, R. H., (2009) Inositol lipid-dependent functions in *Saccharomyces cerevisiae*: analysis of phosphatidylinositol phosphates. Methods Mol Biol 462: 59-74.

33. Letcher, A. J., Schell, M. J., Irvine, R. F., (2008) Do mammals make all their own inositol hexakisphosphate? Biochem J 416: 263-270.

34. McConnell, F. M., Stephens, L. R., Shears, S. B., (1991) Multiple isomers of inositol pentakisphosphate in Epstein-Barr-virus- transformed (T5-1) B-lymphocytes. Identification of inositol 1,3,4,5,6-pentakisphosphate, D-inositol 1,2,4,5,6-pentakisphosphate and L-inositol 1,2,4,5,6-pentakisphosphate. Biochem J 280 (Pt 2): 323-329.

35. Irvine, R. F., Schell, M. J., (2001) Back in the water: the return of the inositol phosphates. Nat Rev Mol Cell Biol 2: 327-338.

36. Loss, O., Wu, C. T., Riccio, A., Saiardi, A., (2013) Modulation of inositol polyphosphate levels regulates neuronal differentiation. Mol Biol Cell 24: 2981-2989.

37. Guo, Z., He, L., (2007) A binary matrix for background suppression in MALDI-MS of small molecules. Anal Bioanal Chem 387: 1939-1944.

Figure 1. PAGE analysis of *D. discoideum* cell extract reveal the presence of three major bands.

Inositol phosphates were extracted from 10ml culture growth of wild type (WT) *D. discoideum* (AX2 strain) and the IP_6-Kinase (*ip6k* null) and phospholipase C mutant (*plc* null) grown at a density of $2\text{-}4\times10^6$. About 30-40 microliters of neutralised cell extract (equivalent to 1/20 of the total volume) was resolved on 35.5% PAGE [26] and visualized with Toluidine blue (A) and DAPI staining (B). The figure shows the result of a representative experiment that was repeated three times.

Figure 2. Treatment by Phytase, Ddp1 and acidic degradation define IP_6, IP_7, and IP_8, in *D. discoideum* cell extract.

Wild type *D. discoideum* cell extract (-) was incubated with phytase (Phy) (A), recombinant diphosphoinositol polyphosphate phosphohydrolase (DDP1) (B) or treated with acid at high temperature (C). The inositol phosphate nature of the three major bands detectable by Toluidine stain is demonstrated by the Phytase treatment (A), an enzyme able to remove the phosphate group from any position of the inositol rings. The pyrophosphate nature of the two slower migrating bands is demonstrated by their disappearance after DDP1 treatment (B) and by the well-known acidic sensitivity of the phosphoanhydride bond (C). The figure shows the result of a representative experiments repeated three to four times.

Figure 3. Mass spectrometry analysis of inositol pyrophosphates purified from *D. discoideum* cell extract.

Gel purified inositol pyrophosphates (A) were subjected to mass spectrometry (B,C). The comparison of the *m/z* spectrum of IP_7 (B) and IP_8 (C) is shown. The peaks in the spectra describing inositol pyrophosphates purified from *D. discoideum* are in agreement with the theoretical values for molecular weight that are deduced to be 738.82 Da and 818.78 Da respectively.

Figure 4. Characterization of *D. discoideum* IP_5 species.

Half of the acidic cell extract (from 5ml culture) of WT *D. discoideum* was incubated on ice (-) while the second half was incubated at 90^oC for 20min (Acid). Both samples were thenneutralised and resolved on 35.5% PAGE together with the six possible IP_5 isomers. Inositol phosphates were visualised by Toluidine staining. Densitometry analysis of treated versus untreated sample was performed and IP_6 and IP_5s bands intensity compared. (A)

Acidic treatment reveals the distinct presence of three IP_5 species, which are otherwise barely detectable, indicating that *D. discoideum* possesses a complex IP_5-derived inositol pyrophosphate metabolism. (B) Schematic representation of inositol pyrophosphate metabolism in *D. discoideum*. The gray arrow to $(PP)_2$-IP_3 indicates a likely potentially step. The dashed arrow from inositol to IP_3 indicates uncharacterized enzymatic steps. The figure shows the result of a representative experiment that was repeated three times.

Figure 5. PAGE analysis of inositol pyrophosphate during *D. discoideum* development.
Amoeba development program was induced as described in material and methods. The inositol phosphates extracted at the indicated time points were resolved on 35% PAGE and visualised with Toluidine. (A) The analysis of wild type (WT) *D. discoideum* developmental program reveal a 2.6 fold increase in the IP_8/IP_6 ratio at the late stage of development, as quantified by densitometry quantified (Bottom), average +/- SD of four independent experiments. (B) To the contrary inositol pyrophosphates are not induced during IP_6-Kinase (*ip6k* null) developmental program. The figure shows the result of a representative experiment that was repeated four times for the WT and two times for *ip6k1* null.

Figure 6. No alteration of IP_7 and IP_8 metabolism after cAMP treatment.
Vegetative growing *D. discoideum* were incubated for the indicated time with 50µM cAMP. The incubation was terminated with equal volume of 2M Perchloric acid to extract the inositol phosphates. These were resolved on 35% PAGE and stained with Toluidine blue. Two independent experiments are shown with short (left) and long (right) cAMP incubation time. The figure shows the result of a representative experiment that was repeated three times.

Figure S1. IP_5 isomerisation by acid treatment.
To verify that acid treatment of IP_5 can induce movement of phosphate groups around the inositol ring we incubated 2nmol of IP_6 and 2nmol of I(1,3,4,5,6)P_5 with1M Perchloric acid for 30 min in ice as well as for 5 and 30 minutes at 90°C. IP_6 is totally unaffected by these treatments. Untreated I(1,3,4,5,6)P_5 (lane 2) is 95% pure as demonstrated by its migration as a major single band. Low temperature acid treatment has no effect on I(1,3,4,5,6)P_5, whilst high temperature induces rapid isomerisation. Just five minute at high temperature are sufficient to substantially convert I(1,3,4,5,6)P_5 into other IP_5 isomeric forms. Densitometry analysis confirmed that the total IP_5 Toluidine staining did not change upon acid treatment, indicating the absence of acid induced IP_5 degradation to lower inositol phosphates.

Figure S2. Differential Toluidine Blue staining capability of IP_8 and IP_6.

To ascertain the relative efficiency of staining of IP_8 and IP_6 by Toluidine blue serial amounts of IP_8 from 1nmol (A) to 16nmol (E) were incubated in the presence of 1M Percloric acid in 20µl (sample from A' to E') for 30 min at 90°C. Untreated (from A to E) and acid treated (from A' to E') samples were resolved on 35% PAGE. To avoid loss of material during the neutralization step, acid treated samples were directly loaded on the gel causing a slight retardation in migration in these lanes (as shown by the different migration of Bromophenol blue (BBF) between treated and untreated samples). Once stained with Toluidine blue, the gel was analyzed with Image J software. Densitometry analysis enabled each pair of samples (treated and untreated) to be plotted on a graph. The areas of the peaks in these graphs correspond to the relative staining of the IP_6 and IP_8 bands on the gel. Depicted are the analyses of samples D_D' and E_E'. Dividing the densitometry derived values for untreated IP_8 by those for the acid generated IP_6 indicates the difference in staining efficiency of the two molecules by Toluidine blue. On average IP_8 is stained 1.27+/-0.08 (+/- SD) better than IP_6. A virtually identical result was obtained from a second, independent experiment also run in quintuplicate. The experimentally calculated value of 1.27 is in good accordance with the theoretical value of 1.33 reflecting the presence of eight phosphates groups in IP_8 rather than the six in IP_6 (8/6 =1.33).

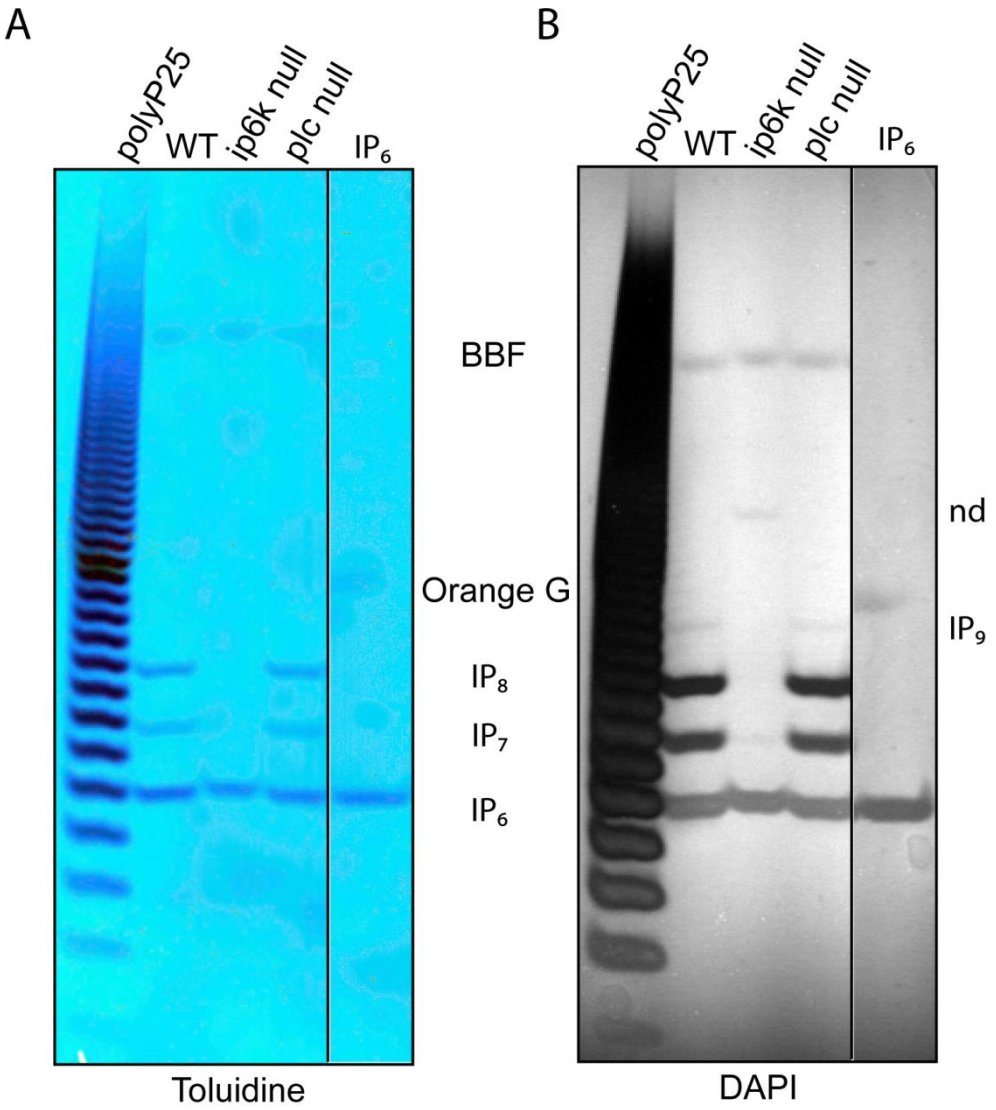
A
polyP25
WT
ip6k null
plc null
IP6
Toluidine
BBF
Orange G
IP8
IP7
IP6
B
polyP25
WT
ip6k null
plc null
IP6
DAPI
nd
IP9

Figure 1

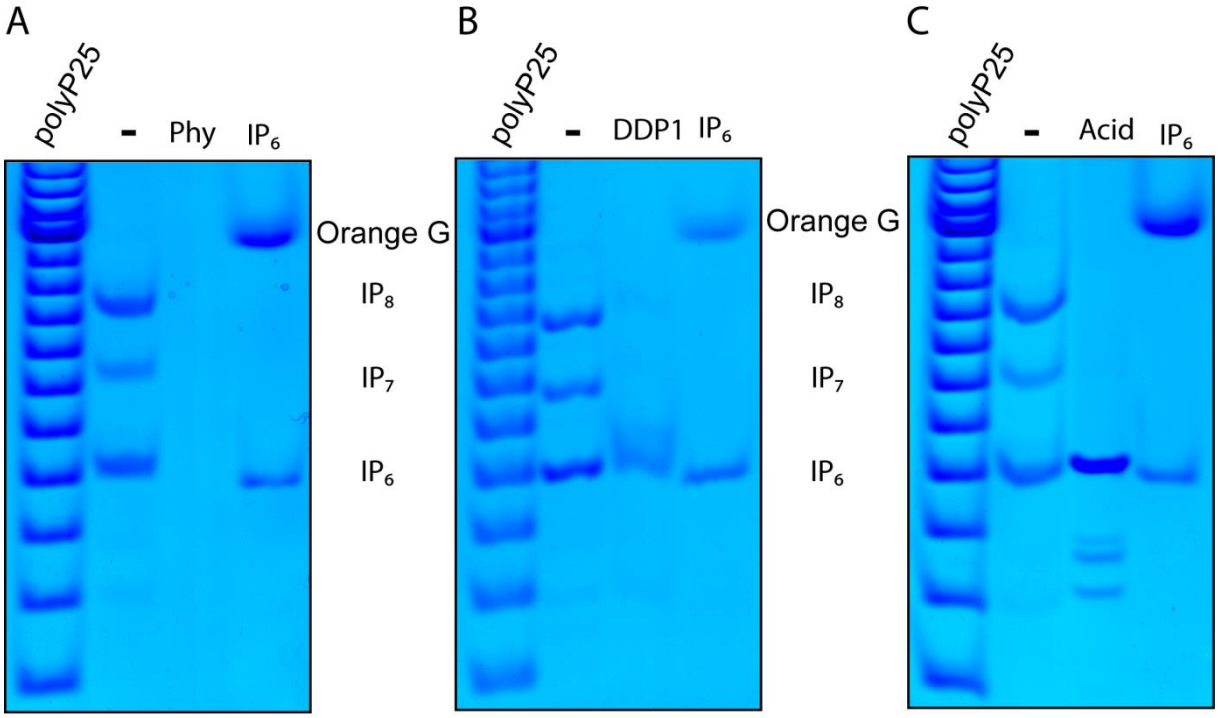
A
polyP25
-
Phy
IP6
Orange G
IP8
IP7
IP6
B
polyP25
-
DDP1
IP6
Orange G
IP8
IP7
IP6
C
polyP25
-
Acid
IP6

Figure 2

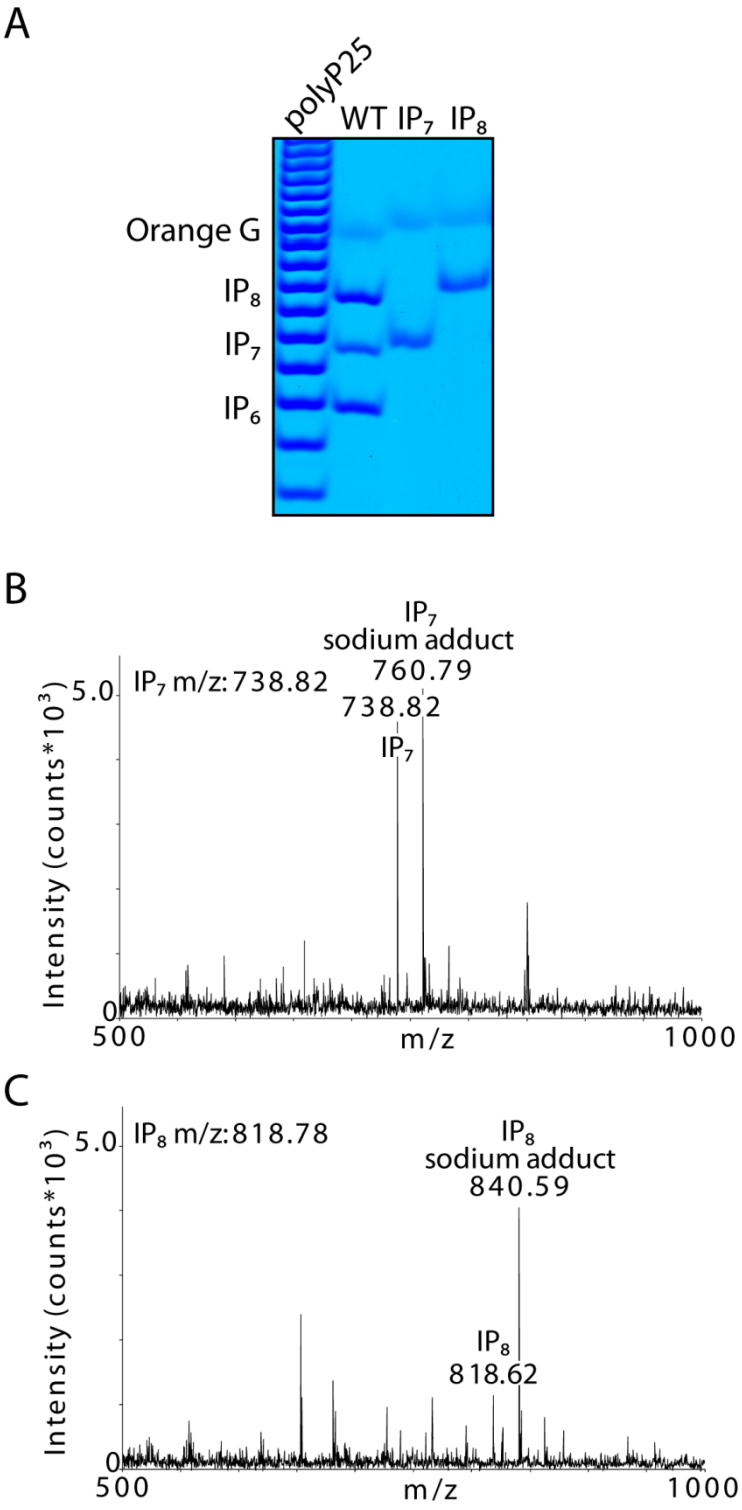
A
polyP25
WT IP7 IP8
Orange G
IP8
IP7
IP6
B
IP7
sodium adduct
760.79
IP7 m/z: 738.82
738.82
IP7
Intensity (counts*10^3)
5.0
0
500
m/z
1000
C
IP8 m/z: 818.78
IP8
sodium adduct
840.59
IP8
818.62
Intensity (counts*10^3)
5.0
0
500
m/z
1000

Figure 3

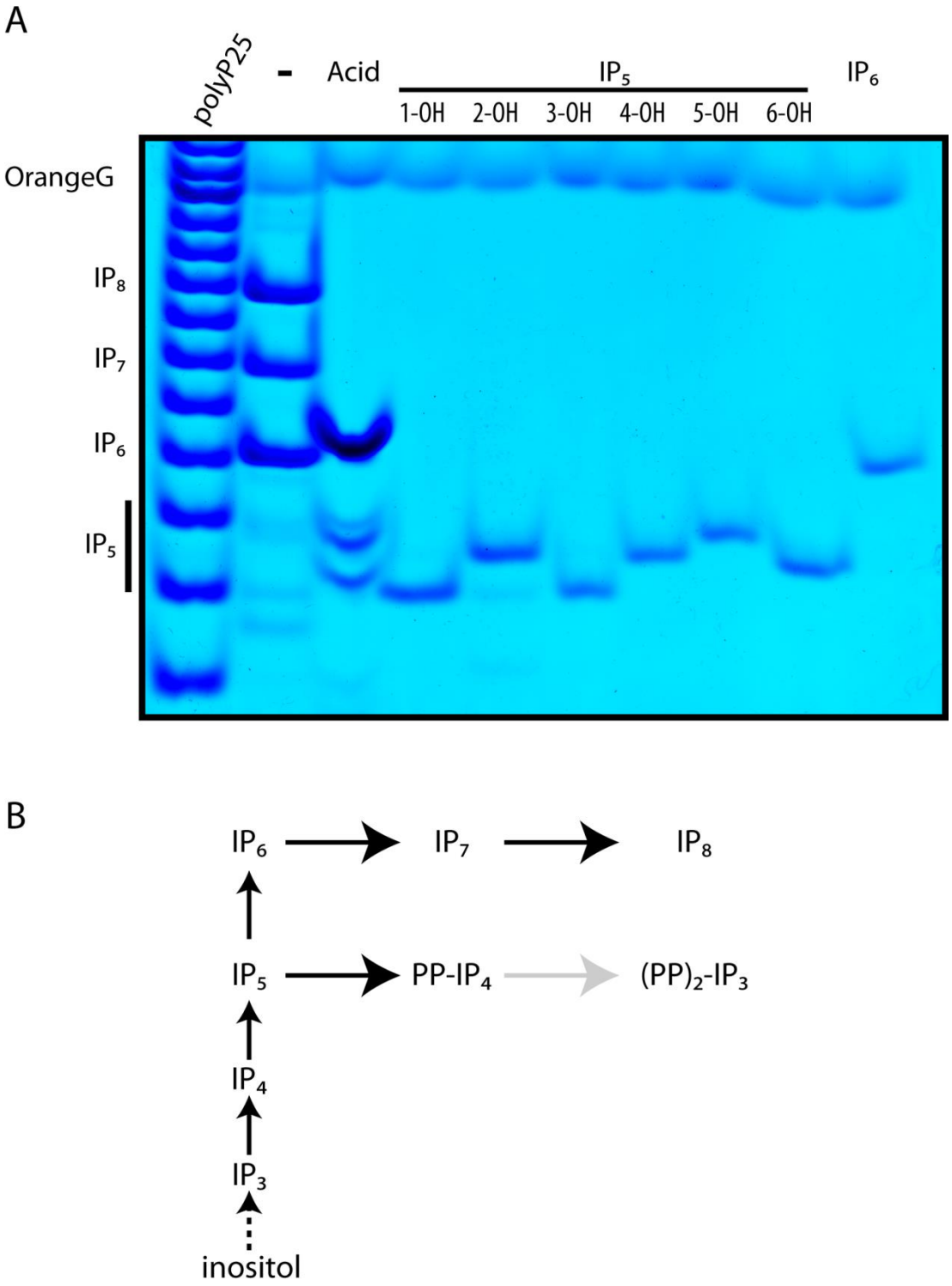
A
polyP25
-
Acid
IP5
IP6
1-OH
2-OH
3-OH
4-OH
5-OH
6-OH
OrangeG
IP8
IP7
IP6
IP5
B
IP6
IP7
IP8
IP5
PP-IP4
(PP)2-IP3
IP4
IP3
inositol

Figure 4

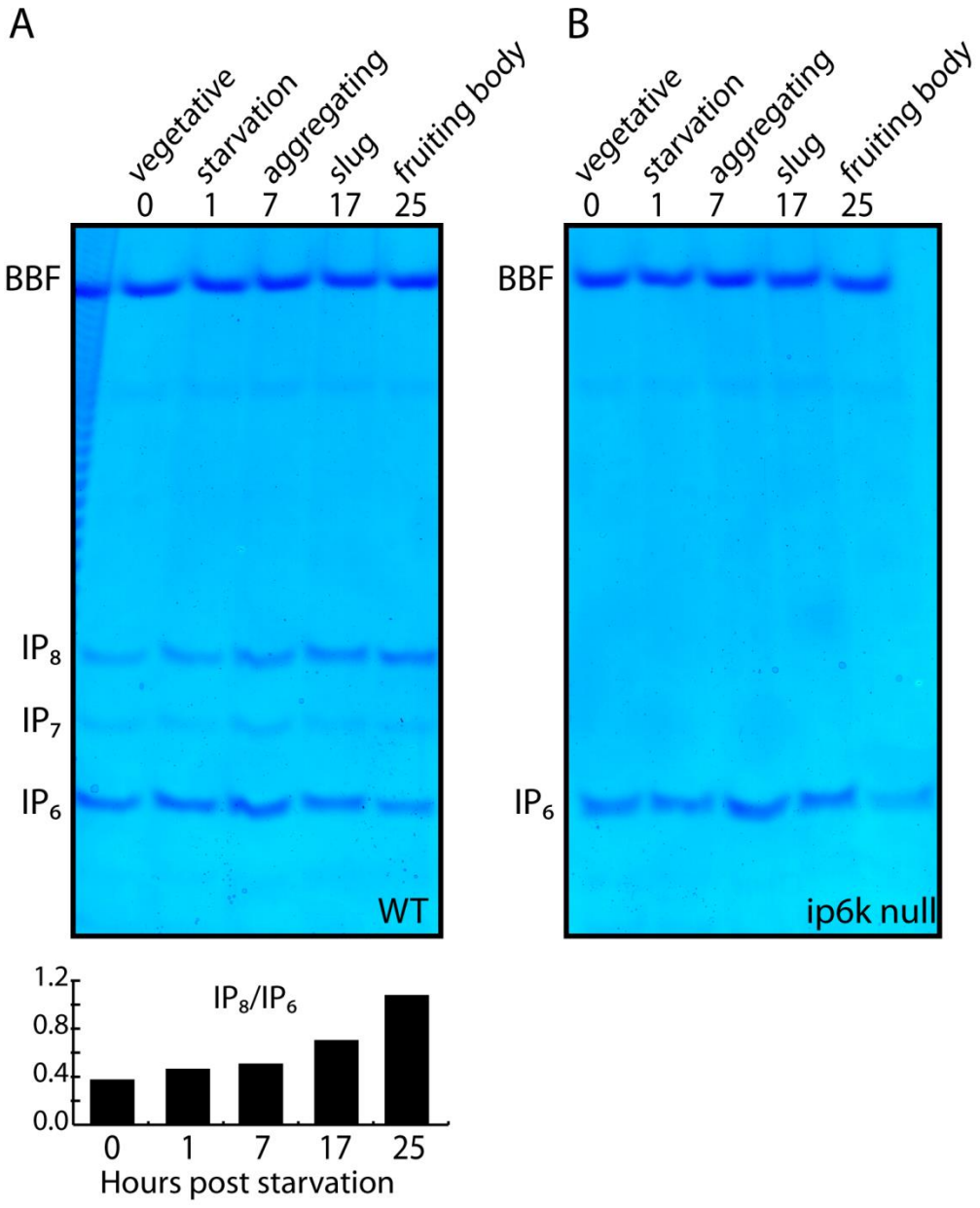
A
B
vegetative
starvation
aggregating
slug
fruiting body
0
1
7
17
25
BBF
IP8
IP7
IP6
WT
ip6k null
IP8/IP6
1.2
0.8
0.4
0.0
Hours post starvation

Figure 5

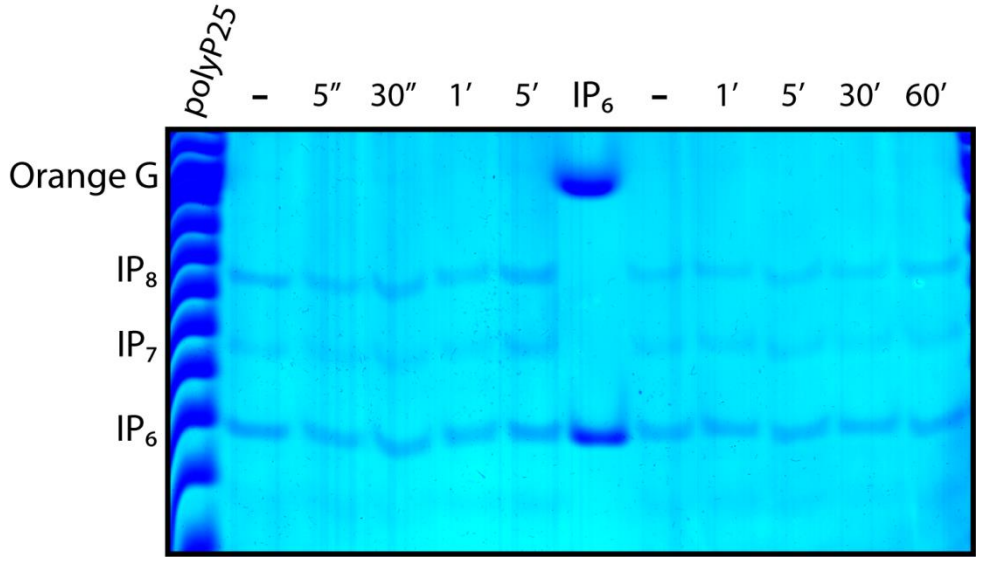

Figure 6

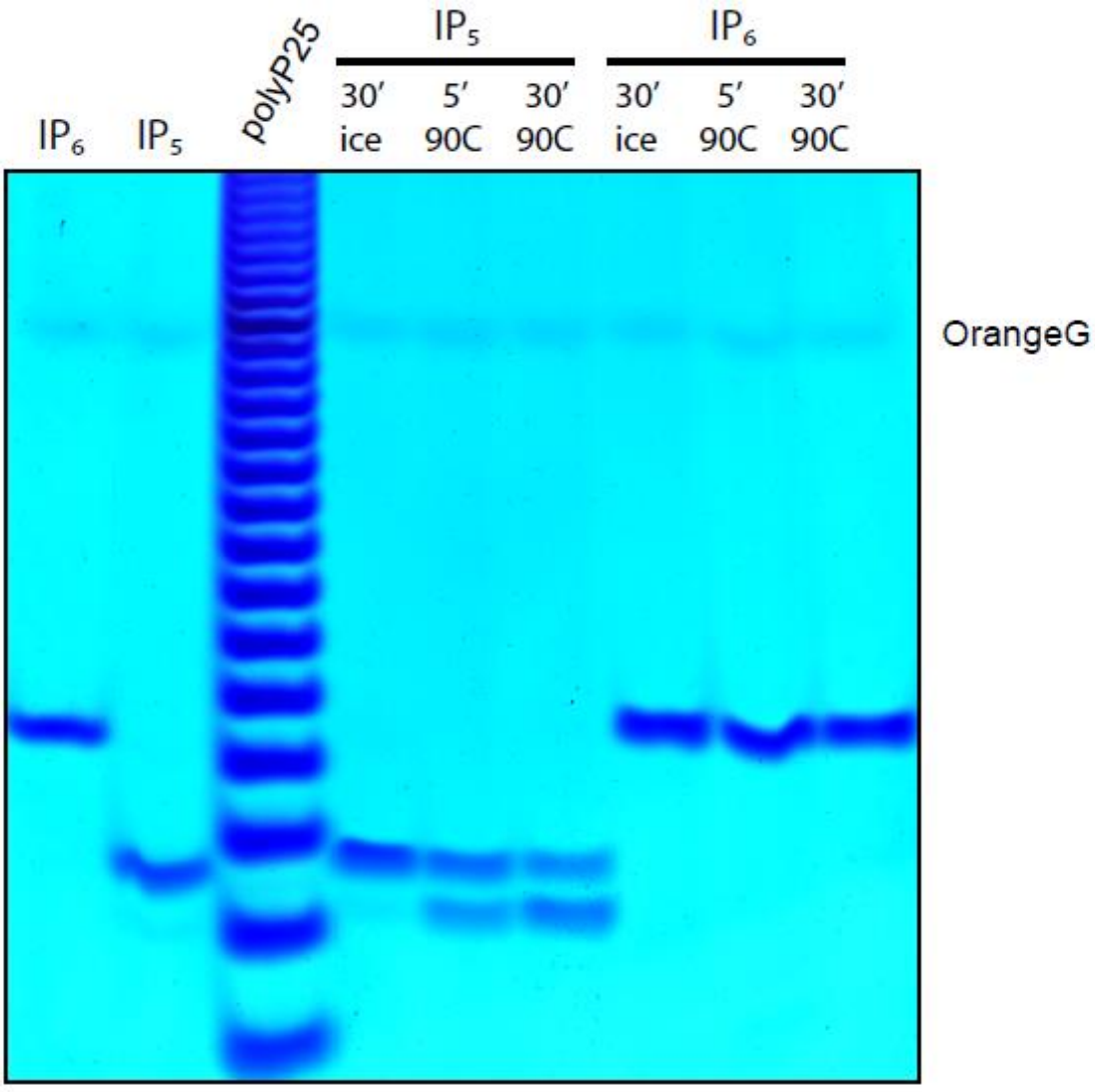
IP6
IP5
polyP25
IP5
30′ ice
5′ 90C
30′ 90C
IP6
30′ ice
5′ 90C
30′ 90C
OrangeG

Figure S1

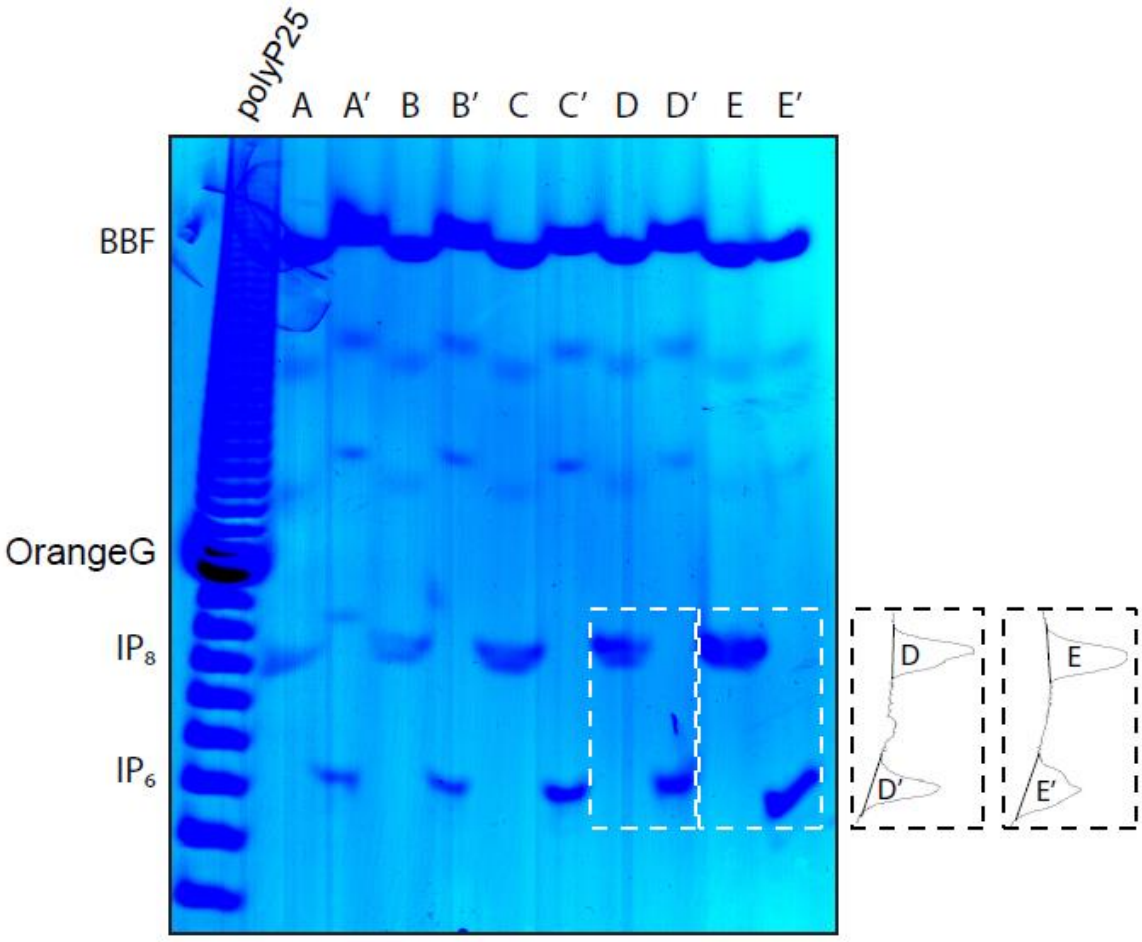

Figure S2

CHAPTER III

Conclusive remarks

In my thesis I reported the investigation of inositol pyrophosphates by PAGE in *Dictyostelium discoideum (D. discoideum)*. We found that this amoeba possesses three bands corresponding to IP_6 and its derivative inositol pyrophosphates, IP_7 and IP_8. We also demonstrated that cAMP does not induce inositol pyrophosphates synthesis as previously reported.

Our study also revealed much higher levels of inositol pyrophosphates in the vegetative state and a three-fold increase in IP_8 during development of *D. discoideum* than previously detected. We used biochemical analysis and genetic evidences to confirm the nature of these bands. We also used mass spectrometry to determine the mass of the purified bands.

Additionally, we discovered that this amoeba possesses three different inositol pentakisphosphates (IP_5) isomers. Furthermore, by analyzing the existence of an elaborated IP_5 derived inositol pyrophosphates metabolism, we evidenced the presence of inositol pyrophosphate generated from IP_5, such PP-IP_4 and likely also $(PP)_2$-IP_3. The inositol pyrophosphates PP-IP_4 and $(PP)_2$-IP_3 possessing six and seven phosphates groups migrate very closely (or co-migrate) with the more abundant IP_6 and IP_7 species.

We also identified in *D. discoideum* a 'new molecule', IP_9, so far detected only from in vitro biochemical reactions; however we were unable to determine the mass of the IP_9 band.

On the whole, these results have allowed us to re-evaluate the regulation of inositol pyrophosphate metabolism during the amoeba development. It has been possible to obtain these results, firstly because *D. discoideum* possesses high levels of this class of molecules and consequently because the PAGE technology has showed huge potential to study inositol pyrophosphate metabolism in this amoeba.

APPENDIX

Common polymorphisms in nitric oxide synthase (NOS) genes influence quality of aging and longevity in humans

Montesanto A., Crocco P., Tallaro F., Pisani F., Mazzei B., Mari V., Corsonello A., Lattanzio F., Passarino G., Rose G.

Department of Biology, Ecology and Earth Science, University of Calabria, 87036 Rende, Italy.

Biogerontology (2013) 14:177–186
DOI 10.1007/s10522-013-9421-z

RESEARCH ARTICLE

Common polymorphisms in nitric oxide synthase (*NOS*) genes influence quality of aging and longevity in humans

Alberto Montesanto · Paolina Crocco · Federica Tallaro · Francesca Pisani · Bruno Mazzei · Vincenzo Mari · Andrea Corsonello · Fabrizia Lattanzio · Giuseppe Passarino · Giuseppina Rose

Received: 29 January 2013 / Accepted: 3 April 2013 / Published online: 10 April 2013

Abstract Nitric oxide (NO) triggers multiple signal transduction pathways and contributes to the control of numerous cellular functions. Previous studies have shown in model organisms that the alteration of NO production has important effects on aging and lifespan. We studied in a large sample (763 subjects, age range 19–107 years) the variability of the three human genes (*NOS1, -2, -3*) coding for the three isoforms of the NADPH-dependent enzymes named NO synthases (NOS) which are responsible of NO synthesis. We have then verified if the variability of these genes is associated with longevity, and with a number of geriatric parameters. We found that gene variation of *NOS1* and *NOS2* was associated with longevity. In addition *NOS1* rs1879417 was also found to be associated with a lower cognitive performance, while *NOS2* rs2297518 polymorphism showed to be associated with physical performance. Moreover, SNPs in the *NOS1* and *NOS3* genes were respectively associated with the presence of depression symptoms and disability, two of the main factors affecting quality of life in older individuals. On the whole, our study shows that genetic variability of *NOS* genes has an effect on common age related phenotypes and longevity in humans as well as previously reported for model organisms.

Keywords NOS · Longevity · Aging · Nitric oxide · Polymorphisms

Alberto Montesanto and Paolina Crocco contributed equally to this study.

Electronic supplementary material The online version of this article (doi:10.1007/s10522-013-9421-z) contains supplementary material, which is available to authorized users.

A. Montesanto · P. Crocco · F. Tallaro · F. Pisani · G. Passarino · G. Rose (✉)
Department of Biology, Ecology and Earth Science, University of Calabria, 87036 Rende, Italy
e-mail: pinarose@unical.it

B. Mazzei · V. Mari · A. Corsonello
Italian National Research Center on Aging (INRCA), 87100 Cosenza, Italy

F. Lattanzio
Scientific Direction of Italian National Research Center on Aging (INRCA), 60124 Ancona, Italy

Introduction

Nitric oxide (NO) is one of the most widespread signaling molecules in nature. By interacting with different intracellular targets, NO triggers multiple signal transduction pathways thus contributing to the control of almost every cellular function (Liaudet et al. 2000). NO is produced during the oxidation of L-arginine to L-citrulline by a family of NADPH-dependent enzymes named NO synthases (NOS), with three isoforms in mammals encoded by three distinct *NOS* genes, named neuronal (*nNOS* or *NOS1*), inducible (*iNOS* or *NOS2*), and endothelial (*eNOS* or *NOS3*). Although all isoforms share a similar

structure, the mechanisms that control their activity are quite different. *NOS1* and *NOS3* are constitutively expressed and Ca^{2+}/calmodulin-dependent, while the inducible form (*NOS2*) is induced by inflammatory stimuli and is Ca^{2+}/calmodulin-independent (Förstermann and Sessa 2012). The activity of each of these isoforms is fine-tuned by a variety of transcriptional and post-translational modifications, which may also influence the specific targeting of NOS to subcellular compartments (Oess et al. 2006). Although all three isoforms can be found in numerous tissues, the specific cell type where NOS enzymes are located is of critical importance in determining the specific outcomes of the NO signalling pathways (Villanueva and Giulivi 2010). In neuronal cells NO, which is produced principally by *NOS1,* functions as regulator of neuronal transmission, cerebral blood flow and synaptic plasticity thus acting as a neuromodulator and neuroprotective agent (Calabrese et al. 2007; Feil and Kleppisch 2008; Garthwaite 2008). In endothelial cells NO, mainly produced by *NOS3,* acts as a regulator of vascular homeostasis being involved in the regulation of smooth muscle relaxation, and in the inhibition of platelet aggregation (Kader et al. 2000; Moncada and Higgs 2006). NO produced by *NOS2* particularly in macrophages, is mainly involved in the maintenance of the immune-inflammatory response (Moilanen et al. 1997; Wink et al. 2011). The biological effects of NO, however, largely depend on the amount of NO produced. High amounts of NO or its derivative reactive nitrogen species (RNS), such as peroxynitrite (ONOO–), a highly reactive radical produced by the reaction between NO and superoxide anion (O_2^-), can trigger nitrosative modifications of proteins, lipids and nucleic acids, which in turn may impinge on cellular signaling pathways leading to cytotoxicity, neurodegeneration, and apoptotic cell death (Beckman and Koppenol 1996; Pacher et al. 2007; Calcerrada et al. 2011).

Oxidative stress is a well established hallmark of the aging process and there is strong evidence for a causal role of NO and RNS therein (McCann et al. 1998; Drew and Leeuwenburgh 2002; Torregrossa et al. 2011). Markers of nitrosative stress injury, such as nitrosylation and nitration of proteins, have been shown to increase as a function of age (Toprakci et al. 2000; Kanski et al. 2005; Kim et al. 2006). Moreover, a growing number of studies indicate that the availability and biological activity of NO is impaired during aging, and that this is a key contributing factor to the onset of age related phenotypes such as vascular and brain aging (van der Loo et al. 2000; Taddei et al. 2001; Napoli and Ignarro 2009; Brown 2010; Kawamoto et al. 2012). Although the enhanced production of O_2^- that accompanies the aging process, as well as the age-related depletion of some essential NOS substrates and cofactors, may affect the amount of bioavailable NO, an impaired activity and expression of *NOSs* has been reported to occur with age which contributes to alterations in NO signaling, and to the subsequent failure of many of the body's physiological processes (Yang et al. 2004; Strosznajder et al. 2004; Yoon et al. 2010; Cau et al. 2012; Jung et al. 2012).

Supportive evidence for a role of *NOSs* in healthy aging and lifespan extension has come from studies with knockout models. It has been shown, for instance, that in mice lacking all three *NOS* isoforms the survival rate is reduced by 80 % (Tsutsui et al. 2009). Moreover, a reduction in survival rate of about 50 %, and an attenuation of caloric restriction-induced life extension has been observed in *nos3* knockout mice (Dere et al. 2002; Nisoli et al. 2005).

Given this background, the present paper addresses the hypothesis that *NOS* genetic variants affect human aging and longevity. We analyzed common and potentially functional *NOS* SNPs in a sample group of 763 individuals from the south of Italy ranging from 19 to 107 years of age. Moreover, since the increase with age in ROS/RNS-mediated stress is accompanied by the deterioration of cognitive and physical abilities, which is one of the most important components of the quality of life in the elderly that adversely affects successful aging and longevity, we also explored the impact of *NOSs* variability on cognitive and physical performances. In this case, subjects aged 65–91 years, that is the age range where a significant increase of overall impairments occur, were analyzed.

Materials and methods

Sample

The sample analyzed in the present study included 763 (417 females and 346 males) 19–107 years old subjects (median age 81 years). All subjects were born in Calabria (southern Italy) and their parents and grandparents were native of the same area.

The sample was collected during several campaigns of recruitment (De Rango et al. 2011). Subjects older than 65 years went through a multidimensional geriatric assessment carried out by a geriatrician. In addition, each of these subjects was submitted to a home based interview by a trained operator, with the administration of a structured questionnaire for the collection of socio-demographic information, evaluation of physical, cognitive, depressive status, sensory deficits, medications, and self-reported health status. Subjects with dementia and/or neurologic disorders were not included. White blood cells (WBC) from blood buffy coats were used as source of DNA.

The analyses were carried out by dividing the sample into two sex- and age-specific classes obtained according to the survival functions of the Italian population from 1890 onward (Passarino et al. 2006). In particular, the graphs of the second derivative of these survival functions indicated that at 88 years for males and 91 for females a significant change in the slope of these functions occurs. We used these two age and sex-specific cut-offs to categorize the sample into rationally defined "thresholds of longevity". For this reason in the present study men younger than 88 and women younger than 91 years will be defined as controls ($N = 442$), while men older than 88 and women older than 91 years will be defined as cases ($N = 321$).

Ethics statement

All the subjects gave their written informed consent to use their anonymous genetic and phenotypic data for genetic studies on aging and longevity. The recruitment campaigns received the approval of the Ethical committee of the University of Calabria.

SNPs selection

Polymorphisms within the *NOS* genes were selected from literature data, and using information from public databases (http://www.ncbi.nih.gov/, http://www.hapmap.org/). The a priori selection was based on the following criteria: minor allele frequency (MAF) >10 % in Caucasians, putative functional significance (non-synonymous SNPs, SNPs located in the 5′- and 3′-UTR regions), SNPs previously investigated in association studies. For each gene the selected SNPs are reported in Table 1.

Table 1 Polymorphisms within the *NOS* genes analysed in the present study

Gene symbol	dbSNP ID	Allele (major/minor)	Physical location	Function annotation
NOS1	rs1879417	T/C	Promoter	
	rs2682826	C/T	3′UTR	
NOS2	rs10459953	G/C	5′UTR	
	rs2297518	G/A	Exon 16	Ser608Leu
NOS3	rs10277237	G/A	Promoter	
	rs1799983	G/T	Exon 7	Asp298Glu

Geriatric assessment

The variability of genes that we tested for association with longevity was also investigated in relation to accepted biomarkers of the aging process that evaluate physical, cognitive, and psychological status in the elderly population. To this purpose a subgroup of the control sample whose subjects underwent a geriatric assessment (subjects 65–91 years of age) was further analyzed ($N = 317$).

Functional activity

The management of activities of daily living (bathing, dressing, toileting, transfer from bed to chair and feeding) was assessed using a modification of the Katz' Index of ADL (Katz et al. 1970). The assessment was based on what the subject was able to do at the time of the visit. The score is given counting the number of activities in which the participant is dependent or independent at the time of the visit. In our analyses ADL scores were dichotomized as one if the subject was not independent in all five items and zero otherwise.

Physical performance

Hand grip (HG) strength was measured by using a handheld dynamometer (SMEDLEY's dynamometer TTM) while the subject was sitting with the arm close to his/her body. The test was repeated three times with the stronger hand. The maximum of these values was used in the analyses. Since HG strength is affected by age, sex and height, the scores were corrected for these factors. When a test was not carried out, it was specified if it was due to physical disabilities or because the subject refused to participate.

Depression

The Geriatric Depression Scale (GDS) is an instrument designed to measure depression in the elderly consisting of a series of yes/no questions in reference to how they felt on the day of administration (Sheikh and Yesavage 1986). A score above five is suggestive of moderate depression, while a score above ten is suggestive of severe depression. In our analyses GDS scores were dichotomized as one if the subject showed depression symptoms (GDS $>$ 5) and zero otherwise.

Cognitive performance

Mini mental state examination (MMSE) test was used to evaluate the cognitive performance in the analysed sample. It is a 30-item questionnaire that assesses orientation, episodic memory, attention, language, and construction functions (Folstein et al. 1975). Since the test is affected by age and educational status, the MMSE scores were normalized for these variables according to a standardized procedure (Grigoletto et al. 1999). In our analyses MMSE scores were dichotomized as 1 if the subject showed a normal cognitive function (MMSE $\geq$ 23) and zero otherwise.

Statistical analyses

For each polymorphism of the *NOS* genes, allele frequencies were estimated by counting genes from the observed genotypes. The Hardy–Weinberg equilibrium (HWE) was tested using the exact test proposed by Wigginton et al. (2005). Standard errors for alleles were computed according to the hypothesis of the multinomial distribution. Pairwise measures of linkage disequilibrium (LD) between the analyzed loci were calculated with the Haploview 4.2 (Barrett et al. 2005). The amount of LD was quantified by Lewontin's coefficient (D′).

Single-locus analysis

In order to test the association between the analysed phenotypes and the variability of the *NOS* genes the *RobustSNP* algorithm (a robust association test suitable for both quantitative and binary traits which also takes into account covariates) recently proposed by So and Sham (2011) was adopted. This test was based on the score test and has been implemented in the R package *RobustSNP*.

In the present study the *RobustSNP* algorithm will be applied to estimate how the variability of genes analyzed in the present study influences (i) the predisposition to human longevity (ii) the variability of functional parameters including cognitive function, functional performance and depression status. In particular, in the regression models used to test the association between the variability of analyzed genes and the human longevity, the variable sex was used as covariate In the association analyses involving the functional parameters, covariate adjustment included sex, age and height when HG scores were analyzed, only age and sex when disability and depression status were investigated. As mentioned before MMSE scores were normalized for age and educational status according to a standardized procedure reported in Grigoletto et al. (1999).

Interaction analysis

In order to explore the interaction effects between the analyzed polymorphisms on the analyzed phenotypes (longevity and functional parameters), the recently developed Model-based multifactor dimensionality reduction (MB-MDR) algorithm will be applied (Calle et al. 2010).

Results

Genetic analyses

Table 2 summarizes the main characteristics of the analyzed sample stratified by age-group as previously defined. The age distributions in males and females are reported in supplementary Fig. 1.

Supplementary Table 1 shows the genotype frequencies in cases and controls. All SNPs followed the HWE in the control group ($p > 0.05$). No linkage disequilibrium was detected at any of the loci.

NOS gene polymorphisms and longevity

Different genetic models (dominant, additive and recessive) were used to test association, using for each SNP the minor allele as reference. Table 3 shows

Table 2 Socio-demographic characteristics and functional parameters (ADL, HG, GDS and MMSE) in the total sample and stratified for group membership

	Controls ($N = 442$)[a]	Cases ($N = 321$)[a]	Total ($N = 763$)
Age			
Mean (SD)	64.9 (18.1)	96.2 (3.3)	78.2 (20.8)
Range	19–91	89–107	19–107
Body mass index (BMI)			
Mean (SD)	27.1 (4.3)	23.3 (4.1)	25.1 (4.6)
Range	15.01–45.35	12.98–40.55	12.98–45.35
Hand grip strength[b]			
Mean (SD)	22.24 (9.40)	12.67 (6.47)	16.99 (9.24)
Range	4.00–55.00	0.00–42.0	0.00–55.00
Activities of daily living (ADL)[b] [*n* (%)]			
Disable (<5)	55 (17.4)	220 (68.5)	275 (43.1)
Non disable (=5)	262 (82.6)	101 (31.5)	363 (56.9)
Geriatric Depression Scale (GDS)[b] [*n* (%)]			
Depressed (≥5)	107 (33.8)	74 (23.1)	181 (28.4)
Non depressed (<5)	210 (66.2)	247 (76.9)	457 (71.6)
Mini mental state examination (MMSE)[c] [*n* (%)]			
Normal (≥23)	202 (66.66)	–	
Impaired (<23)	101 (33.33)		

ADL scores were dichotomized as one if the subject was not independent in all 5 items and 0 otherwise. GDS scores were dichotomized as 1 if the subject showed depression symptoms (GDS > 5) and 0 otherwise (see "Materials and Methods")

[a] Men younger than 88 and women younger than 91 years will be defined as controls. Men older than 88 and women older than 91 years will be defined as cases

[b] Data available only for subjects older than 65 years

[c] Data available only for subjects belonging to the control group older than 65 years

results obtained using the *RobustSNP* algorithm. After adjusting for sex, we found that *NOS1* rs1879417 and *NOS2* rs2297518 were significantly associated with the longevity phenotype. The additive model for rs1879417 and the recessive one for rs2297518 resulted to be the most likely genetic models, in which the presence of the relevant alleles (allele C for rs1879417 and allele A for rs2297518 variation) decreases the probability to attain longevity ($p_{Model} = 0.008$ and $p_{Model} = 0.031$, respectively). After adjusting for multiple testing (due to the three different tested genetic models), the *NOS1* rs1879417 remained statistically significant ($p_{Adj} = 0.018$), while *NOS2* rs2297518 remained only marginally associated with longevity ($p_{Adj} = 0.066$).

NOS gene polymorphisms and functional parameters

Subjects 65–91 years of age ($N = 317$) were further analyzed for examining the association between the variability of *NOS* genes and physical (HG and ADL) and cognitive (MMSE and GDS) abilities. Table 4 reports the results of the association tests for the three genetic models using the minor allele for each SNP as reference, and after adjusting for the appropriate parameters (see "Materials and Methods").

The *NOS1* rs1879417 was found significantly associated with cognitive performance in an additive manner ($p_{Model} = 0.045$) with subjects carrying the less frequent C allele showing lowest MMSE scores. However, after adjustment for multiple comparisons this association failed to reach statistical significance ($p_{Adj} = 0.093$). In addition, we found that *NOS1* rs2682826 variation significantly influenced the GDS performance ($p_{Model} = 0.015$). Subjects with at least one T allele (less frequent allele) showed a significant higher probability to have depression symptoms than subjects homozygous for the allele G (dominant model). After adjustment for multiple comparisons this association remained statistically significant ($p_{Adj} = 0.033$).

A borderline association was observed between *NOS2* rs2297518 and HG scores ($p_{Model} = 0.049$), with subjects homozygous for the less frequent allele A showing higher HG scores than those carrying at least one copy of the wild type G allele.

Finally, a significant association was found between *NOS3* rs10277237 and ADL performance ($p_{Model} = 0.002$) with subjects homozygous for the minor allele A (recessive model) showing significantly lower probability to be disable than those carrying at least one G allele. After adjustment for multiple comparisons this association remained statistically significant ($p_{Adj} = 0.004$).

Interaction analysis

By using the MB-MDR approach, we did not find any significant interaction effect among the *NOS* gene polymorphisms and the analysed phenotypes.

Table 3 Results of the *RobustSNP* association test with the longevity phenotype in the analyzed sample

SNP	Gene	MAF	*z*-score	p_{Model}	Model	p_{Adj}
rs1879417	*NOS1*	49.0	−2.659	0.008	Additive	0.018
rs2682826		37.0	0.919	0.358	Recessive	0.589
rs10459953	*NOS2*	29.5	−1.022	0.307	Additive	0.522
rs2297518		25.3	−2.163	0.031	Recessive	0.066
rs10277237	*NOS3*	29.0	−0.574	0.566	Dominant	0.805
rs1799983		32.5	0.743	0.457	Dominant	0.703

Model refers to the most likely genetic model among the dominant (DOM), recessive (REC) and additive (ADD) ones. p_{model} refers to the *p* value for the most likely genetic model. p_{Adj} refers to the *p* value adjusted for multiple comparisons (due to the three different tested genetic models). *z*-score represents the *z*-statistics for the regression analyses

MAF minor allele frequency

Discussion

Nitrosative stress is now widely recognized as a significant causal factor in the physiological decline that characterizes the aging process in many tissues. Age-related alterations in nitric oxide synthase activity and/or expression and the consequent alterations in NO production and bioactivity are likely to contribute to this decline.

In the present study, we provide evidence that the variability of *NOS* genes affects common age related phenotypes and longevity. We found an association between *NOS1*-rs1879417 ($p_{Model} = 0.008$; $p_{Adj} = 0.018$) and *NOS2*-rs2297518 ($p_{Model} = 0.031$; $p_{Adj} = 0.066$) and longevity, indicating that variation in these genes may influence human aging and lifespan.

The analysis of a subgroup of subjects in the age range 65–91 years showed that the same variants were also weakly associated with geriatric parameters that are predictors of the age related physiological decline. In particular, the *NOS1* rs1879417-C allele, that we found associated with a lower probability of survival to very old age, was also associated with lower cognitive performance (MMSE score < 23). This association is in line with several evidences. First, it is well established that the glutamate–NO–cGMP pathway plays a role in learning and memory processes and cognitive performance during aging (Domek-Łopacińska and Strosznajder 2010; Paul and Ekambaram 2011). Second, recent studies indicate that *nos1* knockout mice have impaired cognitive functions (Kirchner et al. 2004; Weitzdoerfer et al. 2004; Zoubovsky et al. 2011). Third, changes in the expression and/or activity of *NOS1* have been observed in different cognitive brain areas of aged rats and senescence accelerated mice (SAM), a murine model of age-related cognitive impairment and deterioration of learning and memory (Law et al. 2002; Colas et al. 2006; Han et al. 2010). It is also of interest that the rs1879417 is located in the promoter region of *NOS1*, upstream of a fairly complex transcriptional regulatory region (Bros et al. 2006). Polymorphisms in this region, which affect gene expression and neuronal transcriptome, have been associated with neurological disorders such as schizophrenia and Alzheimer's disease (Reif et al. 2011a, b). Based on this, it is conceivable that the association observed might reflect the linkage disequilibrium between the rs1879417 and these functional variants.

As for *NOS2* gene, we also found that the rs2297518 has a modest impact on HG strength, one of the most effective death predictor in the elderly.

This finding is consistent with researches reporting that the NOS2/NO/ONOO– overproduction induced by TNFα via NF-κB may be one of the underlying causes of sarcopenia (Hall et al. 2011). Our finding that the rs2297518-A allele, which reduces the chance of survival to very old age, is associated with higher HG scores seems somehow in contrast with the idea that higher HG strength is predictive of increased survival in the elderly population. This result is just weakly significant, and certainly needs to be verified. On the other hand it may reflect pleiotropic contrasting effects and functions of the iNOS NO in different cell types In this view, it can be hypothesized that the possible harmful effect exerted by the rs2297518-A allele in some cell-types (for instance a low NO production in macrophages) is more relevant for

Table 4 Results of the *RobustSNP* association test with the functional parameters (ADL, HG, GDS and MMSE) in the subjects belonging to the control group older than 65 years ($N = 317$)

SNP		ADL				HG				GDS				MMSE			
		z-score	p_{Model}	Model	p_{Adj}	*z*-score	p_{Model}	Model	p_{Adj}	*z*-score	p_{Model}	Model	p_{Adj}	*z*-score	p_{Model}	Model	p_{Adj}
rs1879417	*NOS1*	−0.866	0.386	DOM	0.622	1.313	0.189	REC	0.339	0.555	0.579	ADD	0.822	−2.004	0.045	ADD	0.094
rs2682826		1.148	0.251	DOM	0.444	0.667	0.505	REC	0.757	2.438	0.015	DOM	0. 033	−0.561	0.575	DOM	0.816
rs10459953	*NOS2*	−0.064	0.949	REC	0.997	1.658	0.097	REC	0.197	0.950	0.342	REC	0.569	1.401	0.161	ADD	0.303
rs2297518		0.496	0.620	ADD	0.858	1.968	0.049	REC	0.100	1.891	0.059	DOM	0.122	1.640	0.101	REC	0.201
rs10277237	*NOS3*	−3.135	0.002	REC	0.004	0.633	0.526	REC	0.769	1.732	0.083	DOM	0.165	0.774	0.439	DOM	0.678
rs1799983		0.909	0.363	REC	0.592	0.897	0.370	REC	0.608	1.324	0.185	REC	0.342	0.571	0.568	DOM	0.810

Model refers to the most likely genetic model among the dominant (DOM), recessive (REC) and additive (ADD) ones. p_{model} refers to the *p* value for the most likely genetic model. p_{Adj} refers to the *p* value adjusted for multiple comparisons (due to the three different tested genetic models). *z*-score represents the *z*-statistics for the regression analyses

survival than its beneficial effect in other cell-types (i.e. low production of RNS in muscle cells).

For two of the six variants analyzed we found association with geriatric conditions but not with longevity. Specifically the SNP rs2682826 in the *NOS1* gene and the SNP rs10277237 in the *NOS3* gene were respectively associated with GDS ($p_{Model} = 0.015$; $p_{Adj} = 0.033$) and Activity of Daily Living ($p_{Model} = 0.002$; $p_{Adj} = 0.004$), two of the main factors affecting quality of life in older individuals. Depression is a complex disorder where, inflammation, oxidative/nitrosative stress, and reduced hippocampal neurogenesis make a substantial contribution (Maes et al. 2009). It has been found that NOS1-derived NO negatively affects neurogenesis and that the over-expression of *NOS1* in the hippocampus following chronic mild stress exposure suppresses hippocampal neurogenesis and induces depression (Zhou et al. 2007). We found that carriers of the minor rs2682826-T allele have a higher probability to be depressed. In line with our observation, the rs2682826-T allele has been found to be a susceptibility factor for recurrent depressive disorder, and for traits where depression is a co-morbidity factor such as Parkinson disease (Gałecki et al. 2011; Hancock et al. 2008). The rs2682826 is located in the 3′UTR of exon 29, downstream from the translation termination site of the *NOS1* (C276T). Differences in protein production elicited by this variation, that lies close to several miRNAs binding sites (Ibarrola-Villava et al. 2011) could be at the basis of the observed association.

Another interesting finding of our study was the association between the *NOS3* rs10277237 and ADL scores. Subjects homozygous for the rs10277237-A allele had significantly better ADL performance compared with subjects with the other two genotypes. The inability of older adults to perform basic self care independently is a consequence of a decline in physiological functions of multiple tissues. A contributor to this general decay is likely to be the reduction in endothelial cell function caused by the age-related impairment in the release of NO by NOS3. Indeed, this has the effect of reducing blood flow to all tissues in the body and thus the availability of nutrients for energy needs. Age-related changes in energy production and fuel utilization via mitochondrial dysfunction may also contribute to the decline in physical performance and disability among older adults. To this regard, evidence in literature indicate that NO

generation by NOS3 is required for mitochondrial biogenesis and function. In fact, *nos3*$^{-/-}$ mice have fewer mitochondria, and lower β-oxidative activity and energy expenditure than wild-type controls (Nisoli et al. 2003; Le Gouill et al. 2007). In this context, it is also worth noting that recent studies have reported the existence of a mitochondrial NOS (mtNOS) isoform that seems to be both constitutive, mainly a post-translational isoform of NOS1, and inducible (Elfering et al. 2000; Lòpez et al. 2006; Finocchietto et al. 2009). Because of its action on complex I and IV, NO in mitochondria may have important effects on oxidative phosphorylation and ROS/RNS production (Finocchietto et al. 2009). These effects may be amplified in a pro-oxidant environment like in the case of aged individuals, with consequences particularly in tissues such as brain and skeletal muscle which are highly dependent on mitochondrial function.

In conclusion, it is worth mentioning that the causative genetic variations in LD with the studied SNPs remain to be identified and that the associations between *NOS* alleles and aging phenotypes we observed, in most cases would not hold after Bonferroni correction for multiple comparisons, indicating that it will be useful to replicate this study. On the other hand, this study availed of a population (Calabria, Southern Italy) which is characterized by high genetic homogeneity and a scarce level of immigration due to geographical, historical and social reasons. Consequently it is likely we avoided false positive results due to population stratification. On the other hand, it is also important to underline that all the results were in line with previous data and in particular with data from model organisms. This allows us to consider *NOS* genes to have an important role on the age related homeostatic and physiological decline which is at the basis of most of the age related phenotypes and longevity (Fried et al. 2001; Montesanto et al. 2010).

Acknowledgments The research leading to these results has received funding from the European Union's Seventh Framework Programme (FP7/2007-2011) under Grant agreement No. 259679 and from "Fondi di Ateneo" of the University of Calabria.

References

Barrett JC, Fry B, Maller J, Daly MJ (2005) Haploview: analysis and visualization of LD and haplotype maps. Bioinformatics 21:263–265

Beckman JS, Koppenol WH (1996) Nitric oxide, superoxide, and peroxynitrite: the good, the bad, and ugly. Am J Physiol 271:C1424–C1437

Bros M, Boissel JP, Gödtel-Armbrust U, Förstermann U (2006) Transcription of human neuronal nitric oxide synthase mRNAs derived from different first exons is partly controlled by exon 1-specific promoter sequences. Genomics 87:463–473

Brown GC (2010) Nitric oxide and neuronal death. Nitric Oxide 23:153–165

Calabrese V, Mancuso C, Calvani M, Rizzarelli E, Butterfield DA, Stella AM (2007) Nitric oxide in the central nervous system: neuroprotection versus neurotoxicity. Nat Rev Neurosci 8:766–775

Calcerrada P, Peluffo G, Radi R (2011) Nitric oxide-derived oxidants with a focus on peroxynitrite: molecular targets, cellular responses and therapeutic implications. Curr Pharm Des 17:3905–3932

Calle ML, Urrea V, Malats N, Van Steen K (2010) mbmdr: an R package for exploring gene–gene interactions associated with binary or quantitative traits. Bioinformatics 26:2198–2199

Cau SB, Carneiro FS, Tostes RC (2012) Differential modulation of nitric oxide synthases in aging: therapeutic opportunities. Front Physiol 3:218

Colas D, Gharib A, Bezin L, Morales A, Guidon G, Cespuglio R, Sarda N (2006) Regional age-related changes in neuronal nitric oxide synthase (nNOS), messenger RNA levels and activity in SAMP8 brain. BMC Neurosci 7:81

De Rango F, Montesanto A, Berardelli M, Mazzei B, Mari V, Lattanzio F, Corsonello A, Passarino G (2011) To grow old in southern Italy: a comprehensive description of the old and oldest old in Calabria. Gerontology 57:327–334

Dere E, De Souza Silva MA, Topic B, Fiorillo C, Li JS, Sadile AG, Frisch C, Huston JP (2002) Aged endothelial nitric oxide synthase knockout mice exhibit higher mortality concomitant with impaired open-field habituation and alterations in forebrain neurotransmitter levels. Genes Brain Behav 1:204–213

Domek-Łopacińska KU, Strosznajder JB (2010) Cyclic GMP and nitric oxide synthase in aging and Alzheimer's disease. Mol Neurobiol 41:129–137

Drew B, Leeuwenburgh C (2002) Aging and the role of reactive nitrogen species. Ann NY Acad Sci 959:66–81

Elfering SL, Sarkela TM, Giulivi C (2000) Biochemistry of mitochondrial nitric-oxide synthase. J Biol Chem 277:38079–38086

Feil R, Kleppisch T (2008) NO/cGMP-dependent modulation of synaptic transmission. Handb Exp Pharmacol 184:529–560

Finocchietto PV, Franco MC, Holod S, Gonzalez AS, Converso DP, Arciuch VG, Serra MP, Poderoso JJ, Carreras MC (2009) Mitochondrial nitric oxide synthase: a masterpiece of metabolic adaptation, cell growth, transformation, and death. Exp Biol Med (Maywood) 234:1020–1028

Folstein MF, Folstein SE, McHugh PR (1975) "Mini-mental state". A practical method for grading the cognitive state of patients for the clinician. J Psychiatr Res 12:189–198

Förstermann U, Sessa WC (2012) Nitric oxide synthases: regulation and function. Eur Heart J 33:829–837

Fried LP, Tangen CM, Walston J, Newman AB, Hirsch C, Gottdiener J, Seeman T, Tracy R, Kop WJ, Burke G,

McBurnie MA (2001) Cardiovascular health study collaborative research group. Frailty in older adults: evidence for a phenotype. J Gerontol A 56:M146–M156

Gałecki P, Maes M, Florkowski A, Lewiński A, Gałecka E, Bienkiewicz M, Szemraj J (2011) Association between inducible and neuronal nitric oxide synthase polymorphisms and recurrent depressive disorder. J Affect Disord 129:175–182

Garthwaite J (2008) Concepts of neural nitric oxide-mediated transmission. Eur J Neurosci 27:2783–2802

Grigoletto F, Zappalà G, Anderson DW, Lebowitz BD (1999) Norms for the mini-mental state examination in a healthy population. Neurology 53:315–320

Hall DT, Ma JF, Marco SD, Gallouzi IE (2011) Inducible nitric oxide synthase (iNOS) in muscle wasting syndrome, sarcopenia, and cachexia. Aging (Albany NY) 3:702–715

Han S, Rudd JA, Hu ZY, Zhang L, Yew DT, Fang M (2010) Analysis of neuronal nitric oxide synthase expression and increasing astrogliosis in the brain of senescence-accelerated-prone 8 mice. Int J Neurosci 120:602–608

Hancock DB, Martin ER, Vance JM, Scott WK (2008) Nitric oxide synthase genes and their interactions with environmental factors in Parkinson's disease. Neurogenetics 9:249–262

Ibarrola-Villava M, Peña-Chilet M, Fernandez LP, Aviles JA, Mayor M, Martin-Gonzalez M, Gomez-Fernandez C, Casado B, Lazaro P, Lluch A, Benitez J, Lozoya R, Boldo E, Pizarro A, Martinez-Cadenas C, Ribas G (2011) Genetic polymorphisms in DNA repair and oxidative stress pathways associated with malignant melanoma susceptibility. Eur J Cancer 47:2618–2625

Jung J, Na C, Huh Y (2012) Alterations in nitric oxide synthase in the aged CNS. Oxid Med Cell Longev 2012:718976

Kader KN, Akella R, Ziats NP, Lakey LA, Harasaki H, Ranieri JP, Bellamkonda RV (2000) eNOS-overexpressing endothelial cells inhibit platelet aggregation and smooth muscle cell proliferation in vitro. Tissue Eng 6:241–251

Kanski J, Hong SJ, Schöneich C (2005) Proteomic analysis of protein nitration in aging skeletal muscle and identification of nitrotyrosine-containing sequences in vivo by nano-electrospray ionization tandem mass spectrometry. J Biol Chem 280:24261–24266

Katz S, Downs TD, Cash HR, Grotz RC (1970) Progress in development of the index of ADL. Gerontologist 10:20–30

Kawamoto EM, Vasconcelos AR, Degaspari S, Böhmer AE, Scavone C et al (2012) Age-related changes in nitric oxide activity, cyclic GMP, and TBARS levels in platelets and erythrocytes reflect the oxidative status in central nervous system. Age (Dordr) 35(2):331–342

Kim CH, Zou Y, Kim DH, Kim ND, Yu BP, Chung HY (2006) Proteomic analysis of nitrated and 4-hydroxy-2- nonenal-modified serum proteins during aging. J Gerontol A 61:332–338

Kirchner L, Weitzdoerfer R, Hoeger H, Url A, Schmidt P, Engelmann M, Villar SR, Fountoulakis M, Lubec G, Lubec B (2004) Impaired cognitive performance in neuronal nitric oxide synthase knockout mice is associated with hippocampal protein derangements. Nitric Oxide 11:316–330

Law A, O'Donnell J, Gauthier S, Quirion R (2002) Neuronal and inducible nitric oxide synthase expressions and activities in the hippocampi and cortices of young adult, aged cognitively unimpaired, and impaired Long-Evans rats. Neuroscience 112:267–275

Le Gouill E, Jimenez M, Binnert C, Pierre-Yves J, Thalmann S, Nicod P, Scherrer U, Vollenweider P (2007) eNOS knockout mice have defective mitochondrial beta-oxidation. Diabetes 56:2690–2696

Liaudet L, Soriano FG, Szabó C (2000) Biology of nitric oxide signaling. Crit Care Med 28:N37–N52

Lòpez LC, Escames G, Tapias V, Utrilla P, Leo′n J, Acuna-Castroviejo D (2006) Identification of an inducible nitric oxide synthase in diaphragm mitochondria from septic mice: its relation with mitochondrial dysfunction and prevention by melatonin. Int J Biochem Cell Biol 38:267–278

Maes M, Yirmyia R, Noraberg J, Brene S, Hibbeln J, Perini G, Kubera M, Bob P, Lerer B, Maj M (2009) The inflammatory & neurodegenerative (I&ND) hypothesis of depression: leads for future research and new drug developments in depression. Metab Brain Dis 24:27–53

McCann SM, Licinio J, Wong ML, Yu WH, Karanth S, Rettori V (1998) The nitric oxide hypothesis of aging. Exp Gerontol 33:813–826

Moilanen E, Moilanen T, Knowles R, Charles I, Kadoya Y, Al-Saffar N, Revell PA, Moncada S (1997) Nitric oxide synthase is expressed in human macrophages during foreign body inflammation. Am J Pathol 150:881–887

Moncada S, Higgs EA (2006) The discovery of nitric oxide and its role in vascular biology. Br J Pharmacol 147:S193–S201

Montesanto A, Lagani V, Martino C, Dato S, De Rango F, Berardelli M, Corsonello A, Mazzei B, Mari V, Lattanzio F, Conforti D, Passarino G (2010) A novel population-specific approach to define frailty. Age (Dordr) 32(3):385–395

Napoli C, Ignarro LJ (2009) Nitric oxide and pathogenic mechanisms involved in the development of vascular diseases. Arch Pharm Res 32:1103–1108

Nisoli E, Clementi E, Paolucci C, Cozzi V, Tonello C, Sciorati C, Bracale R, Valerio A, Francolini M, Moncada S, Carruba MO (2003) Mitochondrial biogenesis in mammals: the role of endogenous nitric oxide. Science 299:896–899

Nisoli E, Tonello C, Cardile A, Cozzi V, Bracale R, Tedesco L, Falcone S, Valerio A, Cantoni O, Clementi E, Moncada S, Carruba MO (2005) Calorie restriction promotes mitochondrial biogenesis by inducing the expression of *eNOS*. Science 310:314–317

Oess S, Icking A, Fulton D, Govers R, Müller-Esterl W (2006) Subcellular targeting and trafficking of nitric oxide synthases. Biochem J 396:401–409

Pacher P, Beckman JS, Liaudet L (2007) Nitric oxide and peroxynitrite in health and disease. Physiol Rev 87:315–424

Passarino G, Montesanto A, Dato S, Giordano S, Domma F, Mari V, Feraco E, De Benedictis G (2006) Sex and age specificity of susceptibility genes modulating survival at old age. Hum Hered 62:213–220

Paul V, Ekambaram P (2011) Involvement of nitric oxide in learning & memory processes. Indian J Med Res 133:471–478

Reif A, Grünblatt E, Herterich S, Wichart I, Rainer MK, Jungwirth S, Danielczyk W, Deckert J, Tragl KH, Riederer P,

Fischer P (2011a) Association of a functional NOS1 promoter repeat with Alzheimer's disease in the VITA cohort. J Alzheimers Dis 23:327–333

Reif A, Schecklmann M, Eirich E, Jacob CP, Jarczok TA, Kittel-Schneider S, Lesch KP, Fallgatter AJ, Ehlis AC (2011b) A functional promoter polymorphism of neuronal nitric oxide synthase moderates prefrontal functioning in schizophrenia. J Neuropsychopharmacol 14:887–897

Sheikh JI, Yesavage JA (1986) Geriatric Depression Scale (GDS): recent evidence and development of a shorter version. Clinical gerontology: a guide to assessment and intervention. Haworth, New York, pp 165–173

So HC, Sham PC (2011) Robust association tests under different genetic models, allowing for binary or quantitative traits and covariates. Behav Genet 41:768–775

Strosznajder JB, Jeśko H, Zambrzycka A, Eckert A, Chalimoniuk M (2004) Age-related alteration of activity and gene expression of endothelial nitric oxide synthase in different parts of the brain in rats. Neurosci Lett 370:175–179

Taddei S, Virdis A, Ghiadoni L (2001) Age-related reduction of NO availability and oxidative stress in humans. Hypertension 38:274–279

Toprakci M, Ozmen D, Mutaf I, Turgan N, Parildar Z, Habif S, Guner I, Bayindir O (2000) Age-associated changes in nitric oxide metabolites nitrite and nitrate. Int J Clin Lab Res 30:83–85

Torregrossa AC, Aranke M, Bryan NS (2011) Nitric oxide and geriatrics: implications in diagnostics and treatment of the elderly. J Geriatr Cardiol 8:230–242

Tsutsui M, Shimokawa H, Otsuji Y, Ueta Y, Sasaguri Y, Yanagihara N (2009) Nitric oxide synthases and cardiovascular diseases: insights from genetically modified mice. Circ J 73:986–993

van der Loo B, Labugger R, Skepper JN, Bachschmid M, Kilo J, Powell JM, Palacios-Callender M, Erusalimsky JD, Quaschning T, Malinski T, Gygi D, Ullrich V, Lüscher TF (2000) Enhanced peroxynitrite formation is associated with vascular aging. JExp Med 192:1731–1744

Villanueva C, Giulivi C (2010) Subcellular and cellular locations of nitric oxide synthase isoforms as determinants of health and disease. Free Radic Biol Med 49:307–316

Weitzdoerfer R, Hoeger H, Engidawork E, Engelmann M, Singewald N, Lubec G, Lubec B (2004) Neuronal nitric oxide synthase knock-out mice show impaired cognitive performance. Nitric Oxide 10:130–140

Wigginton JE, Cutler DJ, Abecasis GR (2005) A note on exact tests of Hardy–Weinberg equilibrium. Am J Hum Genet 76:887–893

Wink DA, Hines HB, Cheng RY, Switzer CH, Flores-Santana W, Vitek MP, Ridnour LA, Colton CA (2011) Nitric oxide and redox mechanisms in the immune response. J Leukoc Biol 89:873–891

Yang B, Larson DF, Watson RR (2004) Modulation of *iNOS* activity in age-related cardiac dysfunction. Life Sci 75:655–667

Yoon HJ, Cho SW, Ahn BW, Yang SY (2010) Alterations in the activity and expression of endothelial NO synthase in aged human endothelial cells. Mech Ageing Dev 131:119–123

Zhou QG, Hu Y, Hua Y, Hu M, Luo CX, Han X, Zhu XJ, Wang B, Xu JS, Zhu DY (2007) Neuronal nitric oxide synthase contributes to chronic stress-induced depression by suppressing hippocampal neurogenesis. J Neurochem 103:1843–1854

Zoubovsky SP, Pogorelov VM, Taniguchi Y, Kim SH, Yoon P, Nwulia E, Sawa A, Pletnikov MV, Kamiya A (2011) Working memory deficits in neuronal nitric oxide synthase knockout mice: potential impairments in prefrontal cortex mediated cognitive function. Biochem Biophys Res Commun 408:707–712

ACKNOWLEDGEMENTS

First and foremost, I would like to acknowledge my Supervisors, Professor Giuseppina Rose and Doctor Adolfo Saiardi without whom this work would not have been possible. I thank Professor Giuseppina Rose for her patient guidance in my research and for her helpful discussions. I must express my gratitude to Doctor Adolfo Saiardi, for accepting me in his laboratory, for being available for discussion, for correcting my thesis, for providing me the opportunity to join the great experience in the Laboratory for Molecular Cell Biology.

In addition, I would like to thank Professor Giuseppe Passarino for not only giving me the opportunity to work in his laboratory but also being a great mentor. Special thanks go to all the laboratory of Genetics at the University of Calabria.

I would also like to acknowledge the fantastic people that I met in Adolfo's lab. In particular, Cristina and Betty, this year and a half without them it would have been impossible. They are two of the most special people that I have never met. My gratitude also extends to Miranda and Tom for correcting my written and spoken English every time it was needed. I also would like to acknowledge many members of the lab and the institute.

I am particularly grateful to my family, Tullio, Rina and Giovanni, for their infinite love, encouragement and unconditional support. Thanks to all my friends for their friendship and patience throughout these years.